Physics Reports 595 (2015) 1–44

Contents lists available at ScienceDirect

Physics Reports

journal homepage: www.elsevier.com/locate/physrep

Phonon hydrodynamics and its applications in nanoscale heat transport

Yangyu Guo, Moran Wang *

Key Laboratory for Thermal Science and Power Engineering of Ministry of Education, Department of Engineering Mechanics and CNMM, Tsinghua University, Beijing 100084, China

ARTICLE INFO

Article history:
Accepted 22 July 2015
Available online 3 August 2015
editor: G. E. W. Bauer

Keywords:
Phonon hydrodynamics
Nanoscale heat transport
Macroscopic method
Phonon transport
Effective thermal conductivity

ABSTRACT

Phonon hydrodynamics is an effective macroscopic method to study heat transport in dielectric solid and semiconductor. It has a clear and intuitive physical picture, transforming the abstract and ambiguous heat transport process into a concrete and evident process of phonon gas flow. Furthermore, with the aid of the abundant models and methods developed in classical hydrodynamics, phonon hydrodynamics becomes much easier to implement in comparison to the current popular approaches based on the first-principle method and kinetic theories involving complicated computations. Therefore, it is a promising tool for studying micro- and nanoscale heat transport in rapidly developing micro and nano science and technology. However, there still lacks a comprehensive account of the theoretical foundations, development and implementation of this approach. This work represents such an attempt in providing a full landscape, from physical fundamental and kinetic theory of phonons to phonon hydrodynamics in view of descriptions of phonon systems at microscopic, mesoscopic and macroscopic levels. Thus a systematical kinetic framework, summing up so far scattered theoretical models and methods in phonon hydrodynamics as individual cases, is established through a frame of a Chapman–Enskog solution to phonon Boltzmann equation. Then the basic tenets and procedures in implementing phonon hydrodynamics in nanoscale heat transport are presented through a review of its recent wide applications in modeling thermal transport properties of nanostructures. Finally, we discuss some pending questions and perspectives highlighted by a novel concept of generalized phonon hydrodynamics and possible applications in micro/nano phononics, which will shed more light on more profound understanding and credible applications of this new approach in micro- and nanoscale heat transport science.

Contents

---

* Corresponding author. Tel.: +86 10 627 87498.
E-mail address: mrwang@tsinghua.edu.cn (M. Wang).

http://dx.doi.org/10.1016/j.physrep.2015.07.003
0370-1573/

1. Introduction

1.1. Micro- and nanoscale heat transport

Heat transport science is an old discipline dated back to the classical work by J. Fourier who proposed the constitutive law termed after his name in his masterpiece [1]. Accurate description and understanding of heat transport hereafter becomes vital not only in theoretical developments of thermodynamics [2–4] and statistical mechanics [5–7], but also in wide engineering applications for chemical processes [8,9], energy and building [10,11], power production [12,13] and so on. In terms of the physical mechanism of heat transport, different kinds of heat carriers have been proposed to explain the process [14]: molecule, electron, photon and phonon. In the present work, we focus on the heat transport mediated by phonon, which was first introduced to describe the heat conduction in dielectric solid by Peierls [15] and then refined and expanded by subsequent researchers [16–20].

Near the end of last century, with the rapid development of micro- and nanofabrication [21] and nanotechnology [22], as the size of systems drastically shrank down, Fourier's law is considered no longer valid for heat transport due to the sub-continuum effects. Therefore, it became crucial to develop substitutes in theory on micro- and nanoscale heat transport, to tackle the related thermal phenomena in nanosystems, such as the intractable microelectronics cooling problems [23,24] emerging in 1980s. Pioneering investigations were conducted in a systematical way by the group of C.L. Tien and coworkers, and have been thoroughly summarized in Refs. [25,26], leading to the gradual establishment of the field of microscale thermophysical engineering [27]. In recent years, there are increasing and urgent demands on deeper understanding of the fundamental issues in this field, motivated by diverse technology applications such as the thermoelectric energy conversion [28,29], micro- and nanoelectronics and optoelectronics [30], micro- and nanoelectromechanical systems [21], functional nanomaterials [31]. These activities and progresses are summarized in some comprehensive reviews [32–36] and several monographs [14,37–40]. Note that micro- and nanoscale denotes both the temporal aspect when the process characteristic time is comparable to or smaller than the relaxation times of the heat carriers such as in short-pulse laser heating process [41,42], and the spatial aspect when the system characteristic size becoming comparable to or smaller than the mean free paths of the heat carriers such as in thin film heat conduction [43,44]. More detailed discussions of heat transport regimes at micro- and nanoscale could be found in Refs. [25,45–47].

1.2. Overview of current methods

To treat heat transport at micro- and nanoscale, there are logically two categories of methods: theoretical and experimental ones. In this work, we are focusing only on the theoretical methods. In the early stage of developments in this field, kinetic modeling based on the phonon Boltzmann equation [41–44] and simplified molecular dynamics simulations [48–50] were the major tools. With the advancements of molecular dynamic techniques [51–53], density functional perturbation theory [54,55] and high performance computing [56], it becomes possible to perform large-scale simulations using molecular dynamics and first-principle calculations to predict thermal transport properties of bulk- and nanostructures in recent years [34]. Monte Carlo (or lattice Boltzmann method, etc.) solutions of the phonon Boltzmann equation supplemented with information from first-principle calculation, molecular dynamics or lattice dynamics simulation are currently the main trend [53,57–60] in multi-scale modeling of micro- and nanoscale heat transport. Even though the first-principle calculations or molecular dynamics simulations are able to explain what happens at microscale, and the kinetic theory based modeling can capture the statistical behavior of phonons at the mesoscopic scale, people have never faltered in the quest for macroscopic description of phonon transport which has the capability to provide a clear and intuitive physical picture for a better understanding. In summary, there are mainly four macroscopic methods available for nanoscale heat transport in the literature: phonon hydrodynamic model [61,62], dual-phase-lag model [63,64], ballistic–diffusive model [65,66] and thermon gas model [67,68].

All of these macroscopic, mesoscopic and microscopic methods are summarized in Fig. 1. Here the terms 'microscopic', 'mesoscopic' and 'macroscopic' represent modeling the nanoscale heat transport at three different levels of descriptions. 'Microscopic' method provides atomic-scale information, while 'mesoscopic' method produces statistical information such as the particle distribution function, and 'macroscopic' method uses only several state variables for continuum media (i.e. moments of the particle distribution function). In the present work, we aim to clarify the significance of macroscopic methods and focus on the phonon hydrodynamic model, which has never been addressed in the previous reviews [32–34,36].

1.2.1. Microscopic methods

The main idea of microscopic method is through direct simulations of the motion and interactions of atoms in solids by numerically solving the fundamental dynamic equations. In the framework of classical mechanics, Newton's equation is solved, as the foundation of molecular dynamics simulation method. Whereas in the quantum mechanical framework, the Schrödinger equation is solved, corresponding to the first-principle method.

Classical molecular dynamics simulation usually includes two branches [69]: the Green–Kubo (equilibrium) method based on fluctuation–dissipation theorem [70], and direct (non-equilibrium) method by calculating the induced heat flux

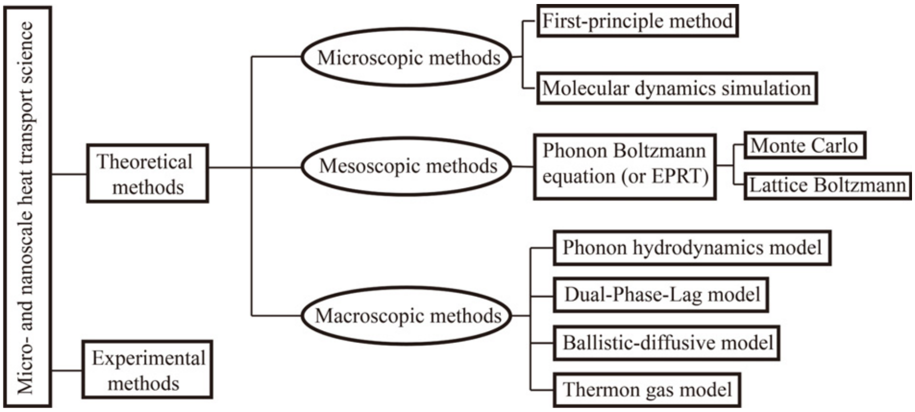

Fig. 1. Current methods in micro- and nanoscale heat transport science.

(or temperature gradient) from the applied temperature gradient (or heat flux). The information of positions and velocities of all the atoms need be stored at each step of the simulation, thus being very time- and computational-source-consuming. To alleviate this situation, combination of molecular dynamics and lattice dynamics simulations has been proposed to obtain the phonon information (dispersion relation, relaxation time) as inputs to the solution of phonon Boltzmann equation and worked well in predicting lattice thermal conductivity [53,69]. Nevertheless, the results of molecular dynamics simulation much depend on the developments of accurate inter-atomic potential functions and usually limit to high-temperature circumstance [60,69].

Therefore, the first-principle method emerges [71], aiming at parameter-free predictions of thermal transport properties over a wide range of temperature. Based on density functional perturbation theory, it obtains the harmonic (second-order) and anharmonic (third-order) interaction force instants for the pairs of atoms and triplets of atoms respectively as inputs to the solution of phonon Boltzmann equation [71]. It worked well in predicting thermal conductivity of diverse categories of bulk materials [71,72] and showed promising potential for nanostructures as well [73].

1.2.2. *Mesoscopic methods*

Mesoscopic methods refer to the kinetic modeling based on phonon Boltzmann equation or its derivatives (such as the Equation of Phonon Radiative Transport, EPRT [44]). Solution of Boltzmann equation is not easy because of its complex collision term [74]. There are usually two trains of thought: a full solution and a single mode relaxation time (SMRT) approximation [14,38]. The full solution needs complicated numerical iteration [71] or *ab initio* variational approach [75]. The SMRT approximation is more preferred [53,58,59,76,77] because of its simplicity although empirical parameters have been utilized, which are often adjusted from experimental data. Monte Carlo method has been used to solve the phonon Boltzmann equation [78], especially for micro- and nanoscale heat transport [60]. Lattice Boltzmann method is an alternative [79] yet still in its infancy [80], which will be further discussed later.

1.2.3. *Macroscopic methods*

In parallel to the developments of microscopic and mesoscopic methods, fruitful efforts have also been put on the macroscopic method for micro- and nanoscale heat transport. The macroscopic approach is based on generalized heat transport equations which are able to describe heat transport in a wide range of scales, including not only the conventional diffusive regime where Fourier's law is valid, but also the so-called ballistic regime and the so-called phonon hydrodynamic regime. Among the available macroscopic methods, one spreading over a large span of time is the phonon hydrodynamics model [62]. Note that the denomination "phonon hydrodynamics" is found in the literature with two slightly different but related meanings. In line of phonon kinetic theory, "phonon hydrodynamics" refers to a particular phonon flow regime with the dominant effect of normal phonon–phonon collisions over resistive collisions, and termed as "classical phonon hydrodynamics" as in Section 3; in macroscopic non-equilibrium thermodynamics, it refers to the use of transport equations analogous to classical hydrodynamic equations, with the heat flux and temperature gradient playing the roles of velocity and pressure gradient respectively, and termed as "phenomenological phonon hydrodynamics" as in Section 4. The details of them will be elucidated soon below. Phonon hydrodynamics was first proposed at the mid-period of last century for studying heat waves in dielectric solid at low temperature [61,81]. Numerous subsequent theoretical work [82–86] was followed by mathematical physicists to refine, develop and extend the original model. The substantial bridging between phonon hydrodynamics and nanoscale heat transport was accomplished recently in the landmark work by Jou and his coworkers [62], based on a heuristic analogy between nanoscale phonon gas flow and rarefied gas flow. It opens up a new field in applying the hydrodynamic approach to analyze nanoscale heat transport, thus simplified the problem and showed an intuitive and clear physical picture consistent with the existing knowledge about hydrodynamics. Many applications are extensively studied, such as the prediction of thermal conductivity of nanostructures [62,87].

The Dual-Phase-Lag (DPL) model [63,64] (or the so-called Jeffrey's type model [88]) was proposed in the end of last century. Its starting point is Fourier's law $\mathbf{q} = -\lambda\nabla T$, which indicates an unphysical instantaneous response between heat flux and temperature gradient [89]. The DPL model proposed new causal response through adding two phase lags into the Fourier's law thus achieving $\mathbf{q}\left(\mathbf{r}, t+\tau_q\right) = -\lambda\nabla T\left(\mathbf{r}, t+\tau_T\right)$, which allows both heat flux as the cause of temperature gradient when $\tau_q<\tau_T$, and temperature gradient as the cause of heat flux when $\tau_q > \tau_T$ [37]. This is a unified model trying to incorporate many different situations of heat transport at different scales by grasping the common feature. From our perspective, the DPL model usually captures well the behavior of heat transport mediated by two (or multi-) carriers (or media), such as the electron–phonon interactions in the laser-heating process in metal [90], superfluid and normal components induced heat wave propagation in superfluid liquid helium [90], multi-phase induced nonhomogeneous heating response in porous media [91] and amorphous media [92]. Another characteristic of DPL model is that the two phase lags have usually to be determined by adjusting to the experimental data of thermal response.

Ballistic-diffusive model [65,66] is an another attempt to transit from mesoscopic kinetic theory to macroscopic equations to describe nanoscale heat transport. It divides the phonon distribution function at a given point into two parts [65]: one from the inside of medium (diffusive part), the other from the boundary of medium (ballistic part). By integrating the phonon Boltzmann equation, two evolution equations are obtained for the internal energy (or heat flux) of the diffusive and ballistic phonons respectively. This model contributes more to the conceptual aspect with only simple 1D and 2D heat conduction benchmarks studied [93–95] rather than to practical applications. Note that the ballistic–diffusive model strictly belongs to a mixed macroscopic–mesoscopic method [96] since the heat flux of ballistic phonons has to be calculated from the kinetic theory.

The thermon gas model, with a history of nearly ten years [67], was to describe heat transport through the classical fluid mechanics equations for heat by introducing a so-called thermomass defined as the equivalent mass of thermal energy based on Einstein's mass-energy equivalence [68]. In this model, heat conductions can be treated as thermon gas flows in media driven by a temperature gradient. Thermon is defined as a unit quasi-particle carrying thermal energy. For solids, the thermon gas is the phonon gas for crystals, attached on the electron gas for pure metals, or just between both for most of other solids. Although predictions based on this model of effective thermal conductivity of nanomaterials have gained good agreements with experimental data [97–99], the theoretical gap between physical picture and constitutive equations has not been perfectly fulfilled. This model was evaluated consistent with the phonon hydrodynamic model, and never beyond the theoretical framework of the phonon hydrodynamics [100,101].

All these major macroscopic models are available to describe or capture the nonlocal effect of the heat flux and the temperature gradient between different locations [102]. Besides, it is worth mentioning that some other similar macroscopic models are also proposed, such as the C-F heat conduction model [103], the stochastic heat equation [104] and so on.

Although the subsequent studies for these macroscopic models have claimed that they all have fundamental bases on the phonon Boltzmann equation [65,100,105], the phonon hydrodynamic model is the most natural and direct production from the phonon Boltzmann equation. The macroscopic constitutive equations of phonon hydrodynamics can be derived directly from the phonon Boltzmann equation, which avoids empirical parameters or pure mathematical terms in other models. Therefore it can provide a clear and intuitive physical picture, and thus converts the abstract and ambiguous heat transport process into a concrete and evident phonon gas flow process, which help us better understand the indiscernible mechanism. In the present work, we focus on reviewing and expatiating the microscopic and mesoscopic physical and mathematical foundations for the phonon hydrodynamic model. Only in this way is it possible to capture the main essences and key features of nanoscale heat transport applications yet still using simple formulations.

1.3. *Objectives and structure of this review*

Therefore, the objectives of the present review include the following aspects: (1) to provide a solid conceptual foundation for phonon hydrodynamics in view of descriptions of phonon systems at different levels; (2) to examine the existing theoretical methods in developing phonon hydrodynamic models from phonon Boltzmann equation, and establish a unified kinetic framework for these models, thus bridging the mesoscopic physics and macroscopic approaches; (3) to summarize the fundamentals and procedures in implementing phonon hydrodynamics to nanoscale heat transport with actual application cases; (4) to give possible perspectives and future trends by revisiting the current status of phonon hydrodynamic model.

This review is organized as: in Section 2, the concepts of phonon, phonon kinetic theory and phonon hydrodynamics are introduced in a systematical way, from the perspective of microscopic, mesoscopic and macroscopic descriptions respectively. Then a unified kinetic framework is established for phonon hydrodynamic model in Section 3 through an asymptotic solution to phonon Boltzmann equation, with also a summary of previous models by diverse methods that could be included as different orders of specific solutions. These theoretical foundations pave the road for actual applications of the phonon hydrodynamics in predicting the thermal transport properties of nanostructures—the main contents in Section 4, where other essential fundamentals for applications including the heat flux boundary and its thermodynamic foundations are introduced as well. Finally, in Section 5 we discuss some open questions and possible perspectives of the phonon hydrodynamic model, after which concluding remarks are made in Section 6.

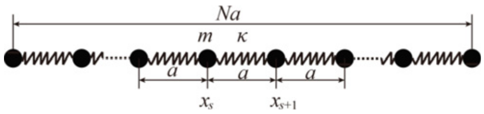

Fig. 2. One-dimensional monoatomic lattice chain.

2. Concepts and foundations

2.1. Phonon

The concept of phonon was first introduced by Einstein [106] and Debye [107] in dealing with the specific heat capacity of dielectric solid. This phonon model is used to describe the equilibrium properties of solid. It was Peierls [15] who generalized the equilibrium phonon model to nonequilibrium heat transport, and proposed the Peierls–Boltzmann transport equation [16] for phonons, inspired from kinetic theory of gases [108].

Phonon is defined as wave packet [14,109] from the perspective of classical mechanics, or minimum energy quantum [38,39,110] from the perspective of quantum mechanics. Therefore we consider the description of phonons in two aspects: classical and quantum mechanical pictures. For simplicity, a one-dimensional monoatomic lattice chain, shown in Fig. 2, is taken to represent the realistic three-dimensional lattice structure in dielectric solid. The interacting atoms are treated as a spring-mass system, with an identical atom mass m, a spring constant κ and a spacing a between the atomic equilibrium positions. N is the total number of atoms, the position of each termed as x_s, with $s = 1, 2, \ldots, N$. Harmonic interaction is assumed between adjacent atoms.

2.1.1. Classical mechanical picture

Based on Newton's equation in classical mechanics, the dynamic relation for lattice vibration is:

$$m\frac{\mathrm{d}^2 x_s}{\mathrm{d}t^2} = \kappa\left(x_{s+1} + x_{s-1} - 2x_s\right). \tag{1}$$

Defining the displacement from corresponding equilibrium position as $u_s = x_s - x_s^0$, we obtain the equation for lattice displacement:

$$m\frac{\mathrm{d}^2 u_s}{\mathrm{d}t^2} = \kappa\left(u_{s+1} + u_{s-1} - 2u_s\right), \tag{2}$$

the solution of which has the following form [38]:

$$u_s = A\exp\left[-i\left(\omega t - ksa\right)\right], \tag{3}$$

with A, ω, k denoting respectively the amplitude, frequency and wave number of lattice vibration, i being the imaginary unit. Substitution of Eq. (3) into Eq. (2) gives rise to the dispersion relation for the wave propagation of lattice vibration:

$$\omega = 2\sqrt{\frac{\kappa}{m}}\left|\sin\frac{ka}{2}\right|, \tag{4}$$

which is a periodic function of k with a period $2\pi/a$. Mathematically, only one period is sufficient to account: $(-\pi/a, \pi/a)$, known as the first Brillouin zone. Any wave number beyond the first Brillouin zone can be shifted into this domain by integer times of periods [110]. Physically, the wave number cannot be larger than π/a because the wave length ($\lambda = 2\pi/k$) cannot be smaller than twice the atomic spacing [38].

The plane harmonic wave described by Eq. (3) does not convey any signal or energy actually. Based on the dispersion relation Eq. (4), the concept of "localized wave packet" is introduced, which is the essential energy or signal carrier. Two plane harmonic waves with slight wave number difference (Δk) around k_0 are described respectively by:

$$u_{s1} = A\exp\left[-i\left(\left(\omega_0 - \Delta\omega\right)t - \left(k_0 - \Delta k\right)sa\right)\right], \tag{5a}$$

$$u_{s2} = A\exp\left[-i\left(\left(\omega_0 + \Delta\omega\right)t - \left(k_0 + \Delta k\right)sa\right)\right]. \tag{5b}$$

Combination of these two waves results in the propagation of a wave packet:

$$u_s = u_{s1} + u_{s2} = \tilde{A}\cos\left(\omega_0 t - k_0 sa\right), \tag{6}$$

with the combinational amplitude $\tilde{A} = 2A\cos\left(\Delta\omega t - \Delta ksa\right)$. The localized wave packet is exactly the classical mechanical picture of phonon. Distinct from the phase speed ($v_p = \omega_0/k_0$) of lattice vibration, the propagating speed of the wave packet or phonon is termed as group speed:

$$v_g = \frac{\Delta\omega}{\Delta k} = \frac{\partial\omega}{\partial k}. \tag{7}$$

2.1.2. Quantum mechanical picture

Schrödinger equation is the fundamental equation in quantum mechanics, which needs the Hamiltonian of the monoatomic lattice chain:

$$H = \sum_s \left[\frac{1}{2} m \dot{x}_s^2 + \frac{1}{2} \kappa \left(x_{s+1} - x_s \right)^2 \right]. \tag{8}$$

Eq. (8) indicates that the monoatomic lattice chain is a coupling interaction system, thus a solution of Schrödinger equation becomes complicated. To decouple the atomic interaction, phonon coordinate is introduced based on a Fourier transformation of the atomic coordinate [110]:

$$Q_k = N^{-1/2} \sum_s x_s \exp\left(-iksa\right). \tag{9}$$

In this way, Eq. (8) turns into a summation of independent harmonic oscillators:

$$H = \sum_k \left[\frac{1}{2} m \dot{Q}_k \dot{Q}_{-k} + \frac{1}{2} m \omega_k^2 Q_k Q_{-k} \right], \tag{10}$$

with the dispersion relation obtained:

$$\omega_k = 2\sqrt{\frac{\kappa}{m}} \left| \sin \frac{ka}{2} \right|. \tag{11}$$

Eq. (11) is identical to Eq. (4) got from the classical mechanics. Combination of Eq. (10) and Schrödinger equation leads to the kinematic equation for each harmonic oscillator [110]:

$$\ddot{Q}_k + \omega_k^2 Q_k = 0, \tag{12}$$

which gives the discrete energy eigenvalue [111]:

$$E_k = \left(n_k + \frac{1}{2} \right) \hbar\omega_k \quad (n_k = 0, 1, 2, \ldots). \tag{13}$$

The minimum energy quantum $\hbar\omega_k$ in Eq. (13), in analogy to the definition of photon, is termed as a phonon, being exactly the quantum mechanical picture. n_k is the energy level of the harmonic oscillator or average number of phonons in the mode (k, ω_k), and obeys the Bose–Einstein statistics. Moreover, a phonon can be treated as a quasi-particle possessing a quasi-momentum $p = h/\lambda = \hbar k$ based on the wave-particle duality in quantum mechanics.

2.2. Phonon kinetic theory

2.2.1. Phonon Boltzmann equation

Analogous to the transport equation proposed by Boltzmann [6,112] for rarefied gas transport, the phonon Boltzmann equation is in prior introduced to phonon transport by Peierls [16]:

$$\frac{\partial f}{\partial t} + \mathbf{v}_g \cdot \nabla f = C\left(f\right), \tag{14}$$

where the phonon distribution function is $f \equiv f(\mathbf{x}, t, \mathbf{k})$, with $f(\mathbf{x}, t, \mathbf{k})\mathrm{d}\mathbf{x}\mathrm{d}\mathbf{k}$ denoting the number of phonons around spatial interval $(\mathbf{x}, \mathbf{x} + d\mathbf{x})$ and wave vector interval $(\mathbf{k}, \mathbf{k} + \mathrm{d}\mathbf{k})$ at certain time t. $\mathbf{k}$ is the wave vector as an extension of wave number k, related to phonon quasi-momentum (crystal momentum) through $\mathbf{p} = \hbar\mathbf{k}$. $\mathbf{v}_g$ is the phonon group velocity, and can be computed from:

$$\mathbf{v}_g = \nabla_{\mathbf{k}} \omega \tag{15}$$

as an extension of Eq. (7). $C(f)$ is the phonon collision term evaluating the effect of phonon scattering processes. Thus phonon Boltzmann equation describes a balance between variation, advection and scattering processes of phonons, adopting the same form of classical balance laws in transport processes [8].

2.2.2. Phonon scattering

Understanding phonon scatterings is crucial to specify the collision term $C(f)$ in Eq. (14). They are usually grouped into two categories [16,109,113]: normal (N) process and resistive (R) process. R process mainly includes three-phonon Umklapp (U) process, phonon-imperfection and phonon-boundary scatterings. In terms of their conservation properties, the number of phonons is not conserved as they can be created or annihilated, such as in three-phonon scattering where two phonons

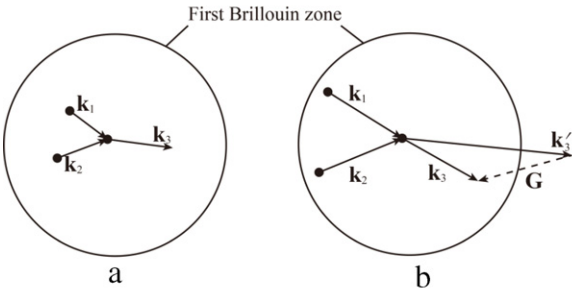

Fig. 3. Three-phonon N process (a) and U process (b) [38].

Table 1
Classification and properties of phonon scatterings.

	Phonon scattering	Momentum	Energy	Effect
N process	Normal process	Conserved	Conserved	Indirect resistance
	Umklapp process	Not conserved	Conserved	Direct resistance
R process	Imperfection scattering	Not conserved	Conserved	Direct resistance
	Boundary scattering	Not conserved	Conserved	Direct resistance

combine into one or one divides into two; N process conserves phonon quasi-momentum while R process does not; the energy of phonons is always conserved in any kind of scattering processes. These features are much different from the conventional conservation laws of molecular number, momentum and energy assumed in rarefied gas transport, in that phonon is a virtual particle whereas molecule is a real particle.

Three-phonon N process and U process make up the main scattering mechanisms in dielectric solid, as shown in Fig. 3. Mathematically they result from additional perturbative third-order terms besides the harmonic terms in Eqs. (1) and (8), and physically they originate in the non-harmonic lattice interaction. The energy and momentum balance equations for them are respectively:

$$\hbar\omega_1 + \hbar\omega_2 = \hbar\omega_3, \tag{16}$$

$$\hbar\mathbf{k}_1 + \hbar\mathbf{k}_2 = \hbar\mathbf{k}_3 + \mathbf{G}, \tag{17}$$

where $\mathbf{G}$ is the reciprocal lattice vector, and $\mathbf{G} = 0$ corresponds to N process whereas $\mathbf{G} \neq 0$ corresponds to U process.

In terms of the effect of N and R processes, both of them will introduce thermal resistance to phonon heat transport, resulting in finite lattice thermal conductivity. R process causes a direct thermal resistance by destroying the phonon quasi-momentum, while N process causes an indirect one by redistributing the phonon frequency spectrum. The effect of N process is often neglected and not satisfactorily treated in modeling lattice thermal conductivity [114]. Merely recently in first-principle method [115] or phenomenological models [116,117] is there a little attention paid on it. Appropriate treatment of R process and N process will be further discussed below.

The portion of different kinds of phonon scatterings varies with the temperature in dielectric solid. At extremely low temperature, the lattice vibrations are in low energy level and small quantities of phonons are produced, which result in scarce scattering rate and long mean free path. Therefore, phonon-boundary interaction becomes the dominant scattering in this regime. With the temperature elevating, both the phonon quantity and three-phonon scattering rate increases. In this regime, N process dominates over R process because the lattice energy level is still low to make the combination of two phonons go beyond the first Brillouin zone, as is shown in Fig. 3(a). When the temperature elevates further to a higher value, the combination of two phonons easily goes outside the first Brillouin zone, as is shown in Fig. 3(b), which fosters the dominance of R process over N process in this regime. Finally, the classification and properties of different kinds of phonon scatterings are summarized in Table 1.

2.2.3. *Callaway's relaxation approximation*

The full collision term in phonon Boltzmann equation is difficult to tackle because of the complex nature of phonon scatterings [16,17], similar to the molecular collision term in Boltzmann equation for rarefied gas [108]. Therefore, inspired by the linear BGK relaxation approximation [74] to molecular collision term, Callaway proposed the dual relaxation approximation to the phonon collision term [113]:

$$C(f) = -\frac{f - f_{\mathrm{R}}^{\mathrm{eq}}}{\tau_{\mathrm{R}}} - \frac{f - f_{\mathrm{N}}^{\mathrm{eq}}}{\tau_{\mathrm{N}}}. \tag{18}$$

In Eq. (18), τ_{R}, τ_{N} are the relaxation times for R and N processes respectively, and the equilibrium distribution functions for R and N processes are respectively the Planck distribution [113] (i.e. Bose–Einstein distribution [38]):

$$f_{\mathrm{R}}^{\mathrm{eq}} = \frac{1}{\exp\left(\hbar\omega/k_{\mathrm{B}}T\right) - 1} \tag{19}$$

Table 2
Relaxation time expressions of N and R processes.

Work	τ_N^{-1}	τ_U^{-1}	τ_i^{-1}	τ_b^{-1}
Callaway [113]	$B_1\omega^2T^3$	$B_2\omega^2T^3$	$A\omega^4$	v_g/L
Holland [118]	$B_{1,L}\omega^2T^3$ $B_{1,T}\omega T^4$	$B_{2,i}\omega^2/\sinh(\hbar\omega/k_BT)$ $(i=L,T)$	$A\omega^4$	v_g/FL
Morelli et al. [123]	$B_{1,i}\omega^2T\exp\left(-\theta_{D,i}/3T\right)\ (i=L,T)$	$B_{2,L}\omega^2T^3\ B_{2,T}\omega T^4$	$A_i\omega^4\ (i=L,T)$	$v_{g,\,i}/L_{eff}\ (i=L,T)$
Mingo [76,119]	Neglected	$B\omega^2T\exp(-C/T)$	$A\omega^4$	v_g/FL
Chantrenne et al. [120]	Neglected	$B_L\omega^2T^{1.5}\ B_T\omega T^4$	$A\omega^4$	v_g/FL
Ward and Broido [124]	$B_1\omega^2T[1-\exp(-3T/\theta_D)]$	$B_2\omega^4T[1-\exp(-3T/\theta_D)]$	–	–
Maldovan [122]	Neglected	$B_i\omega^2T\exp(-C/T)\ (i=L,T)$	$A\omega^4$	–

Notes: a The subscripts i, b denote imperfection and boundary respectively; b The subscripts L, T denote longitudinal and transverse respectively; c F denotes the geometrical factor, with L the geometrical characteristic dimension; d A, B, C are empirical coefficients obtained through fitting the experimental data; e θ_D denotes the Debye temperature; f In Ref. [122], the phonon-boundary scattering is incorporated through a reduced mean free path rather than the relaxation time; g In Ref [124], only the normal process and Umklapp process are studied.

and the displaced Planck distribution [38,113]:

$$f_N^{eq} = \frac{1}{\exp\left[\left(\hbar\omega - \hbar\mathbf{k}\cdot\mathbf{u}\right)/k_BT\right] - 1}, \tag{20}$$

with k_B denoting the Boltzmann constant, T the thermodynamic temperature, $\hbar \equiv h/2\pi$ the reduced Planck constant, and $\mathbf{u}$ the drift velocity of phonons. The drift velocity $\mathbf{u}$ is distinct from the group velocity $\mathbf{v}_g$ and is a space- and time-dependent macroscopic velocity related intimately to heat flux, as to be shown below. As is pointed out in Refs. [116,117], a crucial difference between the R and N processes is that in the former ones the phonons exchange momentum in such a way that each mode tends towards a true (Planck) equilibrium distribution whereas the latter ones result in collective effects leading to displaced Planck distribution.

The relaxation times for N and R processes usually depend on phonon frequency and crystal temperature as $\tau_R(\omega, T)$, $\tau_N(\omega, T)$. However, unified mathematical expressions are still lacking for them to date [114]. Previous work [76,113,118–122] have to adjust empirical coefficients in their relaxation time expressions to fit the experimental data of bulk lattice thermal conductivity. Nevertheless, Callaway's approximation much simplified the collision term and non-doubtfully acts as a milestone in the development of phonon heat transport models. For convenience to future explorations, most of the achieved expressions of relaxation times for N and R processes are summarized in Table 2. It is seen that the main difference of relaxation time expressions lies in the N process and Umklapp process, while those of imperfection and boundary scatterings have nearly consistent forms.

2.3. *Phonon hydrodynamics*

In classical transport theory, hydrodynamics represents the macroscopic level of description for fluid systems [125]. Similarly, phonon hydrodynamics denotes the same level of descriptions for phonon systems. In this section, firstly a brief introduction is given to the description of fluid systems at different levels. Then a consistent conceptual framework is established for phonon systems, and the role of phonon hydrodynamics in phonon transport theory is thus highlighted.

2.3.1. *Description of fluid systems at different levels*

A fluid system could be described at three different levels, to different extent of details with different amount of information [125]. At the microscopic dynamic level, the kinematic details (velocities and positions) of all the particles are known; and at the mesoscopic kinetic level, only the distribution function of a single representative particle is given; while at macroscopic hydrodynamic level, several average variables of many particles such as the mass density and velocity (moments of the single-particle distribution function) are specified. In terms of the dimension of temporal and spatial scales, the dynamic level usually corresponds to the period of particle vibration and force distance between particles, the kinetic level corresponding to the collision relaxation time and mean free path, whereas the macroscopic level corresponds to the flow time and characteristic length of fluid system [126].

Different levels of descriptions for fluid systems need different governing equations. At the dynamic level, all the particles are described by Newton's equation (or Hamiltonian equation) in classical mechanics [127], or by Liouville equation in statistical mechanics [128]; at the kinetic level, Boltzmann transport equation is the evolution equation for the single-particle distribution function; at the hydrodynamic level, the fluid behavior is often determined by the Navier–Stokes equations. The governing equations at different levels are correlated intimately: Boltzmann transport equation could be derived through the BBGKY hierarchy [126] from Liouville equation, while Navier–Stokes equations could be derived through a Chapman–Enskog solution [108] to Boltzmann transport equation. This intimate mathematical connection originates in the physical correlation between them: the macroscopic behavior of fluids is shown based on the mesoscopic statistics of fluid particle mixture, which are ultimately determined by the microscopic dynamics of fluid particles. The relationship between different levels of descriptions of fluid flow system is summarized in Fig. 4(a).

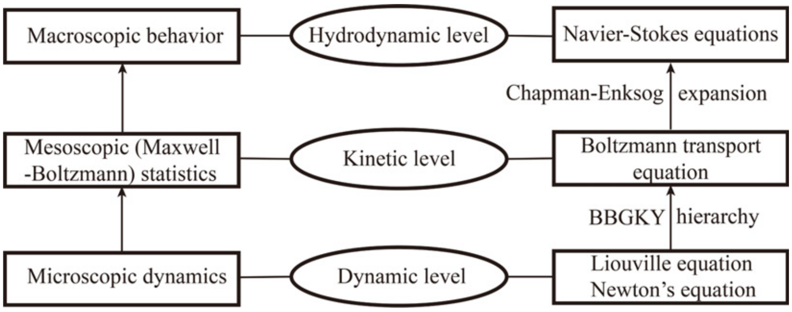

(a) For fluid flow system.

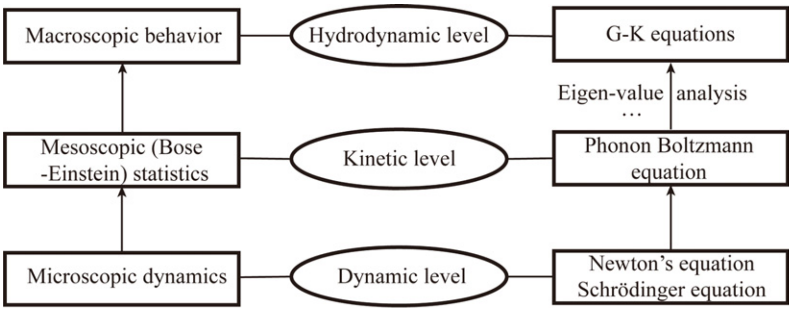

(b) For phonon transport system.

Fig. 4. Hierarchical descriptions for (a) fluid flow and (b) phonon transport systems at different levels.

2.3.2. Hydrodynamic description of phonon systems

The study on phonon hydrodynamics began in the exploration of heat waves [88,129,130] (second sound). Landau [131] and Tisza [132] independently predicted the existence of wavelike propagation of thermal energy (termed as second sound first by Landau [131] in contrast to pressure wave as the first sound) in liquid Helium II based on their two-fluid superfluidity theory [133]. Later, Lifshitz [134] suggested a method for exploring second sound, which was first detected in experiments by Peshkov [135]. These work in liquid Helium motivated the seeking of heat waves in dielectric solid [136,137], because of the same elementary excitations (i.e. phonons) [133]. The early attempt [138] to detect the second sound in quartz and sapphire crystal failed, due to insufficient purity and large anisotropy of crystalline sample [138] on one hand, and ambiguous theoretical foundation [109,139] on the other hand. The first experimental observation of second sound in solid helium [140] was not achieved before the systematical theoretical investigations by the group of Krumhansl [61,81,141, 142]. Their work [61,81] derived the Guyer–Krumhansl (G–K) equation and gave a window condition for the occurrence of second sound, through a solution of linearized phonon Boltzmann equation by Eigen-value analysis method. Based on their results, it is merely feasible to detect the second sound in the hydrodynamic region or phonon Poiseuille flow [143] region, where N process dominates over R process.

The G–K equation is a macroscopic heat transport equation, playing the same role as Navier–Stokes equation in hydrodynamics, and corresponds to the hydrodynamic description of phonon systems. It can be derived from phonon Boltzmann equation at mesoscopic kinetic level based on many different methods as will be summarized in the following section. Section 2.1 actually corresponds to the microscopic description of phonons. The relationship between different levels of descriptions for phonon transport system is summarized in Fig. 4(b).

Finally it is possible to give an intuitive physical picture of the hydrodynamic behavior of phonon systems. As is shown in Section 2.2, phonon quasi-momentum does not destroy in N process. When N process is dominant over R process and its mean free path is much smaller than the dimension of crystalline sample, the momentum conservation is ensured during scattering events just as in gas transport. Thus the local equilibrium can be reached in each small element of the crystalline sample [144], and the macroscopic behavior of phonons resembles that of the classical viscous fluid.

3. Classical phonon hydrodynamics

The field of phonon hydrodynamics was gradually established since the fundamental work by Guyer and Krumhansl [61,81]. Hereafter, further theoretical advances [82,145,146] are achieved by the Eigen-value analysis method applied in Refs. [61,81], with also credible applications in modeling lattice thermal conductivity [147,148]. Other approaches were also proposed such as the approximate method [149], microscopic dynamics method [150] and Green function method [151], and were summarized thoroughly in a review article [152]. In recent years, motivated by the extensive models [108,153–155] for gas transport, several new methods are developed to obtain phonon hydrodynamic models, including the maximum entropy moment method [156,157], Grad's type moment method [84] and Chapman–Enskog method [86,158]. In this section, a brief overview is firstly given to the three classical methods: Eigen-value analysis method, Chapman–Enskog method and moment method. Then a unified kinetic framework is established through a solution to phonon Boltzmann equation with Callaway's relaxation approximation by Chapman–Enskog method. It will be shown that most of previous phonon hydrodynamic models can be included in the present framework as special cases.

3.1. *Diverse branches and methods*

3.1.1. *Eigen-value analysis method*

The Eigen-value analysis method was initially suggested by Peierls [15] and later developed in Ref. [159] to solve the phonon Boltzmann equation in the presence of sole N process. It was first applied to investigate the phonon hydrodynamic behaviors in Refs. [61,81]. In the frame of this method, (14) is cast into an instructive form [61,81,82]:

$$\mathbf{D}^{*}f=\left(\mathbf{R}^{*}+\mathbf{N}^{*}\right)f, \tag{21}$$

with $\mathbf{D}^*$ the drift operator containing transient and advection terms, $\mathbf{R}^*$ and $\mathbf{N}^*$ being the collision operators for R and N processes respectively. In extremely low temperature case where $\mathbf{R}^* \ll \mathbf{N}^*$, the solution of Eq. (21) is obtained in terms of the eigenvectors of $\mathbf{N}^*$ operator. The eigenvectors are grouped into two categories: those having zero eigenvalue and those having nonzero one. The former make up the null space of $\mathbf{N}^*$ operator, where there are merely four eigenvectors: $|\eta_0\rangle$, $|\eta_{1x}\rangle$, $|\eta_{2x}\rangle$ and $|\eta_{3x}\rangle$, which are related intimately to the phonon energy density (E) and the components (q_x, q_y, q_z) of heat flux vector respectively. Thus the solution is expressed as a linear combination of the eigenvectors of $\mathbf{N}^*$ operator:

$$f=\sum_{m}a_{m}\left(\mathbf{x},t\right)\left|\eta_{m}\right\rangle. \tag{22}$$

Substituting Eq. (22) into Eq. (21), they finally got the energy balance equation and the G–K equation [61]:

$$\tau_{\mathrm{R}}\frac{\partial\mathbf{q}}{\partial t}+\mathbf{q}+\lambda\nabla T=\frac{1}{5}v_{\mathrm{g}}^{2}\tau_{\mathrm{N}}\tau_{\mathrm{R}}\left[\nabla^{2}\mathbf{q}+2\nabla\left(\nabla\cdot\mathbf{q}\right)\right], \tag{23}$$

with λ the bulk thermal conductivity, and a coefficient '2' before the gradient of divergence of heat flux, slightly distinct from '1/3' got in Ref. [82] by the same method. Note that Eq. (23) has a similar form to Navier–Stokes equation [133]:

$$\rho\left[\frac{\partial\mathbf{v}}{\partial t}+\left(\mathbf{v}\cdot\nabla\right)\mathbf{v}\right]=-\nabla p+\mu\nabla^{2}\mathbf{v}+\left(\varsigma+\frac{1}{3}\mu\right)\nabla\left(\nabla\cdot\mathbf{v}\right), \tag{24}$$

where ρ, $\mathbf{v}$ and p are the mass density, mass velocity and pressure of fluid, respectively, μ and ς are the shear and bulk viscosity, respectively. This similarity lays a mathematical foundation for the phonon hydrodynamics model, although some tiny differences still exist because of the heat flux term in Eq. (23) while lacking in Eq. (24), and the advection term in Eq. (24) while lacking in Eq. (23). The difference is attributed to some difference between phonons and fluids, as will be explained based on the kinetic framework developed below. Note that a more general equation analogous to Eq. (23), but with different interpretation of the several coefficients, may be found in turbulent superfluid helium [160–163]. We will not enter into this specialized topic, but anyway it is interesting to know about the possibility that the range of an equation of the form as (23) may be more general than for phonons in solids. In fact, an equation analogous to Eq. (23) has been derived from a more general setting by means of a non-equilibrium maximum entropy operator method, not only for phonons, but also for electrons, although the particular range of its application is different for both systems, and more restricted for electrons [164].

3.1.2. *Chapman–Enskog method*

Chapman–Enskog method for the solution of phonon Boltzmann equation includes two derivatives: (1) the continuous asymptotic expansion; (2) the discrete lattice Boltzmann scheme. The latter is taken into account because of two aspects: (1) the lattice Boltzmann equation can be derived from Boltzmann transport equation as a special discretized form [165–167]; (2) the hydrodynamic equations can be recovered from lattice Boltzmann equation by Chapman–Enskog method [155,168]. Thus it is possible to obtain the hydrodynamic description for phonons by the lattice Boltzmann scheme.

I. Continuous form: asymptotic expansion

Chapman–Enskog method was developed along Hilbert expansion [169]—the first perturbative approach to solve the Boltzmann equation, independently by Enskog [170] and Chapman [171] in dealing with rarefied gas transport. Early trace of the application of this method to phonon transport is the aforementioned approximate method [143,149], which assigned the solution by the displaced Planck distribution. The approximate method could be actually treated as a special case of zeroth-order Chapman–Enskog expansion. The closure and stability problems were then discussed by mathematicians for the moment equations of phonon Boltzmann equation in the line of Chapman–Enskog method [172–174]. Substantial progress is not made before the work by Banach and Larecki [86], where Chapman–Enskog expansion was conducted around the displaced Planck distribution and macroscopic heat transport equations were derived within different orders of approximations. Subsequently, they made a solution to the infinite system of moment equations of phonon Boltzmann equation [175] by the same method and analyzed the stability [175,176] of different orders of solutions. These works constitute a solid theoretical foundation for phonon hydrodynamics modeling. However, there is still a distance away from credible applications of the hydrodynamic heat transport equations obtained in Refs. [86,175,176].

II. Discrete form: lattice Boltzmann scheme

Shortly after the lattice Boltzmann scheme was proposed in Refs. [177,178], Guyer [158] applied it to simulate the phonon gas hydrodynamics. Merely N processes of transverse and longitudinal phonons were considered and the isotropic D2Q7 lattice without center-point component was applied, with 2 denoting the dimension and 7 denoting the number of directional components [158]. There are no advances until Jiaung and Ho [179] made a Chapman–Enskog expansion solution to phonon lattice Boltzmann equation under Callaway's relaxation approximation, and achieved a macroscopic heat transport equation similar to G–K equation. It is a milestone in the development of lattice Boltzmann modeling of phonon hydrodynamics, in that this work first bridged the mesoscopic numerical scheme and macroscopic phonon hydrodynamics. On the other hand, it takes into account both N process and R process thus being more credible than merely considering N process in Ref. [158]. Though, the conventional D2Q9 lattice is used, assuming a fictitious larger phonon speed in the diagonal direction than in the straight direction [179]. In the frame of the scheme proposed in Ref. [179], Lee et al. [180,181] devised a novel interfacial boundary collision rule for the simulation of multiphase phonon hydrodynamics to tackle the heat transport between dissimilar materials. In spite of these pioneering work, the lattice Boltzmann modeling is still in its fancy due to the following aspects: (1) dimensionless variables are taken in all of these simulations [158,179–181] with parameters still far away from realistic values of engineering materials; (2) a reasonable lattice structure is still lacking to accurately describe the microscopic dynamics of phonons; (3) treating the frequency spectral characteristic of phonons remains an open question.

There are several other reports [58,79,80,182–184] on lattice Boltzmann modeling of phonon transport in both bulk and nanostructured materials in the last several years. They are not introduced here because from a point of view of the classical phonon hydrodynamics where the N process dominates the phonon transport, their schemes of lattice Boltzmann model deal with only the R process, which is beyond the classical phonon hydrodynamics. Therefore a concept of generalized phonon hydrodynamics and the corresponding lattice Boltzmann implementation will be introduced and discussed in Section 5.

3.1.3. Moment method

Moment method is proposed by Grad [153] as an alternative approach to solve the Boltzmann equation in addition to Chapman–Enskog method. Its basic idea is to construct for high-order moments (the viscous stress and heat flux, etc.) balance equations involving the fluxes of them. To obtain closed expressions for these fluxes and thus a determined system of differential equations, the distribution function is expanded around the equilibrium distribution in Hermite polynomials truncated at a specific order. In the developments of phonon hydrodynamics models, there are mainly two derivatives of moment methods: Grad's type moment method as a kinetic approach, and maximum entropy moment method as a variational approach, as to be introduced respectively.

I. Grad's type moment method

In the spirit of Grad's idea, a modified moment method is proposed to derive the nine-moment phonon hydrodynamics through a closure procedure for the fluxes of high-order moments. The phonon distribution function is expanded around the Planck distribution in early work [185] and around the displaced Planck distribution in subsequent work [84]. The expansion around the displaced Planck distribution in subsequent work hold the advantage that the heat flux is incorporated into the heat transport model in a non-perturbative manner [84,86,175], which is thus still valid for a large value of heat flux in nonlinear problems. Though, to avoid mathematical intricacies without losing physical interpretation, both linear phonon dispersion relation and isotropic gray approximation are assumed in their derivations [84,185]. In a series of work [186] the one-dimensional rotationally symmetric reduction of the nine-moment phonon hydrodynamics was demonstrated to adopt a symmetric hyperbolic form. Symmetric hyperbolicity has at least three benefits for mathematical physicists [186,187]: (1) it guarantees finite propagating speed of disturbances; (2) it ensures well-posedness of Cauchy problems; (3) it allows for the propagation of wave fronts.

Although some fundamental theoretical works have been done, the moment phonon hydrodynamic model is still far away from actual applications. This situation was not remedied until recently the boundary conditions are derived for the macroscopic moment equations [188]. The derivation is based on a Grad's closure by expanding the phonon distribution function around Planck distribution. Three types of boundary conditions have been applied [188]: isotropic scattering, specular scattering and thermalization. The 4-, 9-, 16-, and 25-moment phonon hydrodynamics equations are solved for 1D steady-state heat transfer and 2D phonon Poiseuille flow, with the profiles of both temperature and heat flux distributions obtained. Nevertheless, comparison of theoretical predictions to experimental results is still lacking due to too many simplified assumptions.

Finally, an interesting aspect is noted that nine-moment phonon hydrodynamic model corresponds to the classical thirteen-moment model in hydrodynamics [153,154]. Both of them truncate the moment systems up to third order in the frame of Grad's method. However, the former lacks the zeroth-order moment due to the non-conservation of phonon number. On the other hand, under the linear gray approximations, the phonon momentum density is proportional to heat flux. Therefore another three moments are reduced in phonon hydrodynamics. This explain why at the same level only nine moments exist in phonon hydrodynamics whereas thirteen moments in classical hydrodynamics, and indicates some difference between kinetic theories of phonons and fluids.

II. Maximum-entropy moment method

Maximum entropy method [189] is another closure approach to the moment systems of phonon Boltzmann equation. Based on this method, four-moment [83,156] and nine-moment [85,109,185] phonon hydrodynamics were derived successively. Its basic tenet is to acquire the phonon distribution function by maximizing the phonon entropy density under the constraints of prescribed state variables (energy, quasi-momentum, momentum flux, etc.) with a Lagrange multiplier method [190]. Thus a closed set of balance equations are obtained for all the phonon state variables and Lagrange multipliers, and have been demonstrated [85,157] to admit symmetric hyperbolic form. The linear isotropic phonon dispersion relation is usually assumed in early work [83,85,156,157,185], as in Grad's type moment method. Only recently the influence of nonlinear dispersion is studied on the relation of phonon hydrodynamics to phenomenological theories with internal vector [191] and the propagating speed of weak discontinuity [192] in the frame of four-moment models.

Finally, note that moment phonon hydrodynamic model derived by maximum entropy method was demonstrated [83,109,185] to be consistent with that obtained by extended thermodynamics method, which was proposed [193,194] based on classical kinetic theory of gases.

3.2. A unified kinetic framework

In this subsection, phonon hydrodynamic models will be derived through solving the phonon Boltzmann equation under Callaway's relaxation approximation (18) with Chapman–Enskog method. Therefore a unified kinetic framework is established, which sums up most of previous models derived by different methods. The present derivation is based on the approach proposed in Ref. [86], however, with several differences:

(1) Dimensional variables are used, in contrast to non-dimensional ones in Ref. [86];
(2) Two temporal scales and one spatial scale as in classical hydrodynamics [155] are used, in contrast to infinite temporal and spatial scales in Ref. [86];
(3) Sub-order (sub-first-order and sub-second-order) approximations are also considered of the full zeroth- and first-order expansions in Ref. [86].

3.2.1. Assumptions

As in previous study on deriving the phonon hydrodynamic models, the following approximations are made [84,86,188]:

(1) Debye approximation: the linear phonon dispersion relation introduced by Debye [107]: $\omega = v_g k$ is adopted, with the phonon group velocity (15) reducing to:

$$\mathbf{v}_g = \frac{v_g}{k}\mathbf{k}. \tag{25}$$

(2) Isotropic approximation: the phonon properties in one crystalline direction are representative of that in the whole wave vector space, and thus three identical acoustic phonon branches are considered with the contribution from optical phonon branches neglected.
(3) Gray approximation: a representative phonon branch is considered with constant relaxation times τ_R, τ_N. Although τ_R, τ_N are usually dependent on phonon frequency and crystal temperature, we treat the simple gray case for mathematical simplicity without losing physical interpretation.

3.2.2. Macroscopic variables definitions

Phonon transport is described by several macroscopic state variables [16,109] at the hydrodynamic level. Based on the principles in statistical physics [125], they are obtained by integrating the product of phonon distribution function and corresponding microscopic variables: the energy density of phonons:

$$E = \int \hbar\omega f \frac{3\mathrm{d}\mathbf{k}}{(2\pi)^3}, \tag{26}$$

where 3 represents the number of acoustic phonon branches and 2π results from the elemental volume in the wave vector space, the momentum density of phonons:

$$\mathbf{P} = \int \hbar\mathbf{k} f \frac{3\mathrm{d}\mathbf{k}}{(2\pi)^3} \tag{27}$$

and the heat flux:

$$\mathbf{q} = \int \mathbf{v}_g \hbar\omega f \frac{3\mathrm{d}\mathbf{k}}{(2\pi)^3}. \tag{28}$$

Substitution of Eq. (25) into Eq. (28) gives rise to the relation between heat flux and phonon momentum density:

$$\mathbf{q} = v_g^2\mathbf{P}. \tag{29}$$

The flux of heat flux $\mathbf{Q}$ is defined based on the balance equation of heat flux as in extended thermodynamics [40,187]:

$$\mathbf{Q} = \int \mathbf{v}_g \mathbf{v}_g \hbar\omega f \frac{3d\mathbf{k}}{(2\pi)^3}. \tag{30}$$

It is a second-order symmetric tensor ($\mathbf{Q} = \mathbf{Q}^T$) which could be split into a trace part and a deviatoric (traceless) part as:

$$Q_{ij} = \frac{1}{3} v_g^2 E \delta_{ij} + \int v_{g,<i} v_{g,j>} \hbar\omega f \frac{3d\mathbf{k}}{(2\pi)^3}, \tag{31}$$

with δ_{ij} the unit tensor, and $\langle\rangle$ denoting the deviatoric part.

3.2.3. *Conservation laws and balance equations*

Both N and R processes ensure energy conservation, yielding the following relations under gray approximation:

$$\int \hbar\omega f \frac{3d\mathbf{k}}{(2\pi)^3} = \int \hbar\omega f_R^{eq} \frac{3d\mathbf{k}}{(2\pi)^3}, \qquad \int \hbar\omega f \frac{3d\mathbf{k}}{(2\pi)^3} = \int \hbar\omega f_N^{eq} \frac{3d\mathbf{k}}{(2\pi)^3}. \tag{32}$$

Merely N process ensures momentum conservation thus yielding:

$$\int \hbar\mathbf{k} f \frac{3d\mathbf{k}}{(2\pi)^3} = \int \hbar\mathbf{k} f_N^{eq} \frac{3d\mathbf{k}}{(2\pi)^3}. \tag{33}$$

The balance equations of phonon energy and momentum densities are obtained through an integration of the product of phonon Boltzmann equation and microscopic variables $\hbar\omega$ and $\hbar\mathbf{k}$ respectively:

$$\frac{\partial E}{\partial t} + \nabla \cdot \mathbf{q} = 0, \tag{34}$$

$$\frac{\partial \mathbf{P}}{\partial t} + \frac{1}{v_g^2} \nabla \cdot \mathbf{Q} = -\frac{\mathbf{P}}{\tau_R}. \tag{35}$$

Substitution of Eq. (29) into Eq. (35) gives rise to the balance equation for heat flux (heat transport equation):

$$\frac{\partial \mathbf{q}}{\partial t} + \nabla \cdot \mathbf{Q} = -\frac{\mathbf{q}}{\tau_R}, \tag{36a}$$

or rewritten as when combined with Eq. (31):

$$\frac{\partial \mathbf{q}}{\partial t} + \frac{1}{3} v_g^2 \nabla E + \nabla \cdot \mathbf{Q}_\circ = -\frac{\mathbf{q}}{\tau_R}. \tag{36b}$$

The deviatoric part of $\mathbf{Q}$ is denoted by $\mathbf{Q}_\circ$.

In order to obtain the heat transport equation as an explicit relation between heat flux and temperature (or energy density) gradient, we have to acquire the phonon distribution function in terms of phonon energy density and heat flux. Thus a solution of phonon Boltzmann equation is needed. An exact analytical one is difficult although many approximations have been made. Therefore, a multiscale asymptotic expansion is conducted for the phonon distribution function. Sub-order approximations to each order of expansions are considered to further simplify the solution in the following.

3.2.4. *Multiscale expansion*

Two temporal scales and one spatial scale are applied, with their relations to the normal temporal and spatial scales [155]:

$$\frac{\partial}{\partial t} = \varepsilon \frac{\partial}{\partial t_1} + \varepsilon^2 \frac{\partial}{\partial t_2}, \tag{37}$$

$$\frac{\partial}{\partial x_i} = \varepsilon \frac{\partial}{\partial x_{1i}}, \tag{38}$$

where t_1 and t_2, x_{1i} $(i = 1, 2, 3)$ are the multiscale temporal and spatial variables, and ε is a small parameter which will be explained below. The phonon distribution function is expanded asymptotically as:

$$f = f_0 + \varepsilon f_1 + \varepsilon^2 f_2 + \cdots, \tag{39}$$

with f_0, f_1 and f_2 denoting the zeroth-, first- and second-order approximate components respectively.

The small parameter ε usually denotes *Kn* number (the ratio of mean free path to the characteristic size of fluid system) in classical hydrodynamics [154,155]. Navier–Stokes equation is thus derived through a solution of the Boltzmann equation by Chapman–Enskog expansion up to first order in *Kn*. In contrast, the small parameter here will not be the same because the definitions of mean free path and *Kn* become ambiguous due to two categories of phonon scatterings. Therefore, as in previous work, the small parameter is assumed as the ratio of the relaxation time of N process to that of R process [86,175]:

$$\varepsilon = \frac{\tau_N}{\tau_R}. \tag{40}$$

In this way, we consider the situation where the relaxation time of N process is much smaller than that of R process. Small relaxation time means frequent scatterings whereas large one denotes scarce scatterings. This is reasonable because N process dominates over R process in classical phonon hydrodynamics.

Substituting Eqs. (37)–(39) into Eq. (14), and combining the terms in each order of the small parameter ε, we achieve the approximate components of phonon distribution function respectively:

$$f_0 = f_N^{eq}, \tag{41}$$

$$f_1 = f_R^{eq} - f_N^{eq} - \tau_N \left(\frac{\partial f_0}{\partial t_1} + v_{gi} \frac{\partial f_0}{\partial x_{1i}} \right), \tag{42}$$

$$f_2 = f_N^{eq} - f_R^{eq} + \tau_N \left(\frac{\partial f_0}{\partial t_1} - \frac{\partial f_0}{\partial t_2} - \frac{\partial f_1}{\partial t_1} + v_{gi} \frac{\partial f_0}{\partial x_{1i}} - v_{gi} \frac{\partial f_1}{\partial x_{1i}} \right). \tag{43}$$

Note that in previous work [86,175], it was assumed in prior to expand the phonon distribution function around displaced Planck distribution, which in contrast is obtained naturally in Eq. (41) in the present framework.

Substituting Eq. (39) into the kinetic definitions Eqs. (26)–(30), we can expand the macroscopic variables in several approximate components similarly:

$$E = E_0 + \varepsilon E_1 + \varepsilon^2 E_2 + \cdots, \quad \text{with } E_n = \int \hbar\omega f_n \frac{3d\mathbf{k}}{(2\pi)^3}, \tag{44a}$$

$$\mathbf{P} = \mathbf{P}_0 + \varepsilon \mathbf{P}_1 + \varepsilon^2 \mathbf{P}_2 + \cdots, \quad \text{with } \mathbf{P}_n = \int \hbar\mathbf{k} f_n \frac{3d\mathbf{k}}{(2\pi)^3}, \tag{45a}$$

$$\mathbf{q} = \mathbf{q}_0 + \varepsilon \mathbf{q}_1 + \varepsilon^2 \mathbf{q}_2 + \cdots, \quad \text{with } \mathbf{q}_n = \int \mathbf{v}_g \hbar\omega f_n \frac{3d\mathbf{k}}{(2\pi)^3}, \tag{46a}$$

$$\mathbf{Q} = \mathbf{Q}_0 + \varepsilon \mathbf{Q}_1 + \varepsilon^2 \mathbf{Q}_2 + \cdots, \quad \text{with } \mathbf{Q}_n = \int \mathbf{v}_g \mathbf{v}_g \hbar\omega f_n \frac{3d\mathbf{k}}{(2\pi)^3}. \tag{47}$$

Combined with the conservation relations Eqs. (32), (33), (44a) and (45a) reduce to:

$$E = E_0 = \int \hbar\omega f_N^{eq} \frac{3d\mathbf{k}}{(2\pi)^3}, \qquad E_n = \int \hbar\omega f_n \frac{3d\mathbf{k}}{(2\pi)^3} = 0, \quad \text{for } n \geq 1, \tag{44b}$$

$$\mathbf{P} = \mathbf{P}_0 = \int \hbar\mathbf{k} f_N^{eq} \frac{3d\mathbf{k}}{(2\pi)^3}, \qquad \mathbf{P}_n = \int \hbar\mathbf{k} f_n \frac{3d\mathbf{k}}{(2\pi)^3} = 0, \quad \text{for } n \geq 1. \tag{45b}$$

Taking into account the relation between heat flux and phonon momentum density in Eq. (29), we get from Eq. (45b):

$$\mathbf{q} = \mathbf{q}_0 = \int \mathbf{v}_g \hbar\omega f_N^{eq} \frac{3d\mathbf{k}}{(2\pi)^3}, \qquad \mathbf{q}_n = \int \mathbf{v}_g \hbar\omega f_n \frac{3d\mathbf{k}}{(2\pi)^3} = \mathbf{0}, \quad \text{for } n \geq 1. \tag{46b}$$

Only the zeroth-order approximate component of phonon distribution function contributes to the phonon energy density, momentum density and heat flux, while the higher-order approximate components contribute solely to the flux of heat flux.

Finally, substitution of Eqs. (43)–(47) into the energy and momentum balance equations (34) and (36) gives rise to the following equations at different order of approximations:

$$\frac{\partial E}{\partial t_1} + \frac{\partial}{\partial x_{1i}} q_i = 0, \tag{48a}$$

$$\frac{\partial E}{\partial t_2} = 0, \tag{48b}$$

$$\frac{\partial q_i}{\partial t_1} + \frac{\partial}{\partial x_{1j}} Q_{0ji} = -\frac{1}{\tau_N} q_i, \tag{49a}$$

$$\frac{\partial q_i}{\partial t_2} + \frac{\partial}{\partial x_{1j}} Q_{1ji} = 0. \tag{49b}$$

3.2.5. Zeroth-order expansion solution

The zeroth-order approximate component f_0 is taken into account in this part, and the zeroth-order expansion solution will be obtained. The kinetic expression of the flux of heat flux becomes:

$$\mathbf{Q} = \mathbf{Q}_0 = \int \mathbf{v}_g \mathbf{v}_g \hbar\omega f_0 \frac{3d\mathbf{k}}{(2\pi)^3}. \tag{50}$$

Therefore all the macroscopic variables become dependent merely on f_0. We will achieve the explicit forms of them and the heat transport equation by substituting Eq. (41) into the kinetic definitions of them. However, the drift velocity in displaced Planck distribution Eq. (20) makes the integration in Eqs. (44b)–(46b) and Eq. (50) difficult. Thus in this part, we firstly consider the approximations of Eq. (20) up to first and second order respectively, globally corresponding to sub-first-order and sub-second-order approximations of zeroth-order expansion, and finally the full zeroth-order expansion.

I. Sub-first-order approximation

If the drift velocity term is assumed to be small, then a Taylor expansion of Eq. (20) around Planck distribution Eq. (19) up to first order becomes:

$$f_{\mathrm{N}}^{\mathrm{eq}} \approx f_{\mathrm{R}}^{\mathrm{eq}} + f_{\mathrm{N1}}^{\mathrm{eq}}, \tag{51}$$

with the sub-first-order term $f_{\mathrm{N1}}^{\mathrm{eq}} = f_{\mathrm{R}}^{\mathrm{eq}}\left(1+f_{\mathrm{R}}^{\mathrm{eq}}\right)\hbar\mathbf{k}\cdot\mathbf{u}/k_{\mathrm{B}}T$. This expansion is valid at $|-\hbar\mathbf{k}\cdot\mathbf{u}/k_{\mathrm{B}}T| \gg \hbar\omega/k_{\mathrm{B}}T$, inferring "$u \gg v_g$" when combined with the linear dispersion relation. Substituting Eq. (51) into Eqs. (44b), (46b) and (50) respectively and conducting integrations in the whole wave vector space (the details of computation are shown in Appendix A), we achieve the expressions of the phonon energy density:

$$E = \frac{4\pi^5 (k_{\mathrm{B}}T)^4}{5\left(hv_{\mathrm{g}}\right)^3}, \tag{52}$$

the heat flux:

$$\mathbf{q} = \frac{16\pi^5 (k_{\mathrm{B}}T)^4}{15\left(hv_{\mathrm{g}}\right)^3}\mathbf{u} = \frac{4}{3}E\mathbf{u}, \tag{53}$$

and the flux of heat flux:

$$\mathbf{Q} = \frac{1}{3}v_{\mathrm{g}}^2 E\mathbf{I}. \tag{54}$$

The limit of integration extends from the first Brillouin zone to the whole wave vector space $(-\infty, +\infty)$ which makes the integration much simpler. This simplification is appropriate because heat transport in low temperature dielectric crystals is contributed dominantly by phonons at low energy levels with short wave vectors [83,156]. Eq. (52) shows that phonon energy density is proportional to the quartic power of the temperature, which is quantitatively consistent with previous results obtained by Grad's type moment method [84,186,188], maximum entropy moment method [83,109,156] and Chapman–Enskog method [86,175].

Substitution of Eqs. (52) and (54) into Eqs. (34) and (36) gives rise to the energy balance equation and heat transport equation respectively:

$$C_V\frac{\partial T}{\partial t} + \nabla\cdot\mathbf{q} = 0, \tag{55}$$

$$\tau_{\mathrm{R}}\frac{\partial \mathbf{q}}{\partial t} + \mathbf{q} = -\lambda\nabla T, \tag{56}$$

with the thermal conductivity $\lambda = C_V\tau_{\mathrm{R}}v_{\mathrm{g}}^2/3$ and the heat capacity per unit volume (got from $\mathrm{d}E = C_V\mathrm{d}T$) $C_V = 16\pi^5k_{\mathrm{B}}^4T^3/5\left(hv_{\mathrm{g}}\right)^3$. Eq. (56) is exactly the Cattaneo–Vernotte (C–V) equation [89,195] which adds the thermo inertia effect [40,88,187] into the classical Fourier's law. They are also consistent with the four-field equations obtained in moment phonon hydrodynamics [109,188]. In a word, the celebrated C–V model is achieved through the sub-first-order approximation of zeroth-order expansion solution. Finally note that heat flux is related intimately to drift velocity of phonons in Eq. (53), inferring that the drift velocity is proportional to heat flux as $\mathbf{u} = \frac{3}{4}\frac{\mathbf{q}}{E}$.

II. Sub-second-order approximation

If the Taylor expansion of Eq. (20) around Planck distribution is truncated at second order, we get $f_{\mathrm{N}}^{\mathrm{eq}} = f_{\mathrm{R}}^{\mathrm{eq}} + f_{\mathrm{N1}}^{\mathrm{eq}} + f_{\mathrm{N2}}^{\mathrm{eq}}$, with the sub-second-order term:

$$f_{\mathrm{N2}}^{\mathrm{eq}} = \frac{1}{2}\left(\frac{\hbar\mathbf{k}\cdot\mathbf{u}}{k_{\mathrm{B}}T}\right)^2\exp\left(\frac{\hbar\omega}{k_{\mathrm{B}}T}\right)\left[\exp\left(\frac{\hbar\omega}{k_{\mathrm{B}}T}\right)+1\right]\bigg/\left[\exp\left(\frac{\hbar\omega}{k_{\mathrm{B}}T}\right)-1\right]^3. \tag{57}$$

Through similar procedures as in sub-first-order approximation, we achieve the expressions of the phonon energy density:

$$E = \frac{4\pi^5 (k_{\mathrm{B}}T)^4}{5\left(hv_{\mathrm{g}}\right)^3}\left(1+\frac{10}{3}\chi^2\right), \tag{58}$$

with the ratio of phonon drift speed to group speed $\chi \equiv u/v_{\mathrm{g}}$, the heat flux same as Eq. (53) since Eq. (57) contributes nothing to heat flux:

$$\mathbf{q} = \frac{16\pi^5 \left(k_{\mathrm{B}}T\right)^4}{15\left(hv_{\mathrm{g}}\right)^3}\mathbf{u}, \tag{59}$$

and the flux of heat flux:

$$\mathbf{Q} = \frac{4\pi^5 \left(k_{\mathrm{B}}T\right)^4}{15\left(hv_{\mathrm{g}}\right)^3} v_{\mathrm{g}}^2\mathbf{I} + \frac{8\pi^5 \left(k_{\mathrm{B}}T\right)^4}{15\left(hv_{\mathrm{g}}\right)^3} u^2\mathbf{I} + \frac{16\pi^5 \left(k_{\mathrm{B}}T\right)^4}{15\left(hv_{\mathrm{g}}\right)^3}\mathbf{uu}. \tag{60}$$

The flux of heat flux is reformulated in terms of phonon energy density and heat flux by combining (58)–(60):

$$\mathbf{Q} = \frac{1}{3}v_{\mathrm{g}}^2 E\mathbf{I} + \frac{3v_{\mathrm{g}}}{2v_{\mathrm{g}}E + \sqrt{4v_{\mathrm{g}}^2E^2 - 30q^2}}\left\langle \mathbf{qq}\right\rangle. \tag{61}$$

Substituting Eq. (61) into Eq. (36), we acquire the heat transport equation:

$$\frac{\partial \mathbf{q}}{\partial t} + \frac{1}{3}v_{\mathrm{g}}^2\nabla E + \nabla\cdot\frac{3v_{\mathrm{g}}\left\langle \mathbf{qq}\right\rangle}{2v_{\mathrm{g}}E + \sqrt{4v_{\mathrm{g}}^2E^2 - 30q^2}} = -\frac{\mathbf{q}}{\tau_{\mathrm{R}}}. \tag{62}$$

Previous work [100] tried to derive the heat transport equation in thermon gas model from phonon Boltzmann equation with Callaway's relaxation approximation. It approximated the phonon distribution function by displaced Planck distribution within second-order Taylor expansion, and is exactly equivalent to the sub-second-order approximation of zeroth-order expansion in the present work. The heat flux expression Eqs. (53) or (59) achieved here is consistent with that obtained in Ref. [100].

III. Full zeroth-order expansion

Finally, the full zeroth-order expansion is considered without any approximations to the displaced Planck distribution. Through similar procedures in sub-first-order and sub-second-order approximations, we achieve the expressions of phonon energy density, heat flux and the flux of heat flux respectively (the details of computation are shown in Appendix B):

$$E = \frac{4\pi^5 \left(k_{\mathrm{B}}T\right)^4}{15\left(hv_{\mathrm{g}}\right)^3}\frac{\chi^2 + 3}{\left(1-\chi^2\right)^3}, \tag{63}$$

$$\mathbf{q} = \frac{16\pi^5 \left(k_{\mathrm{B}}T\right)^4}{15\left(hv_{\mathrm{g}}\right)^3}\frac{1}{\left(1-\chi^2\right)^3}\mathbf{u}, \tag{64}$$

$$\mathbf{Q} = v_{\mathrm{g}}^2\frac{4\pi^5 \left(k_{\mathrm{B}}T\right)^4}{15\left(hv_{\mathrm{g}}\right)^3}\frac{1}{\left(1-\chi^2\right)^2}\mathbf{I} + \frac{16\pi^5 \left(k_{\mathrm{B}}T\right)^4}{15\left(hv_{\mathrm{g}}\right)^3}\frac{1}{\left(1-\chi^2\right)^3}\mathbf{uu}. \tag{65}$$

Eqs. (63)–(65) in one-dimensional forms are consistent with the corresponding expressions obtained in four-moment nonlinear phonon hydrodynamics [149]. It considered a one-dimensional steady-state heat conduction through a cylindrical dielectric solid, with the phonon distribution function approximated by displaced Planck distribution [149].

Combination of Eqs. (63)–(65) gives rise to the expressions of drift velocity and the flux of heat flux respectively in terms of phonon energy density and heat flux:

$$\mathbf{u} = \frac{3v_{\mathrm{g}}\mathbf{q}}{2v_{\mathrm{g}}E + \sqrt{4v_{\mathrm{g}}^2E^2 - 3q^2}}, \tag{66}$$

$$\mathbf{Q} = \frac{1}{3}v_{\mathrm{g}}^2 E\mathbf{I} + \frac{3v_{\mathrm{g}}\left\langle \mathbf{qq}\right\rangle}{2v_{\mathrm{g}}E + \sqrt{4v_{\mathrm{g}}^2E^2 - 3q^2}}. \tag{67}$$

For a small heat flux, Eq. (66) reduces to a linear dependence of drift velocity on heat flux obtained in sub-first-order approximation. Thus it is a generalized relation between **u** and **q** in the region far from equilibrium state, and is consistent with the result of three-dimensional case in Refs. [86,175]. Substituting Eq. (67) into Eq. (36a), we acquire the heat transport equation:

$$\frac{\partial \mathbf{q}}{\partial t} + \frac{1}{3}v_{\mathrm{g}}^2\nabla E + \nabla\cdot\frac{3v_{\mathrm{g}}\left\langle \mathbf{qq}\right\rangle}{2v_{\mathrm{g}}E + \sqrt{4v_{\mathrm{g}}^2E^2 - 3q^2}} = -\frac{\mathbf{q}}{\tau_{\mathrm{R}}}. \tag{68}$$

Eq. (68) is consistent with the phonon hydrodynamic models obtained by maximum entropy moment method [83,85,156], Grad's type moment method [84,186], and Chapman–Enskog method at three dimensional case [86,175]. It is seen that the present order of expansion sum up many previous models derived by different approaches.

3.2.6. First-order expansion solution

In this part, the first-order approximate component f_1 is also taken into account, and the first-order expansion solution will be got. It is obtained by substituting Eq. (41) into Eq. (42):

$$f_1 = f_{\mathrm{R}}^{\mathrm{eq}} - f_{\mathrm{N}}^{\mathrm{eq}} - \tau_{\mathrm{N}} \left(\frac{\partial f_{\mathrm{N}}^{\mathrm{eq}}}{\partial t_1} + v_{\mathrm{g}i} \frac{\partial f_{\mathrm{N}}^{\mathrm{eq}}}{\partial x_{1i}} \right). \tag{69}$$

The following differential relations are got based on the chain rule:

$$\frac{\partial f_{\mathrm{N}}^{\mathrm{eq}}}{\partial t_1} = \frac{\partial f_{\mathrm{N}}^{\mathrm{eq}}}{\partial u_j} \frac{\partial u_j}{\partial t_1} + \frac{\partial f_{\mathrm{N}}^{\mathrm{eq}}}{\partial T} \frac{\partial T}{\partial t_1}, \tag{70}$$

$$\frac{\partial f_{\mathrm{N}}^{\mathrm{eq}}}{\partial x_{1i}} = \frac{\partial f_{\mathrm{N}}^{\mathrm{eq}}}{\partial u_j} \frac{\partial u_j}{\partial x_{1i}} + \frac{\partial f_{\mathrm{N}}^{\mathrm{eq}}}{\partial T} \frac{\partial T}{\partial x_{1i}}. \tag{71}$$

The partial differentials with respect to t_1 $(\partial u_j/\partial t_1,\ \partial T/\partial t_1)$ in Eq. (70) are related to the partial differentials with respect to x_{1i} through Eqs. (48a) and (49a) when combined with Eqs. (63) and (64). Therefore we will achieve f_1 in terms of phonon energy density, heat flux and their spatial gradients by substituting the displaced Planck distribution Eq. (20) into Eqs. (69)–(71). Then the explicit forms of the flux of heat flux and heat transport equation will be acquired. However, the displaced Planck distribution makes the full first-order expansion become extremely complicated and lose its physical indication. The corresponding heat transport equation will be too complex for actual applications, as is shown in previous work [86,175]. Therefore, in the spirit of zeroth-order expansion solution in Section 3.2.5, merely the sub-first-order approximation to the first-order expansion is considered. The full first-order expansion could be referred in Refs. [86,175] and not introduced here due to its lengthy process and lacking of physical interpretation.

I. Sub-first-order approximation

Taylor expansion truncated at first order is assumed for the displaced Planck distribution, as in part I of Section 3.2.5. Thus the expressions of approximate phonon distribution, phonon energy density and heat flux remains the same, and are rewritten here for the sake of convenience:

$$f_{\mathrm{N}}^{\mathrm{eq}} \approx f_{\mathrm{R}}^{\mathrm{eq}} + f_{\mathrm{N}1}^{\mathrm{eq}}, \tag{51}$$

$$E = \frac{4\pi^5 \left(k_{\mathrm{B}} T\right)^4}{5 \left(h v_{\mathrm{g}}\right)^3}, \tag{52}$$

$$\mathbf{q} = \frac{16\pi^5 \left(k_{\mathrm{B}} T\right)^4}{15 \left(h v_{\mathrm{g}}\right)^3} \mathbf{u} = \frac{4}{3} E \mathbf{u}. \tag{53}$$

The zeroth-order component of the flux of heat flux becomes:

$$\mathbf{Q}_0 = \frac{1}{3} v_{\mathrm{g}}^2 E \mathbf{I}. \tag{54}$$

The first-order component of the flux of heat flux will be obtained once the first-order phonon distribution function f_1 is determined.

Substitution of Eq. (51) into Eqs. (69)–(71), supplemented with Eqs. (52)–(54), (48a) and (49a), gives rise to the expression of f_1:

$$f_1 = -\frac{\hbar \mathbf{k} \cdot \mathbf{u}}{k_{\mathrm{B}} T} - \tau_{\mathrm{N}} \left\{ \begin{aligned} & \frac{\hbar k_i}{k_{\mathrm{B}} T} f_{\mathrm{R}}^{\mathrm{eq}} \left(1 + f_{\mathrm{R}}^{\mathrm{eq}}\right) \left(-\frac{v_{\mathrm{g}}^2}{4E} \frac{\partial E}{\partial x_{1i}} + \frac{u_i}{E} \frac{\partial q_j}{\partial x_{1j}} - \frac{3 q_i}{4E\tau_{\mathrm{N}}} \right) \\ & - \frac{1}{C_V} \frac{\partial q_j}{\partial x_{1j}} \left[\begin{aligned} & f_{\mathrm{R}}^{\mathrm{eq}} \left(1 + f_{\mathrm{R}}^{\mathrm{eq}}\right) \frac{\hbar v_{\mathrm{g}} k}{k_{\mathrm{B}} T^2} \\ & + f_{\mathrm{R}}^{\mathrm{eq}} \left(1 + f_{\mathrm{R}}^{\mathrm{eq}}\right) \frac{\hbar v_{\mathrm{g}} k}{k_{\mathrm{B}} T^2} \left(2 f_{\mathrm{R}}^{\mathrm{eq}} + 1\right) \frac{\hbar \mathbf{k} \cdot \mathbf{u}}{k_{\mathrm{B}} T} - f_{\mathrm{R}}^{\mathrm{eq}} \left(1 + f_{\mathrm{R}}^{\mathrm{eq}}\right) \frac{\hbar \mathbf{k} \cdot \mathbf{u}}{k_{\mathrm{B}} T^2} \end{aligned} \right] \\ & + \frac{v_{\mathrm{g}}}{k} \frac{\hbar k_i k_j}{k_{\mathrm{B}} T} f_{\mathrm{R}}^{\mathrm{eq}} \left(1 + f_{\mathrm{R}}^{\mathrm{eq}}\right) \frac{3}{4} \frac{\partial}{\partial x_{1i}} \left(\frac{q_j}{E} \right) \\ & + \frac{v_{\mathrm{g}}}{k} k_i \frac{\partial T}{\partial x_{1i}} \left[\begin{aligned} & f_{\mathrm{R}}^{\mathrm{eq}} \left(1 + f_{\mathrm{R}}^{\mathrm{eq}}\right) \frac{\hbar v_{\mathrm{g}} k}{k_{\mathrm{B}} T^2} \\ & + f_{\mathrm{R}}^{\mathrm{eq}} \left(1 + f_{\mathrm{R}}^{\mathrm{eq}}\right) \frac{\hbar v_{\mathrm{g}} k}{k_{\mathrm{B}} T^2} \left(2 f_{\mathrm{R}}^{\mathrm{eq}} + 1\right) \frac{\hbar \mathbf{k} \cdot \mathbf{u}}{k_{\mathrm{B}} T} - f_{\mathrm{R}}^{\mathrm{eq}} \left(1 + f_{\mathrm{R}}^{\mathrm{eq}}\right) \frac{\hbar \mathbf{k} \cdot \mathbf{u}}{k_{\mathrm{B}} T^2} \end{aligned} \right] \end{aligned} \right\}. \tag{72}$$

Putting Eq. (72) into Eq. (47), we get the following integration because the terms from the odd function part of the integrand vanish:

$$\mathbf{Q}_1 = -\hbar v_g^3 \int \frac{\tau_N \mathbf{kk}}{k} \left\{ \begin{aligned} & -\frac{1}{C_V}\frac{\partial q_j}{\partial x_{1j}} \left[f_R^{eq}\left(1+f_R^{eq}\right)\frac{\hbar v_g k}{k_B T^2} \right] \\ & + \frac{v_g}{k}\frac{\hbar k_i k_j}{k_B T} f_R^{eq}\left(1+f_R^{eq}\right)\frac{3}{4}\frac{\partial}{\partial x_{1i}}\left(\frac{q_j}{E}\right) \\ & + \frac{v_g}{k} k_i \frac{\partial T}{\partial x_{1i}} \left[f_R^{eq}\left(1+f_R^{eq}\right)\frac{\hbar v_g k}{k_B T^2}\left(2f_R^{eq}+1\right)\frac{\hbar \mathbf{k}\cdot\mathbf{u}}{k_B T} - f_R^{eq}\left(1+f_R^{eq}\right)\frac{\hbar \mathbf{k}\cdot\mathbf{u}}{k_B T^2} \right] \end{aligned} \right\} \frac{3d\mathbf{k}}{(2\pi)^3} \tag{73}$$

which could be divided into three parts:

$$\mathbf{Q}_1 = \mathbf{Q}_{1,\mathrm{I}} + \mathbf{Q}_{1,\mathrm{II}} + \mathbf{Q}_{1,\mathrm{III}}, \tag{74a}$$

with each part respectively resulting in finally (the details of computation are seen in Appendix C):

$$\left(\mathbf{Q}_{1,\mathrm{I}}\right)_{mn} = \frac{1}{3} v_g^2 \tau_N \frac{\partial q_i}{\partial x_{1i}} \delta_{mn}, \tag{74b}$$

$$\left(\mathbf{Q}_{1,\mathrm{II}}\right)_{mn} = -\frac{1}{5} v_g^2 E \tau_N \left[\frac{\partial}{\partial x_{1i}}\left(\frac{q_i}{E}\right)\delta_{mn} + \frac{\partial}{\partial x_{1m}}\left(\frac{q_n}{E}\right) + \frac{\partial}{\partial x_{1n}}\left(\frac{q_m}{E}\right) \right], \tag{74c}$$

$$\left(\mathbf{Q}_{1,\mathrm{III}}\right)_{mn} = -\frac{4}{5}\frac{v_g^2 \tau_N}{T}\left(q_i \frac{\partial T}{\partial x_{1i}}\delta_{mn} + q_n \frac{\partial T}{\partial x_{1m}} + q_m \frac{\partial T}{\partial x_{1n}} \right). \tag{74d}$$

If the nonlinear effects resulting from the product of heat flux and temperature gradient are negligible, then Eq. (74d) vanishes and Eq. (74c) reduces to:

$$\left(\mathbf{Q}_{1,\mathrm{II}}\right)_{mn} = -\frac{1}{5} v_g^2 \tau_N \left[\frac{\partial q_i}{\partial x_{1i}}\delta_{mn} + \frac{\partial q_n}{\partial x_{1m}} + \frac{\partial q_m}{\partial x_{1n}} \right]. \tag{75}$$

The first part Eq. (74b) of the flux of heat flux resembles the bulk viscous term in classical hydrodynamics [133]. If it is neglected as the bulk viscosity usually not considered in fluid dynamics, the expression of the flux of heat flux is achieved by combining Eqs. (54) and (75):

$$Q_{mn} = \frac{1}{3} v_g^2 E \delta_{mn} - \frac{1}{5} v_g^2 \tau_N \left[\frac{\partial q_i}{\partial x_i}\delta_{mn} + \frac{\partial q_n}{\partial x_m} + \frac{\partial q_m}{\partial x_n} \right]. \tag{76}$$

Substituting Eq. (76) into Eq. (36a), we achieve the heat transport equation:

$$\tau_R \frac{\partial q_n}{\partial t} + q_n + \frac{1}{3} v_g^2 \tau_R \frac{\partial E}{\partial x_n} = \frac{1}{5} v_g^2 \tau_N \tau_R \left[\frac{\partial^2 q_n}{\partial x_m \partial x_m} + 2\frac{\partial}{\partial x_n}\left(\frac{\partial q_i}{\partial x_i}\right) \right], \tag{77a}$$

or in vector form:

$$\tau_R \frac{\partial \mathbf{q}}{\partial t} + \mathbf{q} + \lambda \nabla T = \frac{1}{5} v_g^2 \tau_N \tau_R \left[\nabla^2 \mathbf{q} + 2\nabla\left(\nabla \cdot \mathbf{q}\right) \right]. \tag{77b}$$

Eq. (77) is exactly the G–K equation (23) obtained by solution of linearized phonon Boltzmann equation with Eigen-value analysis method. If the "bulk viscous term" Eq. (74b) of the flux of heat flux is also taken into account, then the expression of the flux of heat flux is achieved by combining Eqs. (54), (74b) and (75):

$$Q_{mn} = \frac{1}{3} v_g^2 E \delta_{mn} - \frac{1}{5} v_g^2 \tau_N \left[\frac{\partial q_n}{\partial x_m} + \frac{\partial q_m}{\partial x_n} - \frac{2}{3}\frac{\partial q_i}{\partial x_i}\delta_{mn} \right]. \tag{78}$$

Substituting Eq. (78) into Eq. (36a), we achieve the heat transport equation:

$$\tau_R \frac{\partial q_n}{\partial t} + q_n + \frac{1}{3} v_g^2 \tau_R \frac{\partial E}{\partial x_n} = \frac{1}{5} v_g^2 \tau_N \tau_R \left[\frac{\partial^2 q_n}{\partial x_m \partial x_m} + \frac{1}{3}\frac{\partial}{\partial x_n}\left(\frac{\partial q_i}{\partial x_i}\right) \right], \tag{79a}$$

or in vector form:

$$\tau_R \frac{\partial \mathbf{q}}{\partial t} + \mathbf{q} + \lambda \nabla T = \frac{1}{5} v_g^2 \tau_N \tau_R \left[\nabla^2 \mathbf{q} + \frac{1}{3}\nabla\left(\nabla \cdot \mathbf{q}\right) \right]. \tag{79b}$$

Eq. (79) is a revised G–K equation obtained in Ref. [82] with also the Eigen-value analysis method, and recently obtained in moment phonon hydrodynamics by Grad's type method [188]. From our perspective, the slight difference between Eqs. (77) and (79) is attributed to different treatments of the "bulk viscous term" Eq. (74b) in the flux of heat flux. Note that the

Table 3
Correlations between present kinetic framework and previous phonon hydrodynamic models.

Present kinetic framework		Previous work and methods	
Zeroth-order expansion	Full expansion	[149]	Approximate method
		[83,85,156]	Maximum entropy moment method
		[84,186]	Grad's type moment method
		[86,175]	Chapman–Enskog method
	Approximations	Sub-first-order [89,195]	Phenomenological
		Sub-first-order [109]	Maximum entropy moment method
		Sub-second-order [100]	Approximate method
First-order expansion	Full expansion	[86,175]	Chapman–Enskog method
	Approximations	Sub-first-order [143]	Approximate method
		Sub-first-order [61,81,82]	Eigen-value analysis method
		Sub-first-order [196]	Phenomenological
		Sub-first-order [158,179]	Lattice Boltzmann scheme
		Sub-first-order [188]	Grad's type moment method

revised G–K equation (79) has almost the same form as Navier–Stokes equation (24) at negligible advection term and bulk viscosity ζ, except the heat flux term resulting from R process (as shown in the derivation of Eq. (35)). Actually previous work studied phonon hydrodynamic phenomena in very pure alkali-halide crystals by directly applying Navier–Stokes equation to phonon gas flow [196], thus could be included in the present order of approximation.

Recently, a lattice Boltzmann scheme is proposed for phonon hydrodynamics based on a first-order Chapman–Enskog expansion around a truncated displaced Planck distribution within first order [179], which is actually identical to the present sub-first-order approximation. However, an additional term of temperature second-order spatial partial derivative in the energy balance equation is obtained in Ref. [179], and results in an additional four-order spatial partial derivative term in the temperature differential equation. Based on our detailed analysis, this additional term results from the fictitious larger phonon speed in diagonal direction of D2Q9 lattice used in Ref. [179] and will vanish under the isotropic approximation. Thus the lattice Boltzmann scheme is consistent with the present order of expansion.

Therefore, the celebrated G–K equation is derived through a sub-first-order approximation to first-order expansion solution. The present work provides a much more intuitive and simpler way to derive it from phonon kinetic theory, in contrast to the Eigen-value analysis method in previous work [61,81] with obscure mathematics. Finally, the heat flux term in Eq. (77) will vanish in the absence of R process ($\tau_{\mathrm{R}} \to \infty$), where the G–K equation reduces to:

$$\frac{\partial \mathbf{q}}{\partial t} + \frac{1}{3} v_{\mathrm{g}}^2 C_V \nabla T = \frac{1}{5} v_{\mathrm{g}}^2 \tau_{\mathrm{N}} \left[\nabla^2 \mathbf{q} + 2\nabla \left(\nabla \cdot \mathbf{q} \right) \right]. \tag{80}$$

Eq. (80) is consistent with the heat transport equations obtained in previous work [143,158] where only N process is considered.

3.3. *Summary: incorporation of previous models*

A unified kinetic framework is established through a Chapman–Enskog expansion solution to phonon Boltzmann equation in Section 3.2. Different sub-order approximations to zeroth-order and first-order expansions respectively give rise to different heat transport equations obtained in previous phonon hydrodynamic models, which thus could be incorporated into the present theoretical formalism as special cases. The correlations are thoroughly summarized between the present kinetic framework and previous models in Table 3.

4. Phenomenological phonon hydrodynamics

The discussions in Section 3 mainly focus on the derivation of heat transport equations from phonon Boltzmann equation, with actual applications less considered. In last few years, inspired by the progress in microscale gas flow by analytical and experimental method [197–201], DSMC [202–204] and lattice Boltzmann simulations [205–207], people began to apply the hydrodynamic approach to study micro- and nanoscale heat transport [62,98,208,209]. In modeling nanoscale phonon transport, the nonlocal effect plays a relevant role [62], which could be understood from two aspects: (1) physically it comes from the confinement of phonon-boundary scattering; (2) mathematically it may be described by a gradient term of the heat flux. The cross-section heat flux distribution of in-plane phonon transport through a thin film at different Knudsen numbers [38] shown in Fig. 5 is a good manifest of the nonlocal effect. It is seen that at high Kn (for instance, $Kn = 1$) in nanoscale, the heat flux distribution deviates from the usual uniform profile ($Kn = 0.001$ in the diffusive regime) determined by the classical Fourier's law. The non-uniform heat flux distribution resembles much the velocity distribution in micro-channel gas flow, both of them having a non-vanishing value at the boundary. Based on this kind of similarity, the phonon

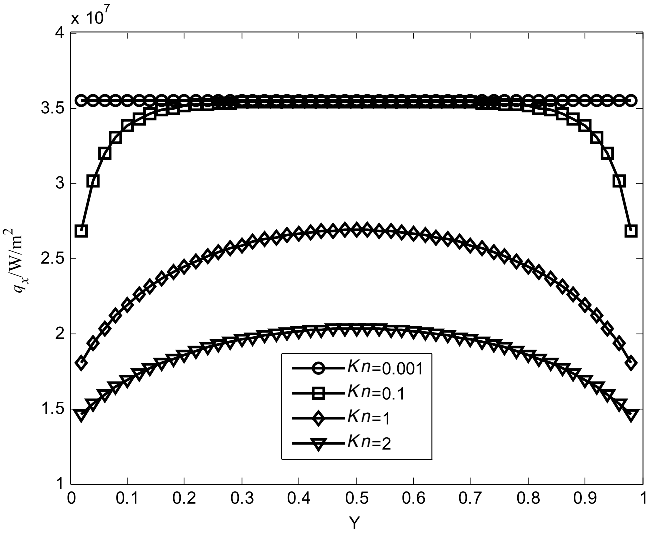

Fig. 5. Analytical solution of cross-section heat flux distribution of in-plane phonon transport through a silicon thin film with diffuse lateral walls; the properties of silicon at 300 K are used; for all the Knudsen numbers, the same temperature gradient of 0.01 K per mean free path is applied.

hydrodynamic model is proposed [62] for nanoscale heat transport. To cover the non-local phonon transport behavior, a G–K like equation with gradient terms of heat flux is applied in prior [62,210]:

$$\tau_{\mathrm{R}}\frac{\partial \mathbf{q}}{\partial t}+\mathbf{q}+\lambda\nabla T=l^2\left[\nabla^2\mathbf{q}+2\nabla\left(\nabla\cdot\mathbf{q}\right)\right], \tag{81}$$

with l the phonon mean free path. Since the application of G–K equation at elevated temperature (such as room temperature) seems lacking of a solid foundation, we use the denomination "phenomenological phonon hydrodynamics" throughout this section, as is already explained at the beginning of Section 1.2.3. Actually, Eq. (81) is slightly different from the original G–K equation (77); but for convenience, we still use the name of "G–K equation" for Eq. (81) hereafter. Though logically a rigorous connection is lost to the kinetic theory discussed in Section 3, historically the phenomenological phonon hydrodynamics provides a simple approach to understand the nanoscale heat transport, which is reasonable in views of both physical picture and mathematical description. To remedy this situation, an extended concept "generalized phonon hydrodynamics" will be proposed and discussed in Section 5. The G–K equation becomes the macroscopic governing equation, acting the same role as the Navier–Stokes equation for gas flow. Thus heat flux boundary condition has also been developed for microscale phonon gas flow, analogous to the velocity slip boundary for microscale gas flow [62].

In this section, firstly an overview is given to the velocity slip boundary for microscale gas flow and heat flux boundary for microscale phonon gas flow. Then the thermodynamic foundations for both G–K equation and heat flux boundary are introduced in the line of extended irreversible thermodynamics [40]. These laid a solid foundation for credible applications of phonon hydrodynamics in predicting the thermal transport properties of nanostructures, as summarized in Section 4.3. Finally, a revisit is made of the difference between phonon and gas flows, and the relationship between phonon hydrodynamics and thermon gas models.

4.1. Origin and fundamentals

4.1.1. Velocity slip boundary in microscale gas flow

In microscale gas flow, the Knudsen number (Kn) is defined as the ratio of molecular mean free path Λ to the characteristic dimension L of gas flow (such as the height of a channel, or the diameter of a pipe) [154]: $Kn=\Lambda/L$. Based on the range of Kn, gas flow is usually grouped into four regimes [198,211]: $Kn\le 0.001$, continuum flow regime; $0.001<Kn<0.1$, slip flow regime; $0.1\le Kn<10$, transitional flow regime; $Kn\ge 10$, free molecular flow regime. The Navier–Stokes equation is derived from Boltzmann equation in the limit of small Kn [125,212], being rigorously valid in continuum flow regime. Therefore the gas flows in other regimes have to be treated through a solution of the Boltzmann equation, which is often intractable and time-consuming. The inefficient kinetic method fosters simple treatment: Navier–Stokes equation is assumed to be still effective for gas flow within slip regime, when supplemented with velocity slip boundary.

The first velocity slip boundary is proposed by Maxwell [213], and adopts the following expression for isothermal gas flow between stationary parallel plates:

$$\mathbf{v}_{\mathrm{w}}=C\Lambda\frac{\partial \mathbf{v}}{\partial n}, \tag{82}$$

with $\mathbf{v}_\mathrm{w}$ the slip velocity of gases at the wall, n denoting the unit normal direction of the wall and C the slip coefficient determined by the surface properties of the plates. Eq. (82) is a first-order boundary, which is later generalized to second-order by Cercignani [214,215]:

$$\mathbf{v}_\mathrm{w} = C_1 \Lambda \frac{\partial \mathbf{v}}{\partial n} - C_2 \Lambda^2 \frac{\partial^2 \mathbf{v}}{\partial n^2}, \tag{83}$$

with C_1, C_2 slip coefficients determined from the solution of Boltzmann equation or experimental measurements. Subsequently, many other velocity slip models were also proposed, which have been summarized thoroughly in the review article [216] and will not be deeply explored here.

4.1.2. *Heat flux boundary in phonon hydrodynamics*

The heat flux boundary is developed in a heuristic way based on the similarity between phonon and gas flows in two aspects: governing equations and physical pictures. For steady-state phonon heat transport in nanostructures, the G–K equation (81) reduces to [62,87,210]:

$$\lambda \nabla T = l^2 \nabla^2 \mathbf{q}. \tag{84}$$

The divergence of heat flux has been vanished at the steady state based on Eq. (34), whereas the heat flux term is negligible in comparison to the Laplacian term of heat flux in nanostructures where l is much larger than the system dimension [62,87,210]. Eq. (84) resembles the steady-state Navier–Stokes equation with negligible nonlinear advection term:

$$\nabla p = \mu \nabla^2 \mathbf{v}, \tag{85}$$

which is applied to describe the Stokes flows at low Reynolds number or parallel flows (such as the Poiseuille flow and Couette flow). In the case of fully-developed Poiseuille flow in a cylindrical pipe or between parallel plates, Eq. (85) gives rise to a parabolic velocity distribution across the flow section. Therefore, Eq. (84) infers a similar behavior of phonon gas Poiseuille flow with a parabolic heat flux distribution across the heat flow section. In analogy to the velocity slip boundary Eq. (82) for microscale gas flow, the heat flux boundary is assumed [62]:

$$\mathbf{q}_\mathrm{w} = Cl \frac{\partial \mathbf{q}}{\partial n}, \tag{86}$$

with q_w the phonon heat flux at the boundary, n denoting the unit normal direction of the boundary and C the boundary coefficient. Subsequently, the first-order boundary Eq. (86) is generalized to a second-order one in the framework of extended irreversible thermodynamics [210]:

$$\mathbf{q}_\mathrm{w} = Cl \frac{\partial \mathbf{q}}{\partial n} - \alpha l^2 \frac{\partial^2 \mathbf{q}}{\partial n^2}, \tag{87}$$

with α an additional boundary coefficient to describe the phonon backscattering effect because of boundary roughness [210]. Note that although the present derivation is under simplified circumstance, the heat flux boundary is still valid for more extensive situations. In a recent work [217], the heat flux boundary condition Eq. (86) is also derived from the discrete Boltzmann transport equation based on a decomposition of the particle distribution function into an equilibrium part and a nonequilibrium part, the gradients of which give rise to the heat flux in the bulk region and heat flux at the boundary respectively. This theoretical study provides a primary microscopic foundation for the heat flux boundary condition Eq. (86); on the other hand, further explorations on the physical nature of boundary heat flux in the future are thus motivated since the derivation in Ref. [217] is mainly from the mathematical perspective.

4.2. *Thermodynamic foundations*

Thermodynamics has a close relation to heat transport science since its early debating on the nature of heat as a form of substance (caloric) or energy [218]. The kinetic (energy) viewpoint finally won and gave rise to the rigorous statement of second law by Clausius and Thomson [218]. Afterwards, the classical irreversible thermodynamics [219] was established independently by Onsager [220,221], Eckart [222,223], Meixner [224] and Prigogine [225] for the near-equilibrium heat transport described by Fourier's law. In recent years, the rapid progress in micro- and nanoscale heat transport induces generalized heat transport equations, which foster the development of irreversible thermodynamic theories [226,227] such as rational thermodynamics [228], rational extended thermodynamics [187], extended irreversible thermodynamics [40], weakly nonlocal thermodynamics [229] and GENERIC [230]. G–K equation is actually a generalized heat transport equation beyond Fourier's law by including the relaxation (memory) and nonlocal effects [46]. Thus Jou and his co-workers have established a solid thermodynamic foundation for G–K equation and phonon hydrodynamics widely applied in micro- and nanoscale heat transport.

In this subsection, a summary is made of the thermodynamic foundations for both the G–K equation and the heat flux boundary. Different branches of thermodynamic theories have been proposed, but the extended irreversible thermodynamics is the main line, with a brief introduction to other formalisms in the following.

4.2.1. Thermodynamic derivation of G–K equation

In classical irreversible thermodynamics for heat transport in rigid solid, the specific energy e is the basic state variable and Fourier's law is a deduction from the linear thermodynamic flux–force relation. To recover the relaxation and nonlocal terms in G–K equation, both the heat flux $\mathbf{q}$ and the flux of heat flux $\mathbf{Q}$ are elevated as additional state variables, being the main idea of extended irreversible thermodynamics. Thus G–K equation was derived [35,231–233] in the extended state variable space based on the generalized second law in extended irreversible thermodynamics. Moreover, the G–K equation was also obtained by the dynamical nonequilibrium temperature method [234,235], weakly nonlocal irreversible thermodynamics [236,237] and minimum entropy production variational principle [238,239]. From our perspective, these thermodynamic formalisms are similar to extended irreversible thermodynamics, and are actually different derivatives of extended thermodynamics [240,241]. As a result, we focused on the derivation of G–K equation in extended irreversible thermodynamics.

We follow the general lines taking e, $\mathbf{q}$, $\mathbf{Q}_\circ$ and Q as the basic state variables. Q is the trace of the flux of heat flux. The present derivation is slightly different from previous work [231] where e, $\mathbf{q}$ and $\mathbf{Q}$ are taken as state variables, and also different from Refs. [232,233] where the evolution equations are assumed in prior for state variables. The specific entropy is dependent on the state variables as $s = s(e, \mathbf{q}, \mathbf{Q}_\circ, Q)$ with the generalized Gibbs equation:

$$ds = \theta^{-1}\mathrm{d}e - v\alpha_1\mathbf{q}\cdot\mathrm{d}\mathbf{q} - v\alpha_2\mathbf{Q}_\circ : \mathrm{d}\mathbf{Q}_\circ - v\alpha_0 Q\,\mathrm{d}Q, \tag{88}$$

with θ the nonequilibrium absolute temperature, v the specific volume, α_0, α_1 and α_2 coefficients to be explained below.

Combined with the energy balance equation (34) ($E = \rho e$), Eq. (88) becomes:

$$\rho\dot{s} = -\theta^{-1}\nabla\cdot\mathbf{q} - \alpha_1\mathbf{q}\cdot\dot{\mathbf{q}} - \alpha_2\mathbf{Q}_\circ : \dot{\mathbf{Q}}_\circ - \alpha_0 Q\dot{Q}, \tag{89}$$

where the dot denotes time derivatives. Comparing Eq. (89) to the local entropy balance equation [219]:

$$\rho\dot{s} = -\nabla\cdot\mathbf{J}^s + \sigma^s, \tag{90}$$

with the expression of entropy flux postulated as [40]:

$$\mathbf{J}^s = \frac{\mathbf{q}}{\theta} + \beta_1\mathbf{Q}_\circ\cdot\mathbf{q} + \beta_2 Q\mathbf{q}, \tag{91}$$

we achieve the expression of entropy production rate:

$$\sigma^s = \mathbf{q}\cdot\left[-\alpha_1\dot{\mathbf{q}} + \nabla(\theta^{-1}) + \beta_1\nabla\cdot\mathbf{Q}_\circ + \beta_2\nabla Q\right] + \mathbf{Q}_\circ : \left[-\alpha_2\dot{\mathbf{Q}}_\circ + \beta_1\left(\nabla\mathbf{q}\right)_\circ^{\mathrm{s}}\right] + Q\left(-\alpha_0\dot{Q} + \beta_2\nabla\cdot\mathbf{q}\right). \tag{92}$$

In Eq. (92), β_1 and β_2 are coefficients to be identified below, and $(\nabla\mathbf{q})_\circ^{\mathrm{s}}$ is the symmetric deviatoric part of the tensor $\nabla\mathbf{q}$. To ensure a non-negative entropy production rate restricted by the second law, linear flux–force relations are assumed:

$$\begin{aligned} \mu_1\mathbf{q} &= -\alpha_1\dot{\mathbf{q}} + \nabla(\theta^{-1}) + \beta_1\nabla\cdot\mathbf{Q}_\circ + \beta_2\nabla Q \\ \mu_2\mathbf{Q}_\circ &= -\alpha_2\dot{\mathbf{Q}}_\circ + \beta_1\left(\nabla\mathbf{q}\right)_\circ^{\mathrm{s}} \\ \mu_0 Q &= -\alpha_0\dot{Q} + \beta_2\nabla\cdot\mathbf{q} \end{aligned} \tag{93a}$$

with μ_0, μ_1, and μ_2 phenomenological coefficients. Eq. (93a) is reformulated as:

$$\begin{aligned} \tau_1\dot{\mathbf{q}} &= -\left(\mathbf{q} + \lambda\nabla\theta\right) + \nabla\cdot\mathbf{Q} \\ \tau_2\dot{\mathbf{Q}}_\circ &= -\mathbf{Q}_\circ + 2\beta''\left(\nabla\mathbf{q}\right)_\circ^{\mathrm{s}} \\ \tau_0\dot{Q} &= -Q + \beta'\nabla\cdot\mathbf{q} \end{aligned} \tag{93b}$$

with the identifications of parameters:

$$\begin{aligned} &\mu_1 = \frac{1}{\lambda\theta^2}, \qquad \alpha_1 = \frac{\tau_1}{\lambda\theta^2}, \qquad \beta_1 = \beta_2 = \mu_1 \\ &\mu_2 = \frac{\mu_1}{2\beta''}, \qquad \alpha_2 = \frac{\tau_2}{2\lambda\theta^2\beta''}, \qquad \mu_0 = \frac{\mu_1}{\beta'}, \qquad \alpha_0 = \frac{\tau_0}{\lambda\theta^2\beta'}. \end{aligned} \tag{94}$$

Usually it is assumed that the relaxation time of the flux of heat flux is negligibly smaller than that of the heat flux, i.e. $\tau_2 \approx 0$, $\tau_0 \approx 0$. Therefore the heat transport equation is obtained by eliminating the flux of heat flux in Eq. (93b):

$$\tau_1\frac{\partial\mathbf{q}}{\partial t} = -\left(\mathbf{q} + \lambda\nabla\theta\right) + \beta''\nabla^2\mathbf{q} + \left(\beta' + \frac{\beta''}{3}\right)\nabla(\nabla\cdot\mathbf{q}). \tag{95}$$

In comparison to the G–K equation (77), the unknown coefficients and parameters in (95) are identified as:

$$\beta' = \frac{1}{3}\tau_{\mathrm{R}}\tau_{\mathrm{N}}v_{\mathrm{g}}^2, \qquad \beta'' = \frac{1}{5}\tau_{\mathrm{R}}\tau_{\mathrm{N}}v_{\mathrm{g}}^2, \qquad \tau_1 = \tau_{\mathrm{R}}. \tag{96}$$

Thus the G–K equation is exactly derived. In some theories, instead, it has been assumed that the relaxation time of the flux of heat flux is of the same order as that of the heat flux. In such a case, it has been proposed to take as independent variables all the higher-order fluxes of heat flux (respectively related to higher-order moments of phonon distribution function), thus leading to a hierarchy of coupled equations for the higher-order fluxes [40,109]. This formalism leads to a continued-fraction expression for the thermal conductivity in terms of the wave vector times the mean free path (or in terms of the Knudsen number) [40]. Under some simplifying assumptions about the relaxation times of the higher-order fluxes (for instance, assuming that all of them are equal, or depend mildly on the tensorial order of the corresponding fluxes) one may get an effective thermal conductivity qualitatively describing the transition from the diffusive to the so-called ballistic regimes of heat transport [46].

Finally, a brief introduction is given to the derivation of the steady-state G–K equation by the minimum entropy production variational principle. Its main idea is to obtain the heat transport equation by minimizing the following functional [238,239]:

$$I = \int_V \sigma^s \mathrm{d}V + \int_V \gamma \nabla \cdot \mathbf{q} \mathrm{d}V, \tag{97}$$

with γ a Lagrange multiplier for the steady-state constraint ($\nabla \cdot \mathbf{q} = 0$), and the entropy production rate for G–K equation obtained in extended irreversible thermodynamics is [238,239]:

$$\sigma^s = \frac{1}{\lambda\theta^2} \left\{ \mathbf{q} \cdot \mathbf{q} + l^2 \left[\nabla\mathbf{q} : (\nabla\mathbf{q})^{\mathrm{T}} + 2 (\nabla \cdot \mathbf{q})^2 \right] \right\}. \tag{98}$$

4.2.2. Thermodynamic derivation of heat flux boundary

The heat flux boundary is derived through similar procedures in the line of extended irreversible thermodynamics. Based on the definitions of specific energy and entropy at the boundary, the heat flux and the flux of heat flux at the boundary, the generalized Gibbs equation becomes [242]:

$$ds_{\mathrm{w}} = \theta_{\mathrm{w}}^{-1} \mathrm{d}e_{\mathrm{w}} - v\alpha_1' \mathbf{q}_{\mathrm{w}} \cdot \mathrm{d}\mathbf{q}_{\mathrm{w}} - v\alpha_2' \mathbf{Q}_{\mathrm{w}} : \mathrm{d}\mathbf{Q}_{\mathrm{w}}, \tag{99}$$

with the subscript "w" denoting quantities at the boundary, and the apostrophe to distinguish the coefficients from those used in previous derivation of G–K equation. The entropy balance equation is still the same as Eq. (90), but only with subscripts "w". The entropy flux is supposed to assume the following form [242]:

$$\mathbf{J}_{\mathrm{w}}^s \cdot \mathbf{n} = \frac{\mathbf{q}_{\mathrm{w}} \cdot \mathbf{n}}{\theta_\infty} - \frac{\mathbf{q} \cdot \mathbf{n}}{\theta_{\mathrm{w}}} + \varpi \mathbf{Q}_{\mathrm{w}} \cdot \mathbf{q}_{\mathrm{w}} \cdot \mathbf{n}, \tag{100}$$

with θ_∞ the environment temperature, ϖ a constant, $\mathbf{n}$ being the unit normal vector of the wall. Combination of Eqs. (90), (99) and (100) gives rise to the expression of entropy production rate:

$$\sigma_{\mathrm{w}}^s = \mathbf{q}_{\mathrm{w}} \cdot \left[\left(\frac{1}{\theta_\infty} - \frac{1}{\theta_{\mathrm{w}}} \right) \mathbf{n} + \varpi \mathbf{Q}_{\mathrm{w}} \cdot \mathbf{n} - \alpha_1' \dot{\mathbf{q}}_{\mathrm{w}} \right] - \alpha_2' \mathbf{Q}_{\mathrm{w}} : \dot{\mathbf{Q}}_{\mathrm{w}}. \tag{101}$$

To ensure non-negative entropy production rate restricted from the second law, linear flux–force relations at the boundary are also assumed:

$$\begin{aligned} \mu_1' \mathbf{q}_{\mathrm{w}} &= \left(\frac{1}{\theta_\infty} - \frac{1}{\theta_{\mathrm{w}}} \right) \mathbf{n} + \varpi \mathbf{Q}_{\mathrm{w}} \cdot \mathbf{n} - \alpha_1' \dot{\mathbf{q}}_{\mathrm{w}} \\ \mu_2' \mathbf{Q}_{\mathrm{w}} &= -\alpha_2' \dot{\mathbf{Q}}_{\mathrm{w}}. \end{aligned} \tag{102}$$

Combined with Eqs. (102), and (93) based on the continuity of the flux of heat flux, the tangential boundary heat flux is derived finally:

$$q_{\mathrm{wt}} = Cl \frac{\partial q}{\partial n}, \tag{103}$$

with the slip coefficient $C = \frac{\varpi}{\mu_1'} \sqrt{\frac{\mu_1}{\mu_2}}$. Eq. (103) is exactly the first-order heat flux boundary Eq. (86). Note that the second-order heat flux boundary condition Eq. (87) can be also obtained by introducing higher-order flux of heat flux into the state variable space [239,242].

Finally, we introduce the main idea of deriving heat flux boundary in another way: the minimum entropy production variational principle. In contrast to Eqs. (97) and (98) in deriving the steady-state G–K equation, additional terms related to the heat flux at the boundary are included into the entropy production rate [239]:

$$I = \int_V \left(\sigma^s + \gamma \nabla \cdot \mathbf{q} \right) \mathrm{d}V + \int_A \frac{l}{\lambda\theta^2 C} \left(\mathbf{q}_{\mathrm{w}} \cdot \mathbf{q}_{\mathrm{w}} \right) \mathrm{d}A. \tag{104}$$

Minimizing the functional equation (104) will result in the first-order heat flux boundary equation (86). Similarly, the second-order heat flux boundary could be obtained by introducing higher-order fluxes.

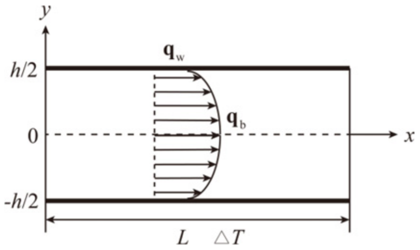

Fig. 6. Phonon gas flow through nano thin film.

4.3. Applications: thermal conductivity predictions of nanostructures

For heat transport in nanostructures, the heat flux distribution can be obtained by a solution of the G–K equation with heat flux boundary. Integration of the heat flux distribution in a cross section of the nanostructure gives rise to the effective thermal conductivity, which usually deviates from the bulk value and decreases with the reduction of nanostructure size [38]. In this subsection, the credible application of phonon hydrodynamics is presented to model the size-dependent thermal conductivity of typical nanostructures: nano thin films and nanowires [62,243–248]. Furthermore, the effect of wall roughness in nanostructures on thermal conductivity is considered by including it into the phonon hydrodynamic model.

4.3.1. Nano thin films

Heat transport through a nano thin film is modeled by phonon gas flow between two parallel plates as is shown in Fig. 6. The length and height of the channel is L and h respectively, whereas the width is much larger than the height with only a unit width is accounted. The temperature difference between the inlet and outlet of the channel is ΔT. Therefore it becomes a two-dimensional temperature-difference driven phonon gas flow, exhibiting a similar physical picture of pressure-difference driven gas Poiseuille flow between parallel plates.

The heat flux through the nano thin film consists of two parts: $\mathbf{q} = \mathbf{q}_b + \mathbf{q}_w$ with $\mathbf{q}_b$ the bulk part and $\mathbf{q}_w$ the boundary part, which are assumed additive independently [62,87,210]. The bulk part is obtained by an analytical solution of Eq. (84) with the conventional boundary condition:

$$\mathbf{q}_b = \frac{\lambda \Delta T}{2l^2 L}\left(\frac{h^2}{4} - y^2\right). \tag{105}$$

The boundary part is obtained by putting Eq. (105) into the first-order heat flux boundary equation (86):

$$\mathbf{q}_w = Cl\frac{\partial \mathbf{q}_b}{\partial n} = -Cl\frac{\partial \mathbf{q}_b}{\partial y} = C\frac{h\lambda \Delta T}{2lL}. \tag{106}$$

Summation of Eqs. (105) and (106) gives the total heat flux:

$$\mathbf{q} = \frac{\lambda \Delta T}{2l^2 L}\left(\frac{h^2}{4} - y^2\right) + C\frac{h\lambda \Delta T}{2lL}. \tag{107}$$

Integration of Eq. (107) across a section of the channel results in the total heat flow rate:

$$Q_h = \int_{-h/2}^{h/2} \mathbf{q}\mathrm{d}y = \frac{\lambda h^2 \Delta T}{2lL}\left(\frac{h}{6l} + C\right), \tag{108}$$

which gives an effective thermal conductivity based on Fourier's law:

$$\lambda_{\mathrm{eff}} = \frac{Q_h L}{h\Delta T} = \frac{\lambda h^2}{12l^2}\left(1 + \frac{6l}{h}C\right). \tag{109}$$

Eq. (109) indicates a size dependence of the thermal conductivity of nano thin film.

This derivation is simple but heuristic for physical interpretation. In realistic situation, the heat flux term should be added to Eq. (84) since it is not negligibly small because the lateral size (h) of thin film spreads from nanoscale to microscale. Through similar procedures, an effective thermal conductivity is derived [62]:

$$\lambda_{\mathrm{eff}} = \lambda\left[1 - \frac{2l}{h}\tanh\left(\frac{h}{2l}\right) + C\tanh\left(\frac{h}{2l}\right)\right]. \tag{110}$$

The comparison of the predictions by Eq. (110) with several different boundary coefficients C to experimental results [249–252] is shown in Fig. 7. Note that in microscale gas flow, the velocity slip coefficient depends on the surface properties of the wall. Similarly, the heat flux boundary coefficients will depend on the properties of the boundary. As scarce work

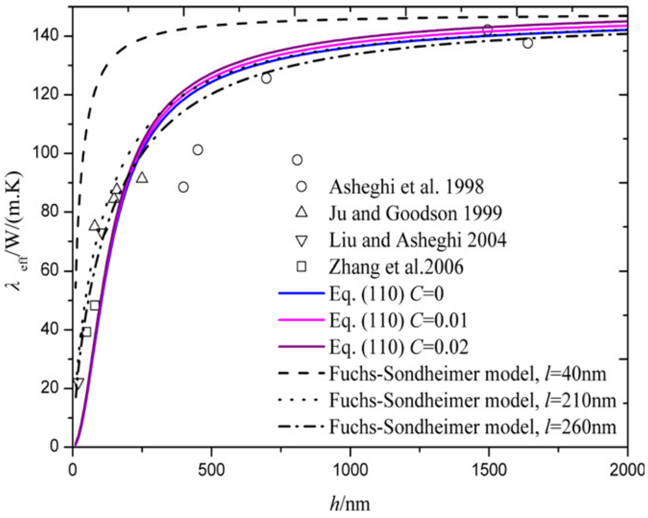

Fig. 7. Effective thermal conductivity of nano thin films modeled by phonon hydrodynamic model (solid lines), Fuchs–Sondheimer model (dash or dot or dash–dot lines) and obtained in experiments (marks).

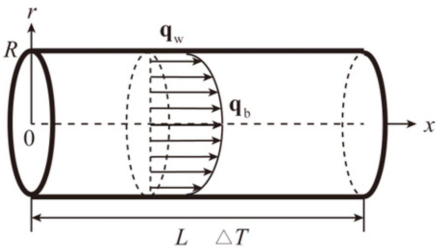

Fig. 8. Phonon gas flow through a nanowire.

has discussed this kind of dependence, several empirical values are adopted for the moment. Further work is needed to understand the relation between the boundary properties and heat flux boundary coefficients in the future. The silicon nano thin film at 300 K is modeled, with bulk thermal conductivity $\lambda = 148$ W/(m.K) and bulk mean free path $l = 40$ nm. It is seen that the phonon hydrodynamic model displays a good performance in predicting the size-dependent thermal conductivity of nano thin films. In addition, a comparison is made between the phonon hydrodynamic model and the classical Fuchs–Sondheimer model [253,254]:

$$\frac{\lambda_{\rm eff}}{\lambda} = 1 - \frac{3(1-s)}{2\xi} \int_0^1 \varphi\left(1-\varphi^2\right) \frac{1-\exp(-\xi/\varphi)}{1-s\exp(-\xi/\varphi)} d\varphi. \tag{111}$$

Eq. (111) is obtained through a solution of phonon Boltzmann equation under gray SMRT approximation, with ξ denoting the inverse of Knudsen number ($Kn = l/h$), s being the specularity parameter [38]. The average mean free path for bulk silicon at 300 K under gray approximation is still inconclusive in the literature, thus three different proposed values $l = 40$ nm, $l = 210$ nm and $l = 260$ nm are adopted respectively. Fully-diffuse wall of the thin film is assumed, thus $s = 0$. Although the Fuchs–Sondheimer model (with $l = 210$ nm or $l = 260$ nm) gives rise to comparable results to the phonon hydrodynamic model as is shown in Fig. 7, the phonon hydrodynamic model holds the following several advantages: (1) Eq. (111) assumes an integral form, which is much more complex than Eq. (110), therefore it is easier to make a qualitative analysis (for instance, the asymptotic analysis) to obtain a physical interpretation based on Eq. (110); (2) Eq. (111) is obtained through a solution of phonon Boltzmann equation, which is only feasible for simple geometries such as the parallel thin film, while phonon hydrodynamics is a macroscopic model and easier to be extended to complex geometries, as to be discussed below.

4.3.2. Nanowires

Heat transport through a nanowire is modeled by phonon gas flow through a circular pipe, as is shown in Fig. 8. The radius and length of the pipe is respectively R and L. The temperature difference between the inlet and outlet of the pipe is ΔT. Therefore it is a two-dimensional temperature-difference driven phonon gas flow, exhibiting a similar physical picture of pressure-difference driven gas Poiseuille flow in a circular pipe.

Through a similar process to the derivations of Eqs. (109) and (110), the steady-state G–K equation (with the heat flux term kept) supplemented with the first-order heat flux boundary equation (86) finally gives rise to an effective thermal

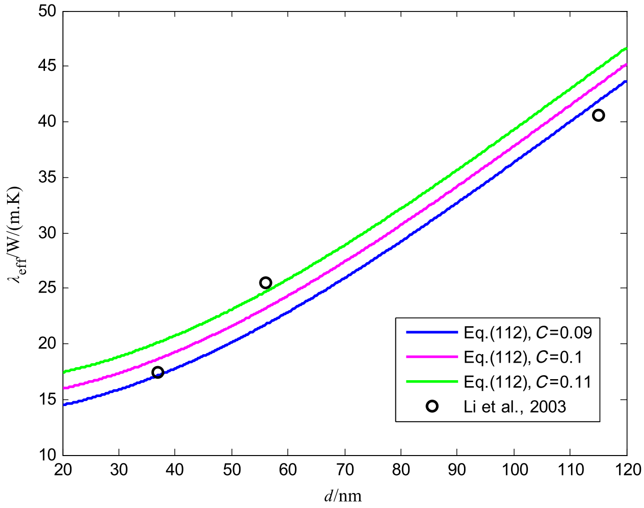

Fig. 9. Effective thermal conductivity of nanowires modeled by phonon hydrodynamic model (solid lines) and obtained in experiments (marks).

conductivity for the nanowire [87,247]:

$$\lambda_{\text{eff}} = \lambda \left\{ 1 - 2Kn \left[\frac{J_1\left(i/Kn\right)}{J_0\left(i/Kn\right)} \right]^2 \left[\frac{J_0\left(i/Kn\right)}{iJ_1\left(i/Kn\right)} + C \right] \right\}, \tag{112}$$

where $Kn = l/R$, and J_0, J_1 are zeroth-order and first-order Bessel functions of the first kind respectively. The comparison of the prediction by Eq. (112) with several boundary coefficients C to experimental results [255] is shown in Fig. 9, with the diameter of the nanowire $d = 2R$. The silicon nanowire at 300 K is modeled, with the bulk properties the same as that used for nano thin film. It is seen that the phonon hydrodynamic model displays a good performance again in predicting the size-dependent thermal conductivity of nanowires. Note that the data of $d = 22$ nm in Ref. [255] is not adopted here. This result cannot be explained well even by phonon kinetic theory [76,119], thus is not included into the present hydrodynamic model. Quantum effect is expected to become relevant at such a small size, but it is not within the present theoretical framework, therefore not investigated here.

In a series of work, the phonon hydrodynamic model is also applied to analyze the size-dependent thermal conductivity of elliptical nanowires, which has the following expression [247]:

$$\lambda_{\text{eff}} = \frac{\lambda}{2Kn} \left[\frac{1}{2Kn} \frac{1}{1 + \left(b/a\right)^2} + CS \right]. \tag{113}$$

In Eq. (113), a, b are respectively the length of semi-long and semi-short axis of the ellipse, $Kn = l/b$, and S is a numerical correction factor for heat flux at the walls adopted from analytical solution of microscale gas flow through elliptical tube and given by $S = 1 - 0.6976 \left[\left(b/a\right)^2 - 1 \right] / \left[1.951 \left(b/a\right)^2 + 1 \right]$ [256].

Moreover, other hydrodynamic methods have been proposed to model the size-dependent thermal conductivity of nano thin films and nanowires. One is the thermon gas model, which treats the heat transport process as an equivalent thermon gas flow. To model the nanoscale heat transport, corrections of the gas-surface confinement effect [97,98] and ends effect [99] are added into the original model, based on the results for the gas flow in micro-channels. The modified thermon gas model gives pretty good predictions of thermal conductivities of nano thin films [98], nanowires [98,99] and nanotubes [97,98] in comparison to the results obtained in experiments or by molecular dynamics simulation. Recently, in the conceptual frame of rarefied gas dynamics, the size-dependent viscosity of thermon gas is extracted from the experimental data of thermal conductivities of nanostructures and substituted into the phonon gas model [257], whence the thermal conductivities of both nano thin films and nanowires have been asserted to be explained well. Another similar model is developed in Ref. [208], where the steady-state G–K equation is analytically solved with the non-dimensional boundary heat flux correlated to a size-dependent effective phonon mean free path.

4.3.3. Roughness effect

The applications discussed above cover the predictions of thermal conductivity of nanostructures with smooth walls. However, in actual engineering, there may be roughness in nanostructures such as the rough nanowires as enhanced thermoelectric materials [258,259]. Because of the clear physical picture of phonon hydrodynamics, it is credible to extend the smooth wall case to the rough one. The second-order heat flux boundary equation (87) is used, with the boundary coefficient α to describe the effect of wall roughness on phonon gas flow [210]. Combined with the correlations between boundary coefficients and geometry parameters ($C = C'(1 - \Delta/D)$, $\alpha = \alpha'\Delta/D$), the effective thermal conductivity of rough nanowire is achieved [243,245]:

$$\lambda_{\mathrm{eff}} = \frac{\lambda}{8Kn^2}\left(1 + 4C'Kn\right) - \frac{\lambda}{2Kn}\left(\frac{\Delta}{D}\right)\left(C' + \alpha'Kn\right). \tag{114}$$

In Eq. (114), $Kn = l/R$, Δ and D denotes respectively the root-mean-square value of the roughness fluctuations and the average distance between adjacent roughness peaks on the wall. It has been reported that the predictions by Eq. (114) agree well with experimental results in a wide range of nanowire diameters and ambient temperatures [243,245].

A similar situation to rough nanowire is the porous nanostructures [260–263], where the roughness (pores) stay inside the structures rather than at the boundary. Based on the abundant models in gas flow through porous media [264], phonon hydrodynamics has been applied to study the influences of porosity and pore size on the effective thermal conductivity of porous silicon, exhibiting good agreement between theoretical predictions and experimental results [209,265]. For instance, the resistance force exerted by a sphere of radius a in viscous fluid flow is given by the Stokes formula $F = 6\pi\mu a v$, with v the relative velocity between the sphere and fluid. In phonon hydrodynamics, Eq. (84) has an identical form to the Stokes equation for fluid flow, with the temperature gradient playing the same role of pressure gradient, the coefficient l^2/λ the role of dynamic viscosity. As the average resistance force (per sphere) exerted by a random array of spheres in viscous fluid flow is given by $F = \frac{6\pi\mu a}{1+A'(\Lambda/a)}\left(1 + \frac{3}{\sqrt{2}}\sqrt{\phi}\right)v$, the thermal resistance of N randomly-distributed pores to the heat flow is thus written as [209]:

$$F_N = 6\pi N\frac{l^2}{\lambda}\frac{a}{1 + A'(l/a)}\left(1 + \frac{3}{\sqrt{2}}\sqrt{\phi}\right)Q_{\mathrm{h}} = A\nabla T, \tag{115}$$

where A' is a numerical function of Kn, and A is the cross-section area of the heat conductor, ϕ being the porosity. Through adding Eq. (115) to the normal diffusive thermal resistance $[f(\phi)\lambda]^{-1}Q_{\mathrm{h}} = A\nabla T$ with $f(\phi) = (1-\phi)^3$, the effective thermal conductivity of porous nanostructure dependent on both the porosity and pore size is obtained [209]:

$$\lambda_{\mathrm{eff}} = \lambda\frac{1}{\frac{1}{f(\phi)} + \frac{9}{2}\phi\frac{(l/a)^2}{1+A'(l/a)}\left(1 + \frac{3}{\sqrt{2}}\sqrt{\phi}\right)}. \tag{116}$$

Moreover, the frequency dependence of the effective thermal conductivity of nanowires is studied [246] by adding a relaxation term to the heat flux boundary [244,246]. Here we do not go into the details of these applications because they follow almost the same line as in modeling the nano thin films and nanowires with smooth walls. The reader could refer to the comprehensive review [87] about them.

The extensive practical applications in nano thin films, nanowires and porous nanostructures indicate that the phonon hydrodynamic model is a promising tool in modeling thermal transport properties of nanostructures. This method holds at least three advantages: clear physical picture of phonon gas flow; relatively small amount of computation in comparison to the kinetic modeling approach; its implementation can adopt the existing models in classical hydrodynamics.

4.4. *Difference between phonon and fluid flow*

The developments and applications of phonon hydrodynamics are mainly inspired by the similarity between phonon and fluid flows. Nevertheless, there are still some differences between them, which are the focus in this part. In the continuum regime, fluid flow is governed by Navier–Stokes equation with non-slip boundary while heat transport is described by Fourier's law. Thus fluid flow between two parallel plates under a pressure gradient will have a parabolic velocity distribution as is shown in Fig. 10(a). In contrast, phonon gas flow under a temperature gradient has a uniform heat flux distribution as is shown in Fig. 10(c). In the slip regime, velocity slip occurs at the wall and the velocity distribution in the bulk stream smoothens, as is shown in Fig. 10(b). In contrast, in phonon gas flow, boundary confinement makes the heat flux distribution depart from a uniform profile to a non-uniform one, as is shown in Fig. 10(d). These are actually distinct features of phonon gas and fluid flows: different trends of variation of the flux profile versus Kn from continuum regime to slip regime. This distinction may be caused by R process which destroys the quasi-momentum in phonon transport. The velocity distribution of microscale gas flow have been extensively studied, while there is only few work [266–268] on the heat flux distribution in nanoscale phonon gas flow. Further investigations should be made about this topic in the future.

4.5. *Comparison of phonon hydrodynamics to thermon gas model*

The principles of thermon gas model have been introduced in Sections 1.2.3 and 4.3.2. When Newton's equation is capable of describing the dynamics of thermon gas flow, the heat transport equation is derived [68,100]:

$$\tau_{\mathrm{T}}\frac{\partial \mathbf{q}}{\partial t} + \mathbf{q} + \lambda\nabla T = -\tau_{\mathrm{T}}\nabla\cdot\left(\frac{\mathbf{q}\mathbf{q}}{E}\right), \tag{117}$$

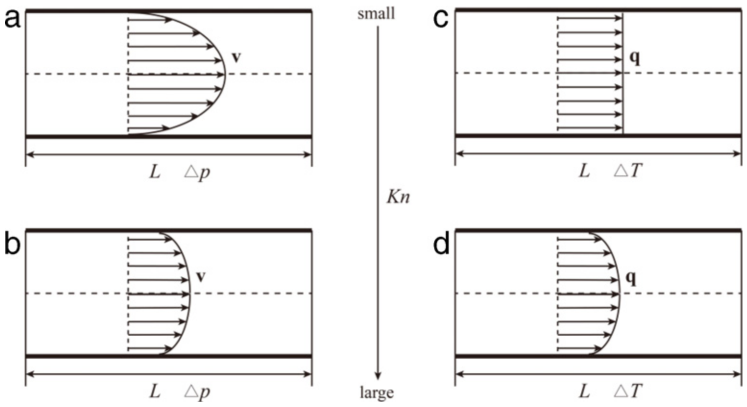

Fig. 10. Comparison between fluid and phonon gas flow.

Table 4
Comparison between phonon hydrodynamics and thermon gas model.

Quantities	Phonon hydrodynamic model	Thermon gas model
Dynamic equation	$\rho\left[\frac{\partial \mathbf{v}}{\partial t}+(\mathbf{v}\cdot\nabla)\,\mathbf{v}\right]=\rho\mathbf{f}-\nabla p+\mu\nabla^2\mathbf{v}$ $+\left(\varsigma+\frac{1}{3}\mu\right)\nabla(\nabla\cdot\mathbf{v})$	$\rho_{\mathrm{T}}\left[\frac{\partial \mathbf{u}_{\mathrm{T}}}{\partial t}+(\mathbf{u}_{\mathrm{T}}\cdot\nabla)\,\mathbf{u}_{\mathrm{T}}\right]=$ $-\nabla p_{\mathrm{T}}+\mathbf{f}_{\mathrm{T}}$
Pressure	$p=\frac{1}{3}E$	$p_{\mathrm{T}}=\gamma\rho_{\mathrm{T}}c_V T=\gamma\rho c_V^2 T^2/c^2$
Mass density	$\rho=\frac{E}{v_{\mathrm{g}}^2}$	$\rho_{\mathrm{T}}=\frac{\rho c_V T}{c^2}=\frac{E}{c^2}$
Drift velocity	$\mathbf{v}=\frac{\mathbf{q}}{E}$	$\mathbf{u}_{\mathrm{T}}=\frac{\mathbf{q}}{\rho c_V T}=\frac{\mathbf{q}}{E}$
Momentum density	$\mathbf{P}=\rho\mathbf{v}=\frac{\mathbf{q}}{v_{\mathrm{g}}^2}$	$\mathbf{P}_{\mathrm{T}}=\rho_{\mathrm{T}}\mathbf{u}_{\mathrm{T}}=\frac{\mathbf{q}}{c^2}$
Resistive force	$\mathbf{f}=-\frac{\mathbf{q}}{\tau_{\mathrm{R}}v_{\mathrm{g}}^2}$	$\mathbf{f}_{\mathrm{T}}=-\frac{6\gamma c_V T}{c^2}\frac{\mathbf{q}}{\tau_{\mathrm{R}}v_{\mathrm{g}}^2}$
Heat transport equation	$\tau_{\mathrm{R}}\frac{\partial \mathbf{q}}{\partial t}+\mathbf{q}+\lambda\nabla T=-\tau_{\mathrm{R}}\nabla\cdot\left(\frac{\mathbf{qq}}{E}\right)+\mu\tau_{\mathrm{R}}v_{\mathrm{g}}^2\nabla^2\frac{\mathbf{q}}{E}$ $+\left(\varsigma+\frac{\mu}{3}\right)\tau_{\mathrm{R}}v_{\mathrm{g}}^2\nabla\left(\nabla\cdot\frac{\mathbf{q}}{E}\right)$	$\tau_{\mathrm{T}}\frac{\partial \mathbf{q}}{\partial t}+\mathbf{q}+\lambda\nabla T=-\tau_{\mathrm{T}}\nabla\cdot\left(\frac{\mathbf{qq}}{E}\right)$
Relaxation times	$\tau_{\mathrm{T}}=\frac{v_{\mathrm{g}}^2}{6\gamma c_V T}\tau_{\mathrm{R}}$	

Note: c is the speed of light.

where τ_{T} denotes the relaxation time of thermon gas with $\tau_{\mathrm{T}}=\tau_{\mathrm{R}}v_{\mathrm{g}}^2/6\gamma c_V T$, γ being the Grüneisen constant of dielectric solid, c_V being the specific heat capacity. Eq. (117) is a generalized heat transport equation beyond Fourier's law and bears similarity to the G–K equation, Eq. (77), except a slight difference on the spatial non-local term of heat flux. Meanwhile, the thermodynamic foundation of the thermon gas model was developed, which [269,270] had no-surprisingly very similar forms to those in extended irreversible thermodynamics for G–K equation [271–273]. The similarities in both mathematical and physical aspects of the two hydrodynamic approaches deserve a further comparison.

The phonon hydrodynamic formalism used in Refs. [196,274] is adopted to make a comparison with the thermon gas model. Many quantities including the pressure, mass density, drift velocity, momentum density, resistance force term and relaxation time of phonon and thermon gas are compared carefully, as is summarized in Table 4. For determination of the relaxation time in both models, the kinetic expression of thermal conductivity $\lambda=C_V\tau_{\mathrm{R}}v_{\mathrm{g}}^2/3$ is used. The heat transport equation in phonon hydrodynamics is a generalized one beyond the G–K equation with an additional nonlinear term usually neglected. Similarity between thermon gas model and phonon hydrodynamic model is explicit. Furthermore, there is usually a ratio between the quantities in the two models, such as v_{g}^2/c^2 between mass densities and between momentum densities. The current analysis contributes to deeper understanding of both models and their relationship.

5. Discussions and perspectives

5.1. Current limitations and possible extensions

All the phonon hydrodynamic models developed based on the kinetic theory are limited to low temperature situation, where N process dominates over R process. Only under this circumstance, could the limit of integration be extended to the whole wave vector space in obtaining the explicit expressions of the macroscopic variables. On the other hand, it is feasible to use the ratio of relaxation times of N process and R process as the small parameter in the Chapman–Enskog solution in Section 3. From the historical perspective, the classical phonon hydrodynamics is originated in seeking second sound, which is possible to be detected only at extremely low temperature and in very pure crystals [81,145]. However, from a physical perspective, the concept of phonon hydrodynamics can be extended beyond its classical definition. In the framework of transport theory shown in Fig. 4(b), phonon hydrodynamics represents more accurately the macroscopic level of description for phonon systems, whereas the G–K equation is merely a special case of hydrodynamic descriptions when N process is the dominated phonon scattering. Another special case is Fourier's law, which is indeed a macroscopic heat transport equation when Umklapp-type R process is dominant. That is to say, there is still a large room for hydrodynamic descriptions in cases where neither N process nor Umklapp-type R process dominates, such as in cases where N process is comparable to Umklapp-type R process, and in nanoscale heat transport where interfacial phonon scattering occurs mainly [38]. We term all these macroscopic models, besides the G–K equation and Fourier's law, as *generalized phonon hydrodynamics*. Under such a new framework, a truly universal hydrodynamic model can be established, and of course, there remains a lot to be done towards that goal. One challenging problem for instance is the integration in a finite range of wave vector space instead of the aforementioned infinite one. Also, a more accurate and detailed understanding and modeling of interfacial phonon transport in nanoscale [34,60] is crucial.

Another limitation in developing phonon hydrodynamic models is the linear approximation. In deriving the G–K equation, nonlinear terms such as the product of heat flux and temperature gradient are neglected. However, nonlinear effects are expected to be very important in nanoscale cases where the heat flux could be extremely high due to the miniature heat flow passage, or in cases under high temperature gradient where the flux-limiter behaviors [275,276] may take place. Some theoretical attempts have been made to investigate the nonlinear effects; for instance, a nonlinear phonon hydrodynamic model [235,277] was developed based on nonequilibrium thermodynamic method, and an exploration was done of the physical consequences of nonlinear terms in a generalized heat transport equation [278]. Nevertheless, to our best knowledge, successful realistic applications of nonlinear phonon hydrodynamics in nanoscale heat transport are seldom reported, and a systematical kinetic derivation of a more general nonlinear theory is still lacking.

5.2. Analysis of N and R process in phonon transport

In modeling micro- and nanoscale phonon transport, the kinetic expression of thermal conductivity tensor is usually given as [14,38,39]:

$$\boldsymbol{\lambda} = \sum_{\nu} \int \tau(\omega)\, \hbar\omega \frac{\mathrm{d}f_{\mathrm{R}}^{\mathrm{eq}}}{\mathrm{d}T} \mathbf{v}_{\mathrm{g}}(\omega)\, \mathbf{v}_{\mathrm{g}}(\omega) \frac{\mathrm{d}\mathbf{k}}{(2\pi)^3}, \tag{118}$$

with ν denoting the phonon branch. Eq. (118) could be derived from phonon Boltzmann equation (14) with SMRT approximation which valued the collision term by $C(f) = \left(f - f_{\mathrm{R}}^{\mathrm{eq}}\right)/\tau(\omega)$. In the neighborhood of equilibrium, phonon distribution function is obtained approximately as $f \approx f_{\mathrm{R}}^{\mathrm{eq}} - \tau(\omega)\left(\mathrm{d}f_{\mathrm{R}}^{\mathrm{eq}}/\mathrm{d}T\right)\mathbf{v}_{\mathrm{g}}(\omega)\cdot\nabla T$. Substitution of this approximate solution into the kinetic expression of heat flux (such as Eq. (28) in the isotropic case) gives rise to Fourier's law and the thermal conductivity expression Eq. (118). To resolve the thermal conductivity, both phonon group velocity and relaxation time must be provided for Eq. (118). The former is computed from the dispersion relation based on (15), whereas the latter is usually obtained in two ways. The popular way is through empirical expressions shown in Table 2, where the empirical parameters are adjusted to fit the bulk thermal conductivity of materials. Different categories of phonon scattering are treated independently and the total relaxation time is derived using the Matthiessen rule [14,44,279]:

$$\frac{1}{\tau(\omega)} = \frac{1}{\tau_{\mathrm{a}}(\omega)} + \frac{1}{\tau_{\mathrm{i}}(\omega)} + \frac{1}{\tau_{\mathrm{b}}(\omega)}, \tag{119}$$

where 'a' denotes the anharmonic phonon scattering [58,121,280,281] (or Umklapp three-phonon scattering process [76,119,120,122]). The other way is through *ab initio* calculation, such as lattice dynamic simulation [58,59] and computing phonon scattering rates from Fermi's golden rule in the first-principle method [71,124].

In summary: (1) the current attempts in modeling size-dependent thermal conductivity of nanostructures are still within the framework of classical Fourier's law, through incorporating the boundary scattering effect by adding an independent contribution to the total relaxation time; (2) there are no unified expressions for the frequency-dependent relaxation times of different kinds of phonon scatterings; (3) N process is often neglected in kinetic modeling of nanoscale phonon transport, or is inappropriately treated as having the same role as R process, as shown in Eqs. (118) and (119).

The treatment of N process is further emphasized because more and more attention is drawn on this issue in last few years. A kinetic-collective model is proposed [114,116,117] to predict lattice thermal conductivity in a wide range of temperature and size. This model is based on two distinct phonon behaviors in kinetic regime at low temperature and in collective regime at elevated temperature, dominated by R process and N process respectively. From our perspective, it is questionable to categorize the collective regime at high temperature where in fact N process is usually scarce in most materials. In microscopic methods: N process and R process are simultaneously taken into account naturally when computing phonon scattering rates by the first-principle calculation [71,72,124]; in lattice dynamics [282] and in molecular dynamics simulation [283], N process is treated as an additional origin of thermal resistance from altering the phonon frequency spectrum. Recent reports [284,285] based on first principle calculations and iterative solutions of linearized phonon Boltzmann equation indicate the dominance of N process and occurrence of hydrodynamic phonon transport even at room temperature in two-dimensional nanomaterials (graphene and so on). This particular phenomenon is mainly attributed to the extremely large anharmonicity and densities of states of long-wavelength phonons characterized by the two-dimensional materials [284], which leads to strong and dominant normal phonon scatterings in a wide range of temperature. An updated review [34] on nanoscale thermal transport also indicated the necessity to go beyond the SMRT approximation and to deal with N process in an appropriate way. As a result of still ambiguous understanding in microscopic and mesoscopic aspects, there is still lacking a widely applicable hydrodynamic model which considers both N and R processes. A rational treatment of N process will be a key point for the advance of generalized phonon hydrodynamics.

5.3. *LBM implementation of phonon hydrodynamics*

Lattice Boltzmann method (LBM) is widely applied in classical hydrodynamics mainly because of its advantages [155,168]: (1) its natural kinetic foundation based on Boltzmann transport equation; (2) its local computational characteristics making it easy to realize parallelization; (3) its simple treatment of complex boundary conditions. With these advantages, LBM will be a promising solver for generalized phonon hydrodynamics in tackling the nanoscale phonon transport problems. Because such problems usually involve multiscale interfaces and complex geometries as in porous nanostructures [260–263] and nano-polycrystalline [286,287] which are potential thermoelectric and thermal barrier materials [288].

Hitherto there are mainly two branches of lattice Boltzmann schemes for phonon transport: one is for the solution of phonon Boltzmann equation with Callaway's relaxation approximation [179] corresponding to hydrodynamics governed by G–K equation; the other is for the solution of phonon Boltzmann equation with SMRT approximation [79,80] corresponding to Fourier's law. The two branches could be unified in the generalized phonon hydrodynamics since the SMRT approximation is a special case of Callaway's relaxation approximation in the limit of $\tau_N \to \infty$. By giving different magnitude of relative values to τ_N and τ_R, LBM will display its robustness in modeling a wide range of phenomena, including those G–K equation and Fourier's law could deal with, and the cases where N process is comparable to R process.

To illustrate the LBM implementation of phonon hydrodynamics, here a brief introduction is given to the LBM scheme for the phonon Boltzmann equation with SMRT approximation. For convenience, the phonon Boltzmann equation is rewritten as the energy density form [79]:

$$\frac{\partial E}{\partial t} + \mathbf{v}_g \cdot \nabla E = -\frac{E - E^{eq}}{\tau_R}, \tag{120}$$

with $E \equiv \int f \hbar\omega D(\omega)\, d\omega$, and $E^{eq} \equiv \int f_R^{eq} \hbar\omega D(\omega)\, d\omega$, $D(\omega)$ being the phonon state density function. Thus the phonon lattice Boltzmann equation is obtained as a discrete form of Eq. (120):

$$E_i(\mathbf{x} + \mathbf{c}_i \Delta t, t + \Delta t) - E_i(\mathbf{x}, t) = -\frac{E_i(\mathbf{x}, t) - E_i^{eq}(\mathbf{x}, t)}{\tau}. \tag{121}$$

In Eq. (121), the non-dimensional relaxation time is $\tau = \tau_R/\Delta t$, Δt being the time step, and the subscripts "i" denote the directional components of a specific lattice structure (for instance D2Q9), with $\mathbf{c}_i$ the lattice velocities in each direction. In this way, phonon transport could be analyzed through an iterative solution of Eq. (121) based on a streaming process and a relaxation process. The macroscopic field variables (temperature, heat flux, etc.) are then obtained through a discrete statistical averaging of the energy density distribution solution E_i.

The field of lattice Boltzmann modeling of phonon transport is still not fully developed. The related fundamental work to be done includes the following aspects: (1) a systematical derivation of the lattice Boltzmann formulation with realistic dimension and clear physical meaning, by bridging the mesoscopic numerical scheme and the macroscopic hydrodynamics; (2) development of practical lattice structures for 2D and 3D cases to avoid the paradox of fictitious phonon speed by capturing more accurately the phonon dynamics; (3) to seek a relatively simple and economic approach to deal with the phonon dispersion spectrum and frequency-dependent relaxation time; (4) to devise proper schemes to treat the interfacial phonon transport, though some attempts were made in Refs. [180,181] but no realistic applications have been reported.

5.4. *Perspectives and open questions*

5.4.1. *Thermal rectification in phononics*

Thermal rectification is an interesting phenomenon where the thermal transport behaviors depend on the sign of temperature gradient [289], viz. the magnitude of heat flux in one direction is different from that in reversed direction. Although such directionality actually exists in conventional heat transport process if we rigorously consider the temperature dependent thermal conductivity of a medium. However, this effect is usually small in macroscale and thus often neglected. With rapidly increasing focus on nanoscale heat transport and artificial manipulation of phononic material properties [290], thermal rectification becomes a hot topic due to its appreciable effect and potential applications in thermal management of micro- and nanoelectronics [289], and in nanoscale phononic devices including thermal diodes, thermal transistors, thermal logic gates and thermal memories potentially used in information processing [291,292]. Actually, thermal rectification holds the similar idea to the current developing field of thermal control by means of heat metamaterials [293], where many interesting phenomena could be designed and applied such as the thermal cloaking [294,295] and thermal camouflage [296].

The usual mechanisms responsible for nanoscale thermal rectification include: nonlinear (anharmonic) lattice chain [297,298], asymmetric nanostructures (such as the graphene [299,300] and silicon [301] ribbons with variable widths, the carbon nano-cone [302]), surface roughness at contacts and interfaces, and hetero-junctions [303]. Different physical explanations have been proposed in literature, such as the overlapping of phonon state density in nonlinear lattice [297,298], phonon lateral confinement effect [300] and phonon transmission characteristic [301] in asymmetric nano ribbons. A sufficient understanding is still lacking though. From our perspective, the generalized phonon hydrodynamics provides an alternative to offer an intuitive explanation. For instance, in heat transport through asymmetric nano ribbons, phonon gas flow, from a hydrodynamic viewpoint, will endure different resistance from the confined boundary in converse directions. Similar analysis can be applied to study the effect of wall roughness or internal pores on the rectification efficiency of nanostructures. It opens a new outlook for investigating the thermal rectification phenomena, and lots of explorations to be done in the future.

5.4.2. Heat waves in temporal microscale

If G–K equation (77) is combined with the energy balance equation (55), a temperature differential equation is obtained:

$$\nabla^2 T + \frac{9\tau_\mathrm{N}}{5}\frac{\partial}{\partial t}\left(\nabla^2 T\right) = \frac{3}{\tau_\mathrm{R} v_\mathrm{g}^2}\frac{\partial T}{\partial t} + \frac{3}{v_\mathrm{g}^2}\frac{\partial^2 T}{\partial t^2}. \tag{122}$$

When N process dominates and R process is negligible ($\tau_\mathrm{N} \to 0,\ \ \tau_\mathrm{R} \to \infty$) in low temperature dielectric solid, Eq. (122) reduces to a pure wave equation:

$$\nabla^2 T = \frac{3}{v_\mathrm{g}^2}\frac{\partial^2 T}{\partial t^2}. \tag{123}$$

Eq. (123) predicts a wave propagation of temperature disturbance (the second sound) with the speed of $v_\mathrm{g}/\sqrt{3}$. Such an ideal heat wave without damping has never been observed in actual experiments. Instead, the observation window for the second sound is [81,109]: $\tau_\mathrm{N} \ll 1/\omega \ll \tau_\mathrm{R}$, with ω the frequency of external heat pulse. Within this window, N process and R process coexist with few R processes but sufficient N processes. Therefore, heat waves in low temperature crystal are mainly attributed to N process. Another similar case is the second sound in superfluid helium made up of a viscous normal fluid and an inviscid superfluid. Its propagating speed is $\sqrt{Ts^2\rho_s/c_p\rho}$ [133], where s is the entropy function, ρ is the total mass density and ρ_s is the mass density of superfluid. The second sound speed vanishes when $\rho_s = 0$ at the so-called λ-phase transition point [133] where all the superfluid transforms into normal fluid. In contrast, at lower temperature below the λ-phase transition point when the superfluid dominates, the second sound with rare damping propagates with a speed about $v_\mathrm{g}/\sqrt{3}$ [133]. Thus the heat waves in low temperature superfluid helium are mainly attributed to the superfluid component.

Moreover, a hot topic has been extensively reported about heat waves in temporal microscale at ambient temperature [88,304–306], when the characteristic time of heat transport is comparable to or smaller than the carrier relaxation time. The C–V equation is a typical model which tries to capture this heat wave behavior by adding a relaxation term of heat flux into Fourier's law. Combination of C–V equation with energy balance equation results in a hyperbolic temperature differential equation, which in turn predicts a propagation of damping temperature wave. However, numerical simulations by MD [307–309] and LBM [310] demonstrate that the C–V equation is unable to describe the short-pulsed laser heating process both in bulk materials and nanostructures (carbon nanotube in Ref. [308] and graphene in Ref. [309]). Experimental attempt [311,312] to seek such heat waves and verify the C–V equation in inhomogeneous medium fails as well, and subsequently, more accurate experiments [313–315] show that Fourier's law could actually explain the results. By contrast, the temporal microscale temperature response behaviors obtained in experiments [305,316] and MD simulation [308,309] fitted reasonably well to the DPL model by adjusting the two phase lags τ_q and τ_T. In spite of this success, the DPL model gives rise to a parabolic temperature differential equation [37], with no supportive evidence of heat waves in temporal microscale.

To sum up, besides the second sound observed in superfluid system and in dielectric solid at low temperature, no experimental reports have been made about the heat waves in temporal microscale at ambient temperature. In fact, the situations are different at low temperature and at ambient temperature, where the key point lies in the local equilibrium hypothesis [219] from a thermodynamic perspective. In the former situation, such as during heat wave propagation in dielectric solid, the mean free path of N process is much smaller than the sample dimension. Thus there are sufficient phonon normal scatterings through the solid from the hot side to the cold side [139], which ensures the local thermal equilibrium. As is also shown in Section 3, the local equilibrium hypothesis is implicitly valid in the derivation of G–K equation, which can explain the heat waves satisfactorily. In the latter situation, the characteristic time is too short to allow sufficient time for heat exchange and thermalization between phonons. Thus the local equilibrium hypothesis is no longer valid [39]. As C–V equation is derived from the phonon Boltzmann equation under local equilibrium, it fails to describe the temporal

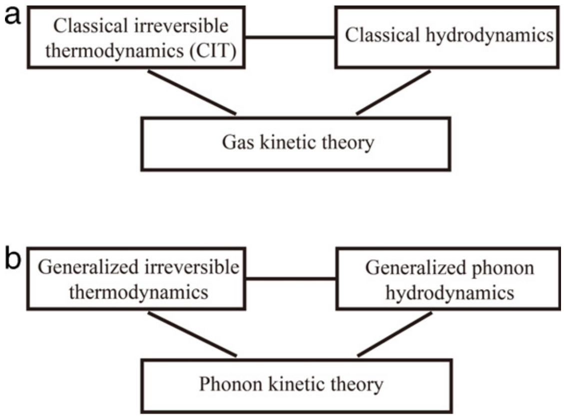

Fig. 11. Theoretical systems of fluid transport (a) and phonon transport (b).

microscale heat transport [317,318]. The existing strong thermal nonequilibrium makes it difficult to find an appropriate macroscopic model to describe the heat transport behavior in this situation.

Finally, from our perspective, the above divergence could be taken as two extreme cases in the generalized phonon hydrodynamics. The second sound observed in low temperature corresponds to N process dominated situation; whereas heat transport in temporal microscale at ambient temperature corresponds to R process dominated one. Further investigation is highly desirable about the temporal microscale phonon heat transport, where a macroscopic model is needed to describe the temperature response behavior. The important question remains to be answered: whether heat waves exist in very short time scale.

5.4.3. Compatible irreversible thermodynamics

Classical irreversible thermodynamics (CIT) has been well developed under the local equilibrium hypothesis. The linear phenomenological thermodynamic force-flux relation ensuring non-negative entropy production gives rise to Newton's shear law. Substitution of the shear law into the momentum balance equation results in the Navier–Stokes equation [219]. That is, CIT provides a solid thermodynamic framework for classical hydrodynamics. In addition, the first-order Chapman–Enskog expansion to Boltzmann transport equation can also yield the Navier–Stokes equation [154]; the entropy balance equation and expressions of entropy flux in CIT can be derived from the kinetic theory of gases [40,219]. Therefore, the gas kinetic theory forms a mesoscopic foundation for both the thermodynamic theory and hydrodynamics. The theoretical system of fluid transport is summarized in Fig. 11(a).

In comparison, compatible irreversible thermodynamics for generalized phonon hydrodynamics is not fully accomplished yet. Although the two extreme cases of Fourier's law and G–K equation have been derived from CIT and extended irreversible thermodynamics (EIT) respectively, they have not essentially gone beyond the near-equilibrium region. It is still an open challenge to establish a thermodynamic formalism valid for far-from-equilibrium region. For processes where the local equilibrium hypothesis is no longer valid, usually the case in nanoscale heat transport such as the heat waves in temporal microscale, the theoretical system of phonon transport shown in Fig. 11(b) provides a future solution, to be finished through further work on both the phonon hydrodynamic models and the thermodynamic formulations.

6. Conclusions

Understanding the laws of heat transport and conversion is a critical task since most of human's activities are pertinent to thermal energy utilization. Heat transport theory is a relatively abstract and obscure branch in physical science because heat could only be felt rather than directly observed. This situation especially worsens when it comes to microscale and nanoscale, where traditional concepts and laws may not be valid. The phonon hydrodynamics provides a potential avenue for heat transport modeling due to its simple and intuitive nature and solid statistical physical roots. A comprehensive introduction is provided in the present work regarding the theoretical foundation and credible application of this model.

A phonon can be treated as a quasi-particle by applying the Boltzmann transport equation a priori, and the coarse graining of the phonon distribution function governed by the Boltzmann equation results in the hydrodynamic heat transport equations. This constitutes a formal theoretical frame for phonon transport in view of microscopic, mesoscopic and macroscopic descriptions. A unified kinetic framework is established through a Chapman–Enskog solution to the phonon Boltzmann equation with Callaway's relaxation approximation. Different orders of expansions and sub-order approximations give rise to different levels of heat transport equations, including both the well-known C–V equation and G–K equation. Previous hydrodynamic models obtained by Eigen-value analysis method, Chapman–Enskog method and moment method can be incorporated into our present framework as special cases. In terms of applications, the essential heat flux boundary is originated from a heuristic analogy to velocity slip boundary in microscale gas flows. In the line of extended irreversible thermodynamics, the hydrodynamic equation and heat flux boundary can also be derived as the constitutive relations in the bulk and boundary region, respectively. In modeling the size-dependent thermal conductivity of nanostructures, the phonon hydrodynamics displays not only a clear qualitative physical picture, but also good quantitative predictions in agreement with experimental results.

Finally, a novel concept of generalized phonon hydrodynamics is proposed, covering the G–K equation and Fourier's law as two extreme cases. In this extended conceptual framework, possible advances are discussed in dealing with phonon N process, developing phonon lattice Boltzmann schemes and exploring the thermal rectification phenomena in micro/nano-phononics. Novel viewpoints are also given to a few open questions including whether the heat waves exist in extremely short time scales at ambient temperature, and the compatible irreversible thermodynamic formulation. Many original references are given throughout this work to reveal the historical logic and the indication for future development. Therefore the authors hope the present work would contribute to the knowledge base about the nanoscale heat transport and its macroscopic modeling.

Acknowledgments

This work is financially supported by the NSF grant of China (Nos. 51176089, 51321002), the Key Basic Scientific Research Program (2013CB228301) and the Tsinghua University Initiative Scientific Research Program. The authors appreciate helpful discussions with Prof. D. Jou, Prof. N. Hadjiconstantinou, Prof. N. Pan, Prof. H. Zhai, Prof. S. Chen and the anonymous reviewers.

Appendix A. The sub-first-order approximation of zeroth-order expansion

A.1. Phonon energy density

$$E = \int \hbar\omega f_{\mathrm{N}}^{\mathrm{eq}} \frac{3\mathrm{d}\mathbf{k}}{(2\pi)^3}. \tag{A.1}$$

Substitution of Eq. (51) into Eq. (A.1) results in:

$$\begin{aligned} E &= \int \left[\hbar\omega f_{\mathrm{R}}^{\mathrm{eq}} + \hbar\omega \frac{\hbar\mathbf{k}\cdot\mathbf{u}}{k_{\mathrm{B}}T} f_{\mathrm{R}}^{\mathrm{eq}}\left(1+f_{\mathrm{R}}^{\mathrm{eq}}\right)\right] \frac{3\mathrm{d}\mathbf{k}}{(2\pi)^3} \\ &= \int \hbar\omega f_{\mathrm{R}}^{\mathrm{eq}} \frac{3\mathrm{d}\mathbf{k}}{(2\pi)^3} + \int \hbar\omega \frac{\hbar\mathbf{k}\cdot\mathbf{u}}{k_{\mathrm{B}}T} f_{\mathrm{R}}^{\mathrm{eq}}\left(1+f_{\mathrm{R}}^{\mathrm{eq}}\right) \frac{3\mathrm{d}\mathbf{k}}{(2\pi)^3}. \end{aligned} \tag{A.2}$$

The second term in Eq. (A.2) vanishes because the integrand is an odd function of wave vector **k**. Thus Eq. (A.2) reduces to:

$$E = \int \hbar\omega f_{\mathrm{R}}^{\mathrm{eq}} \frac{3\mathrm{d}\mathbf{k}}{(2\pi)^3} = \int \hbar\omega \left[\exp\left(\frac{\hbar\omega}{k_{\mathrm{B}}T}\right) - 1\right]^{-1} \frac{3\mathrm{d}\mathbf{k}}{(2\pi)^3}. \tag{A.3}$$

Combined with the linear dispersion relation ($\omega = v_{\mathrm{g}}k$), Eq. (A.3) becomes:

$$\begin{aligned} E &= \frac{3}{(2\pi)^3} \int_0^\infty \hbar v_{\mathrm{g}} k \left[\exp\left(\frac{\hbar v_{\mathrm{g}} k}{k_{\mathrm{B}}T}\right) - 1\right]^{-1} 4\pi k^2 \mathrm{d}k \\ &= \frac{3}{2\pi^2} \hbar v_{\mathrm{g}} \int_0^\infty \left[\exp\left(\frac{\hbar v_{\mathrm{g}} k}{k_{\mathrm{B}}T}\right) - 1\right]^{-1} k^3 \mathrm{d}k. \end{aligned} \tag{A.4}$$

With the well-known Bose integral:

$$\int_0^\infty \frac{x^3}{\exp(x) - 1} \mathrm{d}x = \frac{1}{15}\pi^4, \tag{A.5}$$

Eq. (A.4) finally gives rise to:

$$E = \frac{4\pi^5 (k_{\mathrm{B}}T)^4}{5\left(h v_{\mathrm{g}}\right)^3}. \tag{A.6}$$

A.2. Heat flux

$$\mathbf{q} = \int \mathbf{v}_{\mathrm{g}} \hbar\omega f_{\mathrm{N}}^{\mathrm{eq}} \frac{3\mathrm{d}\mathbf{k}}{(2\pi)^3}. \tag{A.7}$$

Substitution of Eq. (51) into Eq. (A.7) results in:

$$\begin{aligned}\mathbf{q} &= \int \left[\mathbf{v}_{\mathrm{g}}\hbar\omega f_{\mathrm{R}}^{\mathrm{eq}} + \mathbf{v}_{\mathrm{g}}\hbar\omega \frac{\hbar\mathbf{k}\cdot\mathbf{u}}{k_{\mathrm{B}}T} f_{\mathrm{R}}^{\mathrm{eq}}\left(1+f_{\mathrm{R}}^{\mathrm{eq}}\right)\right]\frac{3\mathrm{d}\mathbf{k}}{(2\pi)^3} \\ &= \int \mathbf{v}_{\mathrm{g}}\hbar\omega f_{\mathrm{R}}^{\mathrm{eq}}\frac{3\mathrm{d}\mathbf{k}}{(2\pi)^3} + \int \mathbf{v}_{\mathrm{g}}\hbar\omega\frac{\hbar\mathbf{k}\cdot\mathbf{u}}{k_{\mathrm{B}}T} f_{\mathrm{R}}^{\mathrm{eq}}\left(1+f_{\mathrm{R}}^{\mathrm{eq}}\right)\frac{3\mathrm{d}\mathbf{k}}{(2\pi)^3}.\end{aligned} \tag{A.8}$$

Combined with Eqs. (25), (A.8) becomes after eliminating the phonon group velocity:

$$\mathbf{q} = \hbar v_{\mathrm{g}}^2 \int \mathbf{k} f_{\mathrm{R}}^{\mathrm{eq}}\frac{3\mathrm{d}\mathbf{k}}{(2\pi)^3} + \frac{\left(\hbar v_{\mathrm{g}}\right)^2}{k_{\mathrm{B}}T}\mathbf{u}\cdot\int \mathbf{k}\mathbf{k} f_{\mathrm{R}}^{\mathrm{eq}}\left(1+f_{\mathrm{R}}^{\mathrm{eq}}\right)\frac{3\mathrm{d}\mathbf{k}}{(2\pi)^3}. \tag{A.9}$$

The first term in Eq. (A.9) vanishes for the equilibrium distribution contributes nothing to the heat flux. Thus Eq. (A.9) reduces to:

$$\mathbf{q} = \frac{\left(\hbar v_{\mathrm{g}}\right)^2}{k_{\mathrm{B}}T}\mathbf{u}\cdot\int \mathbf{k}\mathbf{k} f_{\mathrm{R}}^{\mathrm{eq}}\left(1+f_{\mathrm{R}}^{\mathrm{eq}}\right)\frac{3\mathrm{d}\mathbf{k}}{(2\pi)^3}. \tag{A.10}$$

Based on the parity of the integrand, Eq. (A.10) becomes:

$$\begin{aligned}\mathbf{q} &= \frac{\left(\hbar v_{\mathrm{g}}\right)^2}{k_{\mathrm{B}}T}\mathbf{u}\cdot\frac{1}{3}\mathbf{I}\int k^2 f_{\mathrm{R}}^{\mathrm{eq}}\left(1+f_{\mathrm{R}}^{\mathrm{eq}}\right)\frac{3\mathrm{d}\mathbf{k}}{(2\pi)^3} \\ &= \frac{1}{(2\pi)^3}\frac{\left(\hbar v_{\mathrm{g}}\right)^2}{k_{\mathrm{B}}T}\mathbf{u}\int_0^\infty k^2 f_{\mathrm{R}}^{\mathrm{eq}}\left(1+f_{\mathrm{R}}^{\mathrm{eq}}\right)4\pi k^2\mathrm{d}k \\ &= \frac{1}{2\pi^2}\frac{\left(\hbar v_{\mathrm{g}}\right)^2}{k_{\mathrm{B}}T}\mathbf{u}\int_0^\infty k^4 f_{\mathrm{R}}^{\mathrm{eq}}\left(1+f_{\mathrm{R}}^{\mathrm{eq}}\right)\mathrm{d}k \\ &= \frac{1}{2\pi^2}\frac{\left(\hbar v_{\mathrm{g}}\right)^2}{k_{\mathrm{B}}T}\mathbf{u}\int_0^\infty \frac{k^4\exp\left(\frac{\hbar v_{\mathrm{g}}k}{k_{\mathrm{B}}T}\right)}{\left[\exp\left(\frac{\hbar v_{\mathrm{g}}k}{k_{\mathrm{B}}T}\right)-1\right]^2}\mathrm{d}k.\end{aligned} \tag{A.11}$$

With the following integral:

$$\int_0^\infty \frac{x^4\exp(x)}{[\exp(x)-1]}\mathrm{d}x = \frac{4}{15}\pi^4, \tag{A.12}$$

Eq. (A.11) finally gives rise to:

$$\mathbf{q} = \frac{16\pi^5\left(k_{\mathrm{B}}T\right)^4}{15\left(hv_{\mathrm{g}}\right)^3}\mathbf{u}. \tag{A.13}$$

A.3. *The flux of heat flux*

$$\mathbf{Q} = \int \mathbf{v}_{\mathrm{g}}\mathbf{v}_{\mathrm{g}}\hbar\omega f_{\mathrm{N}}^{\mathrm{eq}}\frac{3\mathrm{d}\mathbf{k}}{(2\pi)^3}. \tag{A.14}$$

Substitution of Eq. (51) into Eq. (A.14), combined with Eq. (25), results in:

$$\begin{aligned}\mathbf{Q} &= \hbar v_{\mathrm{g}}^3\int\left[\frac{\mathbf{k}\mathbf{k}}{k}f_{\mathrm{R}}^{\mathrm{eq}} + \frac{\mathbf{k}\mathbf{k}}{k}\frac{\hbar\mathbf{k}\cdot\mathbf{u}}{k_{\mathrm{B}}T}f_{\mathrm{R}}^{\mathrm{eq}}\left(1+f_{\mathrm{R}}^{\mathrm{eq}}\right)\right]\frac{3\mathrm{d}\mathbf{k}}{(2\pi)^3} \\ &= \hbar v_{\mathrm{g}}^3\int\frac{\mathbf{k}\mathbf{k}}{k}f_{\mathrm{R}}^{\mathrm{eq}}\frac{3\mathrm{d}\mathbf{k}}{(2\pi)^3} + \frac{\hbar\mathbf{u}}{k_{\mathrm{B}}T}\cdot\int\frac{\mathbf{k}\mathbf{k}\mathbf{k}}{k}f_{\mathrm{R}}^{\mathrm{eq}}\left(1+f_{\mathrm{R}}^{\mathrm{eq}}\right)\frac{3\mathrm{d}\mathbf{k}}{(2\pi)^3}.\end{aligned} \tag{A.15}$$

The second term in Eq. (A.15) vanishes because the integrand is an odd function of wave vector **k**. Thus Eq. (A.15) reduces to:

$$\mathbf{Q} = \hbar v_{\mathrm{g}}^3\int\frac{\mathbf{k}\mathbf{k}}{k}f_{\mathrm{R}}^{\mathrm{eq}}\frac{3\mathrm{d}\mathbf{k}}{(2\pi)^3}. \tag{A.16}$$

Based on the parity characteristic and combined with Eqs. (A.3), (A.16) reduces to:

$$\mathbf{Q} = \frac{1}{3}\hbar v_{\mathrm{g}}^3\mathbf{I}\int\frac{k^2}{k}f_{\mathrm{R}}^{\mathrm{eq}}\frac{3\mathrm{d}\mathbf{k}}{(2\pi)^3} = \frac{1}{3}v_{\mathrm{g}}^2\mathbf{I}\int\hbar\omega f_{\mathrm{R}}^{\mathrm{eq}}\frac{3\mathrm{d}\mathbf{k}}{(2\pi)^3} = \frac{1}{3}v_{\mathrm{g}}^2E\mathbf{I}. \tag{A.17}$$

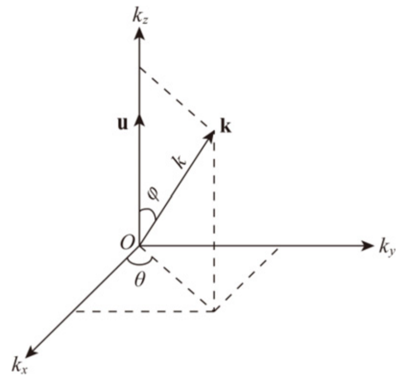

Fig. B.1. Spherical coordinate in wave vector space.

Appendix B. The full zeroth-order expansion

The following integration is conducted in the framework of a spherical coordinate shown in Fig. B.1. The relations between the spherical coordinate variables and wave vector components are:

$$k_x = k \sin\varphi \cos\theta, \tag{B.18a}$$

$$k_y = k \sin\varphi \sin\theta, \tag{B.18b}$$

$$k_z = k \cos\varphi. \tag{B.18c}$$

The differential volume element is:

$$\mathrm{d}\mathbf{k} = k^2 \sin\varphi \mathrm{d}\varphi \mathrm{d}k \mathrm{d}\theta. \tag{B.19}$$

B.1. Phonon energy density

The expression of phonon energy density in the whole zeroth-order expansion is:

$$E = \int \hbar\omega \left[\exp\left(\frac{\hbar\omega - \hbar\mathbf{k}\cdot\mathbf{u}}{k_\mathrm{B}T}\right) - 1\right]^{-1} \frac{3\mathrm{d}\mathbf{k}}{(2\pi)^3}. \tag{B.20}$$

For the sake of simplicity, the drift velocity is set to be parallel to the k_z axis as shown in Fig. B.1, since the integration is invariable under the rotation operation of the coordinates. In this way, Eq. (B.20) reduces to:

$$E = \frac{3}{(2\pi)^3} \int_0^{2\pi} \int_0^{\infty} \int_0^{\pi} \hbar v_\mathrm{g} \left[\exp\left(\frac{\hbar v_\mathrm{g} k - \hbar k u \cos\varphi}{k_\mathrm{B}T}\right) - 1\right]^{-1} k^3 \sin\varphi \mathrm{d}\varphi \mathrm{d}k \mathrm{d}\theta. \tag{B.21}$$

Variable transformations are assumed:

$$m = \frac{\hbar v_\mathrm{g} k - \hbar k u \cos\varphi}{k_\mathrm{B}T}, \tag{B.22}$$

$$x = \cos\varphi. \tag{B.23}$$

With Eqs. (B.22) and (B.23), Eq. (B.21) simplifies into:

$$E = \frac{3}{(2\pi)^2} \hbar v_\mathrm{g} (k_\mathrm{B}T)^4 \int_0^{\infty} \frac{m^3}{\exp(m) - 1} \mathrm{d}m \int_{-1}^{1} \frac{1}{\left(\hbar v_\mathrm{g} - \hbar u x\right)^4} \mathrm{d}x, \tag{B.24}$$

which finally results in:

$$E = \frac{4\pi^5 (k_\mathrm{B}T)^4}{15 \left(h v_\mathrm{g}\right)^3} \frac{\chi^2 + 3}{\left(1 - \chi^2\right)^3}, \tag{B.25}$$

with the ratio of phonon drift speed to group speed $\chi \equiv u/v_\mathrm{g}$.

B.2. Heat flux

The expression of heat flux in the whole zeroth-order expansion is:

$$\mathbf{q} = \int \mathbf{v}_{\mathrm{g}} \hbar\omega \left[\exp\left(\frac{\hbar\omega - \hbar\mathbf{k}\cdot\mathbf{u}}{k_{\mathrm{B}}T} \right) - 1 \right]^{-1} \frac{3\mathrm{d}\mathbf{k}}{(2\pi)^3}. \tag{B.26}$$

Eq. (B.26) simplifies into the following components through variable transformations Eqs. (B.22) and (B.23):

$$q_x = 0, \tag{B.27a}$$

$$q_y = 0, \tag{B.27b}$$

$$q_z = \frac{3}{(2\pi)^2} \hbar v_{\mathrm{g}}^2 (k_{\mathrm{B}}T)^4 \int_0^{\infty} \frac{m^3}{\exp(m) - 1} \mathrm{d}m \int_{-1}^{1} \frac{x}{\left(\hbar v_{\mathrm{g}} - \hbar u x\right)^4} \mathrm{d}x. \tag{B.27c}$$

Combined with Eqs. (A.5), (B.27c) becomes:

$$q_z = \frac{16\pi^5 (k_{\mathrm{B}}T)^4}{15 \left(h v_{\mathrm{g}}\right)^3} \frac{1}{\left(1 - \chi^2\right)^3} u. \tag{B.28}$$

Thus the heat flux finally becomes:

$$\mathbf{q} = \frac{16\pi^5 (k_{\mathrm{B}}T)^4}{15 \left(h v_{\mathrm{g}}\right)^3} \frac{1}{\left(1 - \chi^2\right)^3} \mathbf{u}. \tag{B.29}$$

B.3. The flux of heat flux

The expression of the flux of heat flux in the whole zeroth-order expansion is:

$$\mathbf{Q} = \int \mathbf{v}_{\mathrm{g}} \mathbf{v}_{\mathrm{g}} \hbar\omega \left[\exp\left(\frac{\hbar\omega - \hbar\mathbf{k}\cdot\mathbf{u}}{k_{\mathrm{B}}T} \right) - 1 \right]^{-1} \frac{3\mathrm{d}\mathbf{k}}{(2\pi)^3}. \tag{B.30}$$

Eq. (B.30) simplifies into the following components through variable transformations Eqs. (B.22) and (B.23):

$$Q_{ij} = 0, \quad \text{for } i \neq j, \tag{B.31a}$$

$$Q_{xx} = Q_{yy} = \frac{3}{8\pi^2} \hbar v_{\mathrm{g}}^3 (k_{\mathrm{B}}T)^4 \int_0^{\infty} \frac{m^3}{\exp(m) - 1} \mathrm{d}m \int_{-1}^{1} \frac{1 - x^2}{\left(\hbar v_{\mathrm{g}} - \hbar u x\right)^4} \mathrm{d}x, \tag{B.31b}$$

$$Q_{zz} = \frac{3}{(2\pi)^2} \hbar v_{\mathrm{g}}^3 (k_{\mathrm{B}}T)^4 \int_0^{\infty} \frac{m^3}{\exp(m) - 1} \mathrm{d}m \int_{-1}^{1} \frac{x^2}{\left(\hbar v_{\mathrm{g}} - \hbar u x\right)^4} \mathrm{d}x. \tag{B.31c}$$

Combined with Eq. (A.5), Eq. (B.31b) and Eq. (B.31c) becomes respectively:

$$Q_{xx} = Q_{yy} = v_{\mathrm{g}}^2 \frac{4\pi^5 (k_{\mathrm{B}}T)^4}{15 \left(h v_{\mathrm{g}}\right)^3} \frac{1}{\left(1 - \chi^2\right)^2}, \tag{B.32a}$$

$$Q_{zz} = v_{\mathrm{g}}^2 \frac{4\pi^5 (k_{\mathrm{B}}T)^4}{15 \left(h v_{\mathrm{g}}\right)^3} \frac{1 + 3\chi^2}{\left(1 - \chi^2\right)^3}. \tag{B.32b}$$

Thus the flux of heat flux finally becomes:

$$\begin{aligned} \mathbf{Q} &= Q_{xx} \begin{pmatrix} 1 & 0 & 0 \\ 0 & 1 & 0 \\ 0 & 0 & 0 \end{pmatrix} + Q_{zz} \begin{pmatrix} 0 & 0 & 0 \\ 0 & 0 & 0 \\ 0 & 0 & 1 \end{pmatrix} \\ &= Q_{xx} \mathbf{I} + \left(Q_{zz} - Q_{xx}\right) \hat{\mathbf{u}}\hat{\mathbf{u}} \end{aligned} \tag{B.33}$$

with $\hat{\mathbf{u}}$ denoting a unit vector parallel to $\mathbf{u}$. Substitution of Eqs. (B.32a) and (B.32b) into Eq. (B.33) finally gives rise to:

$$\mathbf{Q} = v_{\mathrm{g}}^2 \frac{4\pi^5 (k_{\mathrm{B}}T)^4}{15 \left(h v_{\mathrm{g}}\right)^3} \frac{1}{\left(1 - \chi^2\right)^2} \mathbf{I} + \frac{16\pi^5 (k_{\mathrm{B}}T)^4}{15 \left(h v_{\mathrm{g}}\right)^3} \frac{1}{\left(1 - \chi^2\right)^3} \mathbf{u}\mathbf{u}. \tag{B.34}$$

Appendix C. The sub-first-order approximation of first-order expansion

C.1. Derivation of $\mathbf{Q}_{1,\mathrm{I}}$

$$\begin{aligned}\mathbf{Q}_{1,\mathrm{I}} &= -\hbar v_{\mathrm{g}}^3 \int \frac{\tau_{\mathrm{N}}\mathbf{kk}}{k}\left\{-\frac{1}{C_V}\frac{\partial q_j}{\partial x_{1j}}\left[f_{\mathrm{R}}^{\mathrm{eq}}\left(1+f_{\mathrm{R}}^{\mathrm{eq}}\right)\frac{\hbar v_{\mathrm{g}} k}{k_{\mathrm{B}}T^2}\right]\right\}\frac{3\mathrm{d}\mathbf{k}}{(2\pi)^3} \\ &= \frac{\hbar^2\, v_{\mathrm{g}}^4\tau_{\mathrm{N}}}{C_V k_{\mathrm{B}}T^2}\frac{\partial q_j}{\partial x_{1j}}\frac{1}{3}\mathbf{I}\int k^2\left[f_{\mathrm{R}}^{\mathrm{eq}}\left(1+f_{\mathrm{R}}^{\mathrm{eq}}\right)\right]\frac{3\mathrm{d}\mathbf{k}}{(2\pi)^3} \\ &= \frac{\hbar^2\, v_{\mathrm{g}}^4\tau_{\mathrm{N}}}{C_V k_{\mathrm{B}}T^2}\frac{\partial q_j}{\partial x_{1j}}\frac{1}{2\pi^2}\mathbf{I}\int_0^{\infty}\frac{k^4\exp\left(\frac{\hbar v_{\mathrm{g}}k}{k_{\mathrm{B}}T}\right)}{\left[\exp\left(\frac{\hbar v_{\mathrm{g}}k}{k_{\mathrm{B}}T}\right)-1\right]^2}\mathrm{d}k.\end{aligned} \tag{C.35}$$

Combined with Eqs. (A.12), (C.35) results in:

$$\left(\mathbf{Q}_{1,\mathrm{I}}\right)_{mn} = \frac{1}{3}v_{\mathrm{g}}^2\tau_{\mathrm{N}}\frac{\partial q_i}{\partial x_{1i}}\delta_{mn}. \tag{C.36}$$

C.2. Derivation of $\mathbf{Q}_{1,\mathrm{II}}$

$$\begin{aligned}\mathbf{Q}_{1,\mathrm{II}} &= -\hbar v_{\mathrm{g}}^3 \int \frac{\tau_{\mathrm{N}}\mathbf{kk}}{k}\left\{\frac{v_{\mathrm{g}}}{k}\frac{\hbar k_i k_j}{k_{\mathrm{B}}T}f_{\mathrm{R}}^{\mathrm{eq}}\left(1+f_{\mathrm{R}}^{\mathrm{eq}}\right)\frac{3}{4}\frac{\partial}{\partial x_{1i}}\left(\frac{q_j}{E}\right)\right\}\frac{3\mathrm{d}\mathbf{k}}{(2\pi)^3} \\ &= -\frac{3}{4}\frac{\partial}{\partial x_{1i}}\left(\frac{q_j}{E}\right)\frac{\hbar^2\, v_{\mathrm{g}}^4\tau_{\mathrm{N}}}{k_{\mathrm{B}}T}\int\frac{\mathbf{kk}k_i k_j}{k^2}f_{\mathrm{R}}^{\mathrm{eq}}\left(1+f_{\mathrm{R}}^{\mathrm{eq}}\right)\frac{3\mathrm{d}\mathbf{k}}{(2\pi)^3}.\end{aligned} \tag{C.37}$$

The following integration is performed:

$$\left[\int\frac{\mathbf{kk}k_i k_j}{k^2}f_{\mathrm{R}}^{\mathrm{eq}}\left(1+f_{\mathrm{R}}^{\mathrm{eq}}\right)\frac{3\mathrm{d}\mathbf{k}}{(2\pi)^3}\right]_{ijmn} = \frac{1}{15}\left(\delta_{ij}\delta_{mn}+\delta_{im}\delta_{nj}+\delta_{in}\delta_{mj}\right)\int k^2 f_{\mathrm{R}}^{\mathrm{eq}}\left(1+f_{\mathrm{R}}^{\mathrm{eq}}\right)\frac{3\mathrm{d}\mathbf{k}}{(2\pi)^3}. \tag{C.38}$$

Substitution of Eq. (C.38) into Eq. (C.37), combined with Eqs. (C.35) and (A.12), results in:

$$\left(\mathbf{Q}_{1,\mathrm{II}}\right)_{mn} = -\frac{1}{5}v_{\mathrm{g}}^2 E\tau_{\mathrm{N}}\left[\frac{\partial}{\partial x_{1i}}\left(\frac{q_i}{E}\right)\delta_{mn}+\frac{\partial}{\partial x_{1m}}\left(\frac{q_n}{E}\right)+\frac{\partial}{\partial x_{1n}}\left(\frac{q_m}{E}\right)\right]. \tag{C.39}$$

C.3. Derivation of $\mathbf{Q}_{1,\mathrm{III}}$

$$\begin{aligned}\mathbf{Q}_{1,\mathrm{III}} &= -\hbar v_{\mathrm{g}}^3 \int \frac{\tau_{\mathrm{N}}\mathbf{kk}}{k}\left\{\frac{v_{\mathrm{g}}}{k}k_i\frac{\partial T}{\partial x_{1i}}\left[f_{\mathrm{R}}^{\mathrm{eq}}\left(1+f_{\mathrm{R}}^{\mathrm{eq}}\right)\frac{\hbar v_{\mathrm{g}}k}{k_{\mathrm{B}}T^2}\left(2f_{\mathrm{R}}^{\mathrm{eq}}+1\right)\frac{\hbar\mathbf{k}\cdot\mathbf{u}}{k_{\mathrm{B}}T}-f_{\mathrm{R}}^{\mathrm{eq}}\left(1+f_{\mathrm{R}}^{\mathrm{eq}}\right)\frac{\hbar\mathbf{k}\cdot\mathbf{u}}{k_{\mathrm{B}}T^2}\right]\right\}\frac{3\mathrm{d}\mathbf{k}}{(2\pi)^3} \\ &= -\frac{\hbar^3\, v_{\mathrm{g}}^5\tau_{\mathrm{N}}}{k_{\mathrm{B}}^2T^3}\frac{\partial T}{\partial x_{1i}}u_j\cdot\int\frac{k_i k_j\mathbf{kk}}{k}f_{\mathrm{R}}^{\mathrm{eq}}\left(1+f_{\mathrm{R}}^{\mathrm{eq}}\right)\left(2f_{\mathrm{R}}^{\mathrm{eq}}+1\right)\frac{3\mathrm{d}\mathbf{k}}{(2\pi)^3} \\ &\quad+\frac{\hbar^2\, v_{\mathrm{g}}^4\tau_{\mathrm{N}}}{k_{\mathrm{B}}T^2}\frac{\partial T}{\partial x_{1i}}u_j\int\frac{k_i k_j\mathbf{kk}}{k^2}f_{\mathrm{R}}^{\mathrm{eq}}\left(1+f_{\mathrm{R}}^{\mathrm{eq}}\right)\frac{3\mathrm{d}\mathbf{k}}{(2\pi)^3}.\end{aligned} \tag{C.40}$$

The second term in Eq. (C.40) is resolved when combined with Eq. (C.38):

$$\frac{\hbar^2\, v_{\mathrm{g}}^4\tau_{\mathrm{N}}}{k_{\mathrm{B}}T^2}\frac{\partial T}{\partial x_{1i}}u_j\left[\int\frac{k_i k_j\mathbf{kk}}{k^2}f_{\mathrm{R}}^{\mathrm{eq}}\left(1+f_{\mathrm{R}}^{\mathrm{eq}}\right)\frac{3\mathrm{d}\mathbf{k}}{(2\pi)^3}\right]_{ijmn} = \frac{1}{5}\frac{v_{\mathrm{g}}^2\tau_{\mathrm{N}}}{T}\left(q_i\frac{\partial T}{\partial x_{1i}}\delta_{mn}+q_n\frac{\partial T}{\partial x_{1m}}+q_m\frac{\partial T}{\partial x_{1n}}\right). \tag{C.41}$$

The first term in Eq. (C.40) is simplified into:

$$\begin{aligned}&-\frac{\hbar^3\, v_{\mathrm{g}}^5\tau_{\mathrm{N}}}{k_{\mathrm{B}}^2T^3}\frac{\partial T}{\partial x_{1i}}u_j\cdot\left[\int\frac{k_i k_j\mathbf{kk}}{k}f_{\mathrm{R}}^{\mathrm{eq}}\left(1+f_{\mathrm{R}}^{\mathrm{eq}}\right)\left(2f_{\mathrm{R}}^{\mathrm{eq}}+1\right)\frac{3\mathrm{d}\mathbf{k}}{(2\pi)^3}\right]_{ijmn} \\ &= -\frac{\hbar^3\, v_{\mathrm{g}}^5\tau_{\mathrm{N}}}{k_{\mathrm{B}}^2T^3}\frac{\partial T}{\partial x_{1i}}u_j\cdot\frac{1}{10\pi^2}\left(\delta_{ij}\delta_{mn}+\delta_{im}\delta_{nj}+\delta_{in}\delta_{mj}\right)\int_0^{\infty}k^5 f_{\mathrm{R}}^{\mathrm{eq}}\left(1+f_{\mathrm{R}}^{\mathrm{eq}}\right)\left(2f_{\mathrm{R}}^{\mathrm{eq}}+1\right)\mathrm{d}k,\end{aligned} \tag{C.42}$$

where the following integration becomes:

$$\int_0^{\infty} k^5 f_{\mathrm{R}}^{\mathrm{eq}}\left(1+f_{\mathrm{R}}^{\mathrm{eq}}\right)\left(2f_{\mathrm{R}}^{\mathrm{eq}}+1\right)\mathrm{d}k=\int_0^{\infty}\frac{k^5\exp\left(\frac{\hbar v_{\mathrm{g}}k}{k_{\mathrm{B}}T}\right)\left[\exp\left(\frac{\hbar v_{\mathrm{g}}k}{k_{\mathrm{B}}T}\right)+1\right]}{\left[\exp\left(\frac{\hbar v_{\mathrm{g}}k}{k_{\mathrm{B}}T}\right)-1\right]^3}\mathrm{d}k. \tag{C.43}$$

The following integral is conducted through integrating by parts:

$$\int_0^{\infty}\frac{x^5\exp(x)\left[\exp(x)+1\right]}{\left[\exp(x)-1\right]^3}\mathrm{d}x=\frac{4}{3}\pi^4. \tag{C.44}$$

Substitution of Eq. (C.43) supplemented with Eq. (C.44), into Eq. (C.42), gives rise to the first term in Eq. (C.40):

$$\begin{aligned}&-\frac{\hbar^3 v_{\mathrm{g}}^5\tau_{\mathrm{N}}}{k_{\mathrm{B}}^2T^3}\frac{\partial T}{\partial x_{1i}}u_j\cdot\left[\int\frac{k_ik_j\mathbf{kk}}{k}f_{\mathrm{R}}^{\mathrm{eq}}\left(1+f_{\mathrm{R}}^{\mathrm{eq}}\right)\left(2f_{\mathrm{R}}^{\mathrm{eq}}+1\right)\frac{3\mathrm{d}\mathbf{k}}{(2\pi)^3}\right]_{mn}\\&=-\frac{v_{\mathrm{g}}^2\tau_{\mathrm{N}}}{T}\left(q_i\frac{\partial T}{\partial x_{1i}}\delta_{mn}+q_n\frac{\partial T}{\partial x_{1m}}+q_m\frac{\partial T}{\partial x_{1n}}\right).\end{aligned} \tag{C.45}$$

Finally, substitution of Eqs. (C.41) and (C.45) into Eq. (C.40) results in:

$$\left(\mathbf{Q}_{1,\mathrm{III}}\right)_{mn}=-\frac{4}{5}\frac{v_{\mathrm{g}}^2\tau_{\mathrm{N}}}{T}\left(q_i\frac{\partial T}{\partial x_{1i}}\delta_{mn}+q_n\frac{\partial T}{\partial x_{1m}}+q_m\frac{\partial T}{\partial x_{1n}}\right). \tag{C.46}$$

References

[1] J. Fourier, Théorie analytique de la chaleur, Firmin Didot Père et Fils, Paris, 1822.
[2] S. Carnot, Réflexions sur la puissance motrice du feu et sur les machines propres à développer cette puissance, Bachelier, Paris, 1824.
[3] W. Thomson, On the Dynamical Theory of Heat, with numerical results deduced from Mr Joule's equivalent of a Thermal Unit, and M. Regnault's Observations on Steam, Trans. R. Soc. Edinb. 20 (1853) 261–288.
[4] R. Clausius, The Mechanical Theory of Heat-with its Applications to the Steam Engine and to Physical Properties of Bodies, John van Voorst, London, 1867.
[5] J.C. Maxwell, On the dynamical theory of gases, Philos. Trans. R. Soc. Lond. 157 (1867) 49.
[6] L. Boltzmann, Lectures on Gas Theory, Cambridge University Press, London, 1964.
[7] J.W. Gibbs, Elementary Principles in Statistical Mechanics, Charles Scribner's sons, New York, 1902.
[8] R.B. Bird, W.E. Stewart, E.N. Lightfoot, Transport Phenomena, Wiley, New York, 1960.
[9] W.M. Deen, Analysis of Transport Phenomena, Oxford University Press, New York, 2011.
[10] M.G. Davies, Building Heat Transfer, John Wiley & Sons Ltd., Chichester, 2004.
[11] H. Janssen, B. Blocken, J. Carmeliet, Conservative modelling of the moisture and heat transfer in building components under atmospheric excitation, Int. J. Heat Mass Transfer 50 (2007) 1128–1140.
[12] A.E. Bergles, J.G. Collier, J.M. Delhaye, G.F. Hewitt, F. Mayinger, Two-phase Flow and Heat Transfer in the Power and Process Industries, Hemisphere Publishing Corporation, New York, 1981.
[13] A. Bejan, Theory of heat transfer-irreversible power-plants, Int. J. Heat Mass Transfer 31 (1988) 1211–1219.
[14] M. Kaviany, Heat Transfer Physics, Cambridge University Press, New York, 2008.
[15] R.E. Peierls, Zur kinetischen Theorie der Wärmeleitung in Kristallen, Ann. Phys. 395 (1929) 1055–1101.
[16] R.E. Peierls, Quantum Theory of Solids, The Clarendon Press, Oxford, 1955.
[17] J.M. Ziman, Electrons and Phonons: The Theory of Transport Phenomena in Solids, The Clarendon Press, Oxford, 1960.
[18] J.A. Reissland, The Physics of Phonons, Wiley, New York, 1973.
[19] W.E. Bron, Nonequilibrium Phonon Dynamics, Plenum Press, New York, 1985.
[20] V.L. Gurevich, Transport in Phonon Systems, North-Holland, Amsterdam, 1986.
[21] M. Gad-el-Hak, The MEMS Handbook: MEMS Design and Fabrication, Taylor & Francis, New York, 2006.
[22] H.S. Nalwa, Encyclopedia of Nanoscience and Nanotechnology, American Scientific Publishers, California, 2004.
[23] F. Honnor, M.A. Thomas, Packaging and cooling problems associated with microelectronics equipment, Microelectron. Reliab. 8 (1969) 331–337.
[24] A. Bejan, Constructal-theory network of conducting paths for cooling a heat generating volume, Int. J. Heat Mass Transfer 40 (1997) 799–816.
[25] C.L. Tien, G. Chen, Challenges in microscale conductive and radiative heat transfer, J. Heat Transfer 116 (1994) 799–807.
[26] C.L. Tien, A. Majumdar, F.M. Gerner, Microscale Energy Transport, Taylor & Francis, Washington, 1998.
[27] G. Chen, A. Majumdar, J. Lukes, Chang-lin Tien's contributions to micro- and nanoscale heat transfer, Annu. Rev. Heat Transfer 14 (2005) 97–102.
[28] A.J. Minnich, M.S. Dresselhaus, Z.F. Ren, G. Chen, Bulk nanostructured thermoelectric materials: current research and future prospects, Energy Environ. Sci. 2 (2009) 466–479.
[29] J.P. Heremans, M.S. Dresselhaus, L.E. Bell, D.T. Morelli, When thermoelectrics reached the nanoscale, Nature Nanotechnol. 8 (2013) 471–473.
[30] R.F. Davis, G. Kelner, M. Shur, J.W. Palmour, J.A. Edmond, Thin film deposition and microelectronic and optoelectronic device fabrication and characterization in monocrystalline alpha and beta silicon carbide, Proc. IEEE 79 (1991) 677–701.
[31] M. Wang, N. Pan, Predictions of effective physical properties of complex multiphase materials, Mater. Sci. Eng. R 63 (2008) 1–30.
[32] D.G. Cahill, W.K. Ford, K.E. Goodson, G.D. Mahan, A. Majumdar, H.J. Maris, R. Merlin, S.R. Phillpot, Nanoscale thermal transport, J. Appl. Phys. 93 (2003) 793–818.
[33] S. Liu, X.F. Xu, R.G. Xie, G. Zhang, B.W. Li, Anomalous heat conduction and anomalous diffusion in low dimensional nanoscale systems, Eur. Phys. J. B 85 (2012) 337.
[34] D.G. Cahill, P.V. Braun, G. Chen, D.R. Clarke, S. Fan, K.E. Goodson, P. Keblinski, W.P. King, G.D. Mahan, A. Majumdar, H.J. Maris, S.R. Phillpot, E. Pop, L. Shi, Nanoscale thermal transport. II. 2003–2012, Appl. Phys. Rev. 1 (2014) 011305.
[35] G. Lebon, Heat conduction at micro and nanoscales: A review through the prism of extended irreversible thermodynamics, J. Non-Equilib. Thermodyn. 39 (2014) 35–59.
[36] A.J. Minnich, Advances in the measurment and computation of thermal phonon transport properties, J. Phys.: Condens. Matter. 27 (2015) 053202.
[37] D.Y. Tzou, Macro- to Microscale Heat Transfer: The Lagging Behavior, Taylor & Francis, Washington, 1996.

[38] G. Chen, Nanoscale Energy Transport and Conversion: A Parallel Treatment of Electrons, Molecules, Phonons, and Photons, Oxford University Press, New York, 2005.
[39] Z.M. Zhang, Nano/microscale Heat Transfer, McGraw-Hill, New York, 2007.
[40] D. Jou, J. Casas-Vázquez, G. Lebon, Extended Irreversible Thermodynamics, Springer, Heidelberg, 2010.
[41] T.Q. Qiu, C.L. Tien, Short-pulse laser heating on metals, Int. J. Heat Mass Transfer 35 (1992) 719–726.
[42] T.Q. Qiu, C.L. Tien, Heat transfer mechanisms during short-pulse laser heating of metals, J. Heat Transfer 115 (1993) 835–841.
[43] M.I. Flik, C.L. Tien, Size effect on the thermal conductivity of high-Tc thin-film superconductors, J. Heat Transfer 112 (1990) 872–881.
[44] A. Majumdar, Microscale heat conduction in dielectric thin films, J. Heat Transfer 115 (1993) 7–16.
[45] M.I. Flik, B.I. Choi, K.E. Goodson, Heat transfer regimes in microstructures, J. Heat Transfer 114 (1992) 666–674.
[46] F.X. Alvarez, D. Jou, Memory and nonlocal effects in heat transport: From diffusive to ballistic regimes, Appl. Phys. Lett. 90 (2007) 083109.
[47] C. Hua, A.J. Minnich, Transport regimes in quasiballistic heat conduction, Phys. Rev. B 89 (2014) 094302.
[48] F.C. Chou, J.R. Lukes, X.G. Liang, K. Takahashi, C.L. Tien, Molecular dynamics in microscale thermophysical engineering, Annu. Rev. Heat Transfer 10 (1999) 141–176.
[49] J.R. Lukes, D.Y. Li, X.G. Liang, C.L. Tien, Molecular dynamics study of solid thin-film thermal conductivity, J. Heat Transfer 122 (2000) 536–543.
[50] A.R. Abramson, C.L. Tien, A. Majumdar, Interface and strain effects on the thermal conductivity of heterostructures: A molecular dynamics study, J. Heat Transfer 124 (2002) 963–970.
[51] A.J.C. Ladd, B. Moran, W.G. Hoover, Lattice thermal conductivity—A comparison of molecular dynamics and anharmonic lattice dynamics, Phys. Rev. B 34 (1986) 5058–5064.
[52] P.K. Schelling, S.R. Phillpot, P. Keblinski, Phonon wave-packet dynamics at semiconductor interfaces by molecular-dynamics simulation, Appl. Phys. Lett. 80 (2002) 2484–2486.
[53] A.J.H. McGaughey, M. Kaviany, Quantitative validation of the Boltzmann transport equation phonon thermal conductivity model under the single-mode relaxation time approximation, Phys. Rev. B 69 (2004) 094303.
[54] A. Debernardi, S. Baroni, E. Molinari, Anharmonic phonon lifetimes in semiconductors from density-functional perturbation theory, Phys. Rev. Lett. 75 (1995) 1819–1822.
[55] S. Baroni, S. de Gironcoli, A. Dal corso, P. Giannozzi, Phonons and related crystal properties from density-functional perturbation theory, Rev. Modern Phys. 73 (2001) 515–562.
[56] V. Alex, K. Joe, H. Amano, H. Aiso, High Performance Computing, Springer, New York, 2003.
[57] J.E. Turney, E.S. Landry, A.J.H. McGaughey, C.H. Amon, Predicting phonon properties and thermal conductivity from anharmonic lattice dynamics calculations and molecular dynamics simulations, Phys. Rev. B 79 (2009) 064301.
[58] D.P. Sellan, J.E. Turney, A.J.H. McGaughey, C.H. Amon, Cross-plane phonon transport in thin films, J. Appl. Phys. 108 (2010) 113524.
[59] J.E. Turney, A.J.H. McGaughey, C.H. Amon, In-plane phonon transport in thin films, J. Appl. Phys. 107 (2010) 024317.
[60] G. Chen, Multiscale simulation of phonon and electron thermal transport, Annu. Rev. Heat Transfer 17 (2014) 1–8.
[61] R.A. Guyer, J.A. Krumhansl, Solution of the linearized phonon Boltzmann equation, Phys. Rev. 148 (1966) 766–788.
[62] F.X. Alvarez, D. Jou, A. Sellitto, Phonon hydrodynamics and phonon-boundary scattering in nanosystems, J. Appl. Phys. 105 (2009) 014317.
[63] D.Y. Tzou, The generalized lagging response in small-scale and high-rate heating, Int. J. Heat Mass Transfer 38 (1995) 3231–3240.
[64] D.Y. Tzou, A unified field approach for heat conduction from macro- to micro-scales, J. Heat Transfer 117 (1995) 8–16.
[65] G. Chen, Ballistic-diffusive heat-conduction equations, Phys. Rev. Lett. 86 (2001) 2297–2300.
[66] G. Chen, Ballistic-diffusive equations for transient heat conduction from nano to macroscales, J. Heat Transfer 124 (2002) 320–328.
[67] Z.-Y. Guo, Motion and transfer of thermal mass-thermal mass and thermon gas, J. Eng. Thermophys. 27 (2006) 631–634.
[68] B.-Y. Cao, Z.-Y. Guo, Equation of motion of a phonon gas and non-Fourier heat conduction, J. Appl. Phys. 102 (2007) 053503.
[69] A.J.H. Mcgaughey, M. Kaviany, Phonon transport in molecular dynamics simulations: formulation and thermal conductivity prediction, Adv. Heat Transfer 39 (2006) 169–255.
[70] R. Kubo, Fluctuation–dissipation theorem, Rep. Progr. Phys. 29 (1966) 255–284.
[71] D.A. Broido, M. Malorny, G. Birner, N. Mingo, D.A. Stewart, Intrinsic lattice thermal conductivity of semiconductors from first principles, Appl. Phys. Lett. 91 (2007) 231922.
[72] L. Lindsay, D.A. Broido, T.L. Reinecke, Ab initio thermal transport in compound semiconductors, Phys. Rev. B 87 (2013) 165201.
[73] W. Li, N. Mingo, L. Lindsay, D.A. Broido, D.A. Stewart, N.A. Katcho, Thermal conductivity of diamond nanowires from first principles, Phys. Rev. B 85 (2012) 195436.
[74] P.L. Bhatnagar, E.P. Gross, M. Krook, A model for collision processes in gases. I. Small amplitude in charged and neutral one-component systems, Phys. Rev. 94 (1954) 511–525.
[75] G. Fugallo, M. Lazzeri, L. Paulatto, F. Mauri, Ab initio variational approach for evaluating lattice thermal conductivity, Phys. Rev. B 88 (2013) 045430.
[76] N. Mingo, Calculation of Si nanowire thermal conductivity using complete phonon dispersion relations, Phys. Rev. B 68 (2003) 113308.
[77] J.-P.M. Peraud, Low Variance Methods for Monte Carlo Simulation of Phonon Transport, Massachusetts Institute of Technology, 2011.
[78] J.-P.M. Peraud, C.D. Landon, N.G. Hadjiconstantinou, Monte Carlo methods for solving the Boltzmann equation, Annu. Rev. Heat Transfer 17 (2014) 205–265.
[79] R.A. Escobar, S.S. Ghai, M.S. Jhon, C.H. Amon, Multi-length and time scale thermal transport using the lattice Boltzmann method with application to electronics cooling, Int. J. Heat Mass Transfer 49 (2006) 97–107.
[80] A. Nabovati, D.P. Sellan, C.H. Amon, On the lattice Boltzmann method for phonon transport, J. Comput. Phys. 230 (2011) 5864–5876.
[81] R.A. Guyer, J.A. Krumhansl, Thermal conductivity, second sound, and phonon hydrodynamic phenomena in nonmetallic crystals, Phys. Rev. 148 (1966) 778–788.
[82] R.J. Hardy, D.L. Albers, Hydrodynamic approximation to the phonon Boltzmann equation, Phys. Rev. B 10 (1974) 3546–3551.
[83] W. Larecki, Symmetric conservative form of low-temperature phonon gas hydrodynamics, Il Nuovo Cimento D 14 (1992) 141–176.
[84] Z. Banach, W. Larecki, Nine-moment phonon hydrodynamics based on the modified Grad-type approach: formulation, J. Phys. A: Math. Gen. 37 (2004) 9805–9829.
[85] Z. Banach, W. Larecki, Nine-moment phonon hydrodynamics based on the maximum-entropy closure: one-dimensional flow, J. Phys. A: Math. Gen. 38 (2005) 8781–8802.
[86] Z. Banach, W. Larecki, Chapman–Enskog method for a phonon gas with finite heat flux, J. Phys. A 41 (2008) 375502.
[87] F.X. Alvarez, V.A. Cimmelli, D. Jou, A. Sellitto, Mesoscopic description of boundary effects in nanoscale heat transport, Nanosc. Syst.: Math. Model. Theory Appl. 1 (2012) 112–142.
[88] D.D. Joseph, L. Preziosi, Heat waves, Rev. Modern Phys. 61 (1989) 41–73.
[89] C. Cattaneo, Sulla conduzione del calore, Atti Sem. Mat. Fis. Univ. Modena 3 (1948) 21.
[90] D.Y. Tzou, Experimental support for the lagging behavior in heat propagation, J. Thermophys. Heat Transfer 9 (1995) 686–693.
[91] A.G. Agwu nnanna, A. Haji-Sheikh, K.T. Harris, Experimental study of local thermal non-equilibrium phenomena during phase change in porous media, Int. J. Heat Mass Transfer 47 (2004) 4365–4375.
[92] D.Y. Tzou, J.K. Chen, Thermal lagging in random media, J. Thermophys. Heat Transfer 12 (1998) 567–574.
[93] R.G. Yang, G. Chen, M. Laroche, Y. Taur, Simulation of nanoscale multidimensional transient heat conduction problems using ballistic-diffusive equations and phonon Boltzmann equation, J. Heat Transfer 127 (2005) 298–306.
[94] J. Ordonez-Miranda, R. Yang, J.J. Alvarado-Gil, A constitutive equation for nano-to-macro-scale heat conduction based on the Boltzmann transport equation, J. Appl. Phys. 109 (2011) 084319.
[95] Y. Zhang, W. Ye, Modified ballistic-diffusive equations for transient non-continuum heat conduction, Int. J. Heat Mass Transfer 83 (2015) 51–63.

[96] G. Lebon, M. Grmela, C. Dubois, From ballistic to diffusive regimes in heat transport at nano-scales, C. R. Mec. 339 (2011) 324–328.
[97] M. Wang, Z.-Y. Guo, Understanding of temperature and size dependences of effective thermal conductivity of nanotubes, Phys. Lett. A 374 (2010) 4312–4315.
[98] M. Wang, N. Yang, Z.-Y. Guo, Non-Fourier heat conductions in nanomaterials, J. Appl. Phys. 110 (2011) 064310.
[99] M. Wang, X. Shan, N. Yang, Understanding length dependences of effective thermal conductivity of nanowires, Phys. Lett. A 376 (2012) 3514–3517.
[100] Y. Dong, B.-Y. Cao, Z.-Y. Guo, Generalized heat conduction laws based on thermomass theory and phonon hydrodynamics, J. Appl. Phys. 110 (2011) 063504.
[101] A. Sellitto, V.A. Cimmelli, A continuum approach to thermomass theory, J. Heat Transfer 134 (2012) 112402.
[102] D.Y. Tzou, Nonlocal behavior in phonon transport, Int. J. Heat Mass Transfer 54 (2011) 475–481.
[103] C.V. Anderson, K.K. Tamma, Novel heat conduction model for bridging different space and time scales, Phys. Rev. Lett. 96 (2006) 184301.
[104] K.R. Naqvi, S. Waldenstrom, Brownian motion description of heat conduction by phonons, Phys. Rev. Lett. 95 (2005) 065901.
[105] M. Xu, L. Wang, Dual-phase-lagging heat conduction based on Boltzmann transport equation, Int. J. Heat Mass Transfer 48 (2005) 5616–5624.
[106] A. Einstein, Die Plancksche Theorie der Strahlung und die Theorie der spezifischen Wärme, Ann. Phys. 327 (1907) 180–190.
[107] P. Debye, Zur Theorie der spezifischen Wärmen, Ann. Phys. 344 (1912) 789–839.
[108] S. Chapman, T.G. Cowling, The Mathematical Theory of Non-uniform Gases, Cambridge University Press, Cambridge, 1953.
[109] W. Dreyer, H. Struchtrup, Heat pulse experiments revisited, Contin. Mech. Thermodyn 5 (1993) 3–50.
[110] C. Kittel, Introduction to Solid State Physics, John Wiley & Sons, New York, 2005.
[111] D.J. Griffiths, Introduction to Quantum Mechanics, Prentice-Hall, Inc., 2005.
[112] L. Boltzmann, Weitere Studien über das Wärmegleichwicht unter Gasmolekülen, Sitzungsber. Akad. Wiss. Wien (II) 66 (1872) 275–370.
[113] J. Callaway, Model for lattice thermal conductivity at low temperatures, Phys. Rev. 113 (1959) 1046–1051.
[114] C. de Tomas, On Thermal Transport by Phonons in Bulk and Nanostructured Semiconductor Materials, Universitat Autonoma de Barcelona, 2014.
[115] A. Ward, D.A. Broido, D.A. Stewart, G. Deinzer, Ab initio theory of the lattice thermal conductivity in diamond, Phys. Rev. B 80 (2009).
[116] C. de Tomas, A. Cantarero, A.F. Lopeandia, F.X. Alvarez, From kinetic to collective behavior in thermal transport on semiconductors and semiconductor nanostructures, J. Appl. Phys. 115 (2014).
[117] C. de Tomas, A. Cantarero, A.F. Lopeandia, F.X. Alvarez, Thermal conductivity of group-IV semiconductors from a kinetic-collective model, Proc. R. Soc. A 470 (2014) 20140371.
[118] M.G. Holland, Analysis of lattice thermal conductivity, Phys. Rev. 132 (1963) 2461–2471.
[119] N. Mingo, L. Yang, D. Li, A. Majumdar, Predicting the thermal conductivity of Si and Ge nanowires, Nano Lett. 3 (2003) 1713–1716.
[120] P. Chantrenne, J.L. Barrat, X. Blase, J.D. Gale, An analytical model for the thermal conductivity of silicon nanostructures, J. Appl. Phys. 97 (2005) 104318.
[121] A.J.H. McGaughey, E.S. Landry, D.P. Sellan, C.H. Amon, Size-dependent model for thin film and nanowire thermal conductivity, Appl. Phys. Lett. 99 (2011) 131904.
[122] M. Maldovan, Thermal conductivity of semiconductor nanowires from micro to nano length scales, J. Appl. Phys. 111 (2012) 024311.
[123] D.T. Morelli, J.P. Heremans, G.A. Slack, Estimation of the isotope effect on the lattice thermal conductivity of group IV and group III–V semiconductors, Phys. Rev. B 66 (2002) 195304.
[124] A. Ward, D.A. Broido, Intrinsic phonon relaxation times from first-principles studies of the thermal conductivities of Si and Ge, Phys. Rev. B 81 (2010) 085205.
[125] K. Huang, Statistical Mechanics, John Wiley & Sons, New York, 1987.
[126] N.N. Bogoliubov, Problems of a dynamical theory in statistical physics, in: J.d. Boer, G.E. Uhlenbeck (Eds.), Studies in Statistical Mechanics, North-Holland Publishing Company, Amsterdam, 1946.
[127] L.D. Landau, E.M. Lifshitz, Mechanics, Elsevier Pte Ltd., Singapore, 2007.
[128] F. Schwabl, Statistical Mechanics, Springer-Verlag, Berlin, 2006.
[129] D.D. Joseph, L. Preziosi, Addendum to the paper "Heat waves", Rev. Modern Phys. 62 (1990) 375–391.
[130] B. Straughan, Heat Waves, Springer, New York, 2011.
[131] L.D. Landau, The theory of superfluidity of helium II, Phys. Rev. 60 (1941) 356–358.
[132] L. Tisza, Sur la théorie des liquides quantiques. Application à l'hélium liquide. II, J. Phys. Radium 1 (1940) 350–358.
[133] L.D. Landau, E.M. Lifshitz, Fluid Mechanics, Elsevier Pte Ltd., Singapore, 2004.
[134] E.M. Lifshitz, Radiation of sound in helium II, J. Phys. USSR 8 (1944) 110.
[135] V.P. Peshkov, "Second sound" in helium II, J. Phys. USSR 8 (1944) 381.
[136] J.C. Ward, J. Wilks, The velocity of second sound in liquid helium near to absolute zero, London, Edinburgh, Dublin Phil. Mag. J. Sci. 42 (1951) 314–316.
[137] J.C. Ward, J. Wilks, Second sound and the thermo-mechanical effect at very low temperatures, London, Edinburgh, Dublin Phil. Mag. J. Sci. 43 (1952) 48–50.
[138] R.J. Von gutfeld, Heat Pulses in Quartz and Sapphire at Low Temperatures, Phys. Rev. Lett. 12 (1964) 641–644.
[139] C.C. Ackerman, R.A. Guyer, Temperature pulses in dielectric solids, Ann. Physics 50 (1968) 128–185.
[140] C.C. Ackerman, B. Bertman, H.A. Fairbank, R.A. Guyer, Second sound in solid helium, Phys. Rev. Lett. 16 (1966) 789–791.
[141] R.A. Guyer, J.A. Krumhansl, Dispersion relation for second sound in solids, Phys. Rev. 133 (1964) A1411–A1417.
[142] E.W. Prohofsky, J.A. Krumhansl, Second-sound propagation in dielectric solids, Phys. Rev. 133 (1964) A1403–A1410.
[143] J. Sussmann, A. Thellung, Thermal conductivity of perfect dielectric crystals in the absence of umklapp processes, Proc. Phys. Soc. 81 (1963) 1122–1130.
[144] E.M. Lifshitz, L.P. Pitaevskii, Physical Kinetics, Pergamon Press, New York, 1981.
[145] R.J. Hardy, Phonon Boltzmann equation and second sound in solids, Phys. Rev. B 2 (1970) 1193–1207.
[146] H. Beck, On the temperature behavior of second sound and Poiseuille flow, Z. Phys. B 20 (1975) 313–322.
[147] W. Bausch, Thermal Conductivity and Poiseuille Flow of Phonons in Dielectric Films and Plates, Phys. Status Solidi b 52 (1972) 253–262.
[148] R. Gurzhi, A. Maksimov, Nonlocal hydrodynamics of phonon gas in dielectrics, JETP Lett. 27 (1978) 236–238.
[149] H. Nielsen, B. Shklosvkii, Heat transfer and second sound in dielectrics at large drift velocities of the phonon gas, Sov. Phys. JETP 29 (1969) 386–390.
[150] A. Efros, Contribution to the theory of elasticity of crystals at low temperatures, Sov. Phys. JETP 27 (1968) 948–951.
[151] P.F. Meier, Green's function approach to phonon hydrodynamics in solids, Phys. Kondens. Mater. 8 (1969) 241–267.
[152] H. Beck, P. Meier, A. Thellung, Phonon hydrodynamics in solids, Phys. Status Solidi a 24 (1974) 11–63.
[153] H. Grad, On the kinetic theory of rarefied gases, Comm. Pure Appl. Math. 2 (1949) 331–407.
[154] H. Struchtrup, Macroscopic Transport Equations for Rarefied Gas Flows, Springer-Verlag, Heidelberg, 2005.
[155] S. Succi, The Lattice Boltzmann Equation for Fluid Dynamics and Beyond, Clarendon Press, Oxford, 2001.
[156] W. Larecki, S. Piekarski, Symmetric conservative form of low-temperature phonon gas hydrodynamics, Il Nuovo Cimento D 13 (1991) 31–53.
[157] W. Larecki, S. Piekarski, Phonon gas hydrodynamics based on the maximum entropy principle and the extended field theory of a rigid conductor of heat, Arch. Mech. 43 (1991) 163–190.
[158] R.A. Guyer, Phonon gas: A lattice Boltzmann description, Phys. Rev. E 50 (1994) 4596–4608.
[159] J.A. Krumhansl, Thermal conductivity of insulating crystals in the presence of normal processes, Proc. Phys. Soc. 85 (1965) 921–930.
[160] M.S. Mongiovi, D. Jou, Nonlocal effects in superfluid turbulence: Application to the low-density- to high-density-state transition and to vortex decay, Phys. Rev. B 71 (2005) 094507.
[161] M.S. Mongiovi, D. Jou, Thermodynamical derivation of a hydrodynamical model of inhomogeneous superfluid turbulence, Phys. Rev. B 75 (2007) 024507.
[162] L. Saluto, M.S. Mongiovi, D. Jou, Longitudinal counterflow in turbulent liquid helium: velocity profile of the normal component, Z. Angew. Math. Phys. 65 (2014) 531–548.

[163] M. Sciacca, A. Sellitto, D. Jou, Transition to ballistic regime for heat transport in helium II, Phys. Lett. A 378 (2014) 2471–2477.
[164] D. Jou, J. Casas-Vazquez, J.R. Madureira, A.R. Vasconcellos, R. Luzzi, Energy transport in a mesoscopic thermo-hydrodynamics, Internat. J. Modern Phys. B 15 (2001) 4211–4222.
[165] X.Y. He, L.S. Luo, A priori derivation of the lattice Boltzmann equation, Phys. Rev. E 55 (1997) R6333–R6336.
[166] X.Y. He, L.S. Luo, Theory of the lattice Boltzmann method: From the Boltzmann equation to the lattice Boltzmann equation, Phys. Rev. E 56 (1997) 6811–6817.
[167] T. Abe, Derivation of the lattice Boltzmann method by means of the discrete ordinate method for the Boltzmann equation, J. Comput. Phys. 131 (1997) 241–246.
[168] S.Y. Chen, G.D. Doolen, Lattice Boltzmann method for fluid flows, Annu. Rev. Fluid Mech. 30 (1998) 329–364.
[169] D. Hilbert, Grundzüge einer allgemeinen Theorie der linearen Integralgleichungen, Teubner Leipzig, 1912.
[170] D. Enskog, Kinetische Theorie der Vorgänge in mässig verdünnten Gasen, Uppsala Univertitet, 1917.
[171] S. Chapman, On the law of distribution of molecular velocities, and on the theory of viscosity and thermal conduction, in a non-uniform simple monatomic gas, Philos. Trans. R. Soc. Lond. 216 (1916) 279–348.
[172] I.V. Karlin, G. Dukek, T.F. Nonnenmacher, Gradient expansions in kinetic theory of phonons, Phys. Rev. B 55 (1997) 6324–6329.
[173] P.A. Zakharchenko, E.V. Radkevich, Central manifold and the problems of the Chapman-Enskog expansion, Dokl. Phys. 49 (2004) 451–455.
[174] V.V. Palin, E.V. Radkevich, Navier–Stokes approximation and problems of the Chapman-Enskog projection for kinetic equations, J. Math. Sci. 135 (2006) 2721–2748.
[175] Z. Banach, W. Larecki, Modified Chapman-Enskog moment approach to diffusive phonon heat transport, Phys. Rev. E 78 (2008) 061137.
[176] Z. Banach, W. Larecki, W. Zajaczkowski, Stability analysis of phonon transport equations derived via the Chapman-Enskog method and transformation of variables, Phys. Rev. E 80 (2009) 041114.
[177] U. Frisch, B. Hasslacher, Y. Pomeau, Lattice-gas automata for the Navier–Stokes equation, Phys. Rev. Lett. 56 (1986) 1505–1508.
[178] G.R. McNamara, G. Zanetti, Use of the Boltzmann equation to simulate lattice-gas automata, Phys. Rev. Lett. 61 (1988) 2332–2335.
[179] W.-S. Jiaung, J.-R. Ho, Lattice-Boltzmann modeling of phonon hydrodynamics, Phys. Rev. E 77 (2008) 066710.
[180] J. Lee, A.K. Roy, B.L. Farmer, Kapitza resistance in the lattice Boltzmann-Peierls-Callaway equation for multiphase phonon gases, Phys. Rev. E 83 (2011) 056706.
[181] J. Lee, S. Sihn, A.K. Roy, B.L. Farmer, The lattice Boltzmann Peierls Callaway equation for mesoscopic thermal transport modeling, Int. J. Smart Nano Mater. 3 (2012) 47–63.
[182] S.S. Ghai, W.T. Kim, R.A. Escobar, C.H. Amon, M.S. Jhon, A novel heat transfer model and its application to information storage systems, J. Appl. Phys. 97 (2004) 10P703.
[183] W.S. Jiaung, J.R. Ho, Lattice Boltzmann study on size effect with geometrical bending on phonon heat conduction in a nanoduct, J. Appl. Phys. 95 (2004) 958–966.
[184] A. Chattopadhyay, A. Pattamatta, Energy transport across submicron porous structures: A lattice Boltzmann study, Int. J. Heat Mass Transfer 72 (2014) 479–488.
[185] Z. Banach, S. Piekarski, Irreducible tensor description. III. Thermodynamics of a low-temperature phonon gas, J. Math. Phys. 30 (1989) 1826–1836.
[186] Z. Banach, W. Larecki, Nine-moment phonon hydrodynamics based on the modified Grad-type approach: hyperbolicity of the one-dimensional flow, J. Phys. A: Math. Gen. 37 (2004) 11053–11072.
[187] I. Müller, T. Ruggeri, Rational Extended Thermodynamics, Springer, New York, 1998.
[188] M.J. Fryer, H. Struchtrup, Moment model and boundary conditions for energy transport in the phonon gas, Contin. Mech. Thermodyn. 26 (2014) 593–618.
[189] W. Dreyer, Maximisation of the entropy in non-equilibrium, J. Phys. A: Math. Gen. 20 (1987) 6505–6517.
[190] I.-S. Liu, Method of Lagrange multipliers for exploitation of the entropy principle, Arch. Ration. Mech. Anal. 46 (1972) 131–148.
[191] W. Larecki, Z. Banach, Consistency of the phenomenological theories of wave-type heat transport with the hydrodynamics of a phonon gas, J. Phys. A 43 (2010) 385501.
[192] W. Larecki, Z. Banach, Influence of nonlinearity of the phonon dispersion relation on wave velocities in the four-moment maximum entropy phonon hydrodynamics, Physica D 266 (2014) 65–79.
[193] I. Müller, Zum Paradoxon der Wärmeleitungstheorie, Z. Phys. 198 (1967) 329–344.
[194] I.-S. Liu, I. Müller, Extended thermodynamics of classical and degenerate gases, Arch. Ration. Mech. Anal. 83 (1983) 285–332.
[195] P. Vernotte, Les paradoxes de la théorie continue de l'équation de la chaleur, C. R. Acad. Sci. 246 (1958) 3154–3155.
[196] S.J. Rogers, Transport of heat and approach to second sound in some isotopically pure Alkali-Halide crystals, Phys. Rev. B 3 (1971) 1440–1457.
[197] E.B. Arkilic, M.A. Schmidt, K.S. Breuer, Gaseous slip flow in long microchannels, J. Microelectromech. Syst. 6 (1997) 167–178.
[198] A. Beskok, G.E. Karniadakis, A model for flows in channels, pipes, and ducts at micro and nano scales, Microsc. Thermophys. Eng. 3 (1999) 43–77.
[199] N. Dongari, A. Agrawal, A. Agrawal, Analytical solution of gaseous slip flow in long microchannels, Int. J. Heat Mass Transfer 50 (2007) 3411–3421.
[200] Q. Lv, X. Liu, E. Wang, S. Wang, Analytical solution to predicting gaseous mass flow rates of microchannels in a wide range of Knudsen numbers, Phys. Rev. E 88 (2013) 013007.
[201] N. Singh, N. Dongari, A. Agrawal, Analytical solution of plane Poiseuille flow within Burnett hydrodynamics, Microfluid. Nanofluid. 16 (2014) 403–412.
[202] G.A. Bird, Molecular Gas Dynamics and the Direct Simulation of Gas Flows, Oxford Unviversity Press, New York, 1994.
[203] C. Shen, J. Fan, C. Xie, Statistical simulation of rarefied gas flows in micro-channels, J. Comput. Phys. 189 (2003) 512–526.
[204] M. Wang, Z. Li, Nonideal gas flow and heat transfer in micro- and nanochannels using the direct simulation Monte Carlo method, Phys. Rev. E 68 (2003) 46704.
[205] X. Nie, G.D. Doolen, S. Chen, Lattice-Boltzmann simulations of fluid flows in MEMS, J. Stat. Phys. 107 (2002) 279–289.
[206] C.Y. Lim, C. Shu, X.D. Niu, Y.T. Chew, Application of lattice Boltzmann method to simulate microchannel flows, Phys. Fluids 14 (2002) 2299–2308.
[207] S. Succi, Mesoscopic modeling of slip motion at fluid-solid interfaces with heterogeneous catalysis, Phys. Rev. Lett. 89 (2002) 064502.
[208] Y. Ma, Size-dependent thermal conductivity in nanosystems based on non-Fourier heat transfer, Appl. Phys. Lett. 101 (2012) 211905.
[209] F.X. Alvarez, D. Jou, A. Sellitto, Pore-size dependence of the thermal conductivity of porous silicon: a phonon hydrodynamic approach, Appl. Phys. Lett. 97 (2010) 033103.
[210] A. Sellitto, F.X. Alvarez, D. Jou, Second law of thermodynamics and phonon-boundary conditions in nanowires, J. Appl. Phys. 107 (2010) 064302.
[211] A. Beskok, Simulations and Models for Gas Flows in Microgeometries, Princeton University, 1996.
[212] H. Struchtrup, P. Taheri, Macroscopic transport models for rarefied gas flows: a brief review, J. Appl. Math. 76 (2011) 672–697.
[213] J.C. Maxwell, On stresses in rarified gases arising from inequalities of temperature, Philos. Trans. R. Soc. Lond. 170 (1879) 231–256.
[214] C. Cercignani, Higher oder slip according to the linearized boltzmann equation, Institute of Engineering Research Report AS-64-19, University of California, Berkeley, 1964.
[215] N.G. Hadjiconstantinou, Comment on Cercignani's second-order slip coefficient, Phys. Fluids 15 (2003) 2352–2354.
[216] W.-M. Zhang, G. Meng, X. Wei, A review on slip models for gas microflows, Microfluid. Nanofluid. 13 (2012) 845–882.
[217] M. Xu, Slip boundary condition of heat flux in Knudsen layers, Proc. R. Soc. A 470 (2014) 20130578.
[218] I. Müller, A History of Thermodynamics the Doctrine of Energy and Entropy, Springer, Heidelberg, 2007.
[219] S.R. De Groot, P. Mazur, Non-equilibrium Thermodynamics, Dover Publications, New York, 1962.
[220] L. Onsager, Reciprocal relations in irreversible thermodynamics I, Phys. Rev. 37 (1931) 405–426.
[221] L. Onsager, Reciprocal relations in irreversible thermodynamics II, Phys. Rev. 38 (1931) 2265–2279.
[222] C. Eckart, The thermodynamics of irreversible processes I: The simple fluid, Phys. Rev. 58 (1940) 267–269.
[223] C. Eckart, The thermodynamics of irreversible processes II: Fluid mixtures, Phys. Rev. 58 (1940) 269–275.
[224] J. Meixner, Zur Theorie der irreversiblen Prozesse, Ann. Phys. 5 (1943) 244–270.

[225] I. Prigogine, Etude Thermodynamique des processus irréversibles, Desoer, Liege, Paris, 1947.
[226] V.A. Cimmelli, Different thermodynamic theories and different heat conduction laws, J. Non-Equilib. Thermodyn. 34 (2009) 299–333.
[227] W. Muschik, Survey of some branches of thermodynamics, J. Non-Equilib. Thermodyn. 33 (2008) 165–198.
[228] C. Truesdell, Rational Thermodynamics, McGraw Hill, New York, 1969.
[229] P. Ván, T. Fülöp, Universality in heat conduction theory: weakly nonlocal thermodynamics, Ann. Phys. 524 (2012) 470–478.
[230] H.C. Öttinger, Beyond the Equilibrium Thermodynamics, John Wiley & Sons, Inc., Hoboken, New Jersey, 2005.
[231] D. Jou, J. Casas-Vázquez, Nonequilibrium absolute temperature, thermal waves and phonon hydrodynamics, Physica A 163 (1990) 47–58.
[232] G. Lebon, M. Torrisi, A. Valenti, A non-local thermodynamic analysis of second sound propagation in crystalline dielectrics, J. Phys.: Condens. Matter. 7 (1995) 1461–1474.
[233] A. Valenti, M. Torrisi, G. Lebon, Heat pulse propagation by second sound in dielectric crystals, J. Phys.: Condens. Matter. 9 (1997) 3117–3127.
[234] V.A. Cimmelli, A. Sellitto, D. Jou, Nonlocal effects and second sound in a nonequilibrium steady state, Phys. Rev. B 79 (2009) 014303.
[235] V.A. Cimmelli, A. Sellitto, D. Jou, Nonequilibrium temperatures, heat waves, and nonlinear heat transport equations, Phys. Rev. B 81 (2010) 054301.
[236] G. Lebon, D. Jou, J. Casas-Vazquez, W. Muschik, Weakly nonlocal and nonlinear heat transport in rigid solids, J. Non-Equilib. Thermodyn. 23 (1998) 176–191.
[237] P. Ván, Weakly nonlocal irreversible thermodynamics-the Guyer-Krumhansl and the Cahn-Hilliard equations, Phys. Lett. A 290 (2001) 88–92.
[238] G. Lebon, P. Dauby, Heat transport in dielectric crystals at low temperature: A variational formulation based on extended irreversible thermodynamics, Phys. Rev. A 42 (1990) 4710–4715.
[239] D. Jou, G. Lebon, M. Criado-Sancho, Variational principles for thermal transport in nanosystems with heat slip flow, Phys. Rev. E 82 (2010) 031128.
[240] D. Jou, J. Casas-Vázquez, G. Lebon, Extended irreversible thermodynamics, Rep. Progr. Phys. 51 (1988) 1105–1179.
[241] I. Müller, T. Ruggeri, Extended Thermodznamcis, Springer, New York, 1993.
[242] G. Lebon, D. Jou, P.C. Dauby, Beyond the Fourier heat conduction law and the thermal no-slip boundary condition, Phys. Lett. A 376 (2012) 2842–2846.
[243] F.X. Alvarez, D. Jou, A. Sellitto, Phonon boundary effects and thermal conductivity of rough concentric nanowires, J. Heat Transfer 133 (2011) 022402.
[244] D. Jou, A. Sellitto, F.X. Alvarez, Heat waves and phonon–wall collisions in nanowires, Proc. R. Soc. A 467 (2011) 2520–2533.
[245] A. Sellitto, F.X. Alvarez, D. Jou, Temperature dependence of boundary conditions in phonon hydrodynamics of smooth and rough nanowires, J. Appl. Phys. 107 (2010) 114312.
[246] A. Sellitto, F.X. Alvarez, D. Jou, Phonon-wall interactions and frequency-dependent thermal conductivity in nanowires, J. Appl. Phys. 109 (2011) 064317.
[247] A. Sellitto, F.X. Alvarez, D. Jou, Geometrical dependence of thermal conductivity in elliptical and rectangular nanowires, Int. J. Heat Mass Transfer 55 (2012) 3114–3120.
[248] A. Sellitto, V.A. Cimmelli, D. Jou, Thermoelectric effects and size dependency of the figure-of-merit in cylindrical nanowires, Int. J. Heat Mass Transfer 57 (2013) 109–116.
[249] M. Asheghi, M.N. Touzelbaev, K.E. Goodson, Y.K. Leung, S.S. Wong, Temperature-dependent thermal conductivity of single-crystal silicon layers in SOI substrates, J. Heat Transfer 120 (1998) 30–36.
[250] Y.S. Ju, K.E. Goodson, Phonon scattering in silicon films with thickness of order 100 nm, Appl. Phys. Lett. 74 (1999) 3005–3007.
[251] W. Liu, M. Asheghi, Phonon-boundary scattering in ultrathin single-crystal silicon layers, Appl. Phys. Lett. 84 (2004) 3819–3821.
[252] H. Zhang, Z. Lv, L. Tian, Z. Tan, L. Liu, Z. Li, Thermal conductivity measurements of ultra-thin single crystal silicon films using improved structure, in: T.A. Tang, G.P. Ru, Y.L. Jiang (Eds.), 8th International Conference on Solid-State and Integrated Circuit Technology, Shanghai, China, 2006.
[253] K. Fuchs, N.F. Mott, The conductivity of thin metallic films according to the electron theory of metals, Math. Proc. Camb. Phil. Soc. 34 (1938) 100–108.
[254] E.H. Sondheimer, The mean free path of electrons in metals, Adv. Phys. 1 (1952) 1–42.
[255] D.Y. Li, Y.Y. Wu, P. Kim, L. Shi, P.D. Yang, A. Majumdar, Thermal conductivity of individual silicon nanowires, Appl. Phys. Lett. 83 (2003) 2934–2936.
[256] I. Graur, F. Sharipov, Gas flow through an elliptical tube over the whole range of the gas rarefaction, Eur. J. Mech. B Fluids 27 (2008) 335–345.
[257] Y. Dong, Z.Y. Guo, Hydrodynamic modeling of heat conduction in nanoscale systems, J. Nanosci. Nanotechnol. 14 (2014) 1–5.
[258] A.I. Hochbaum, R. Chen, R.D. Delgado, W. Liang, E.C. Garnett, M. Najarian, A. Majumdar, P. Yang, Enhanced thermoelectric performance of rough silicon nanowires, Nature 451 (2008) 163–U165.
[259] P. Martin, Z. Aksamija, E. Pop, U. Ravaioli, Impact of phonon-surface roughness scattering on thermal conductivity of thin si nanowires, Phys. Rev. Lett. 102 (2009) 125503.
[260] D. Song, G. Chen, Thermal conductivity of periodic microporous silicon films, Appl. Phys. Lett. 84 (2004) 687–689.
[261] D.W. Song, W.N. Shen, B. Dunn, C.D. Moore, M.S. Goorsky, T. Radetic, R. Gronsky, G. Chen, Thermal conductivity of nanoporous bismuth thin films, Appl. Phys. Lett. 84 (2004) 1883–1885.
[262] J.H. Lee, J.C. Grossman, J. Reed, G. Galli, Lattice thermal conductivity of nanoporous Si: Molecular dynamics study, Appl. Phys. Lett. 91 (2007) 223110.
[263] P.E. Hopkins, P.T. Rakich, R.H. Olsson, I.F. El-Kady, L.M. Phinney, Origin of reduction in phonon thermal conductivity of microporous solids, Appl. Phys. Lett. 95 (2009) 161902.
[264] M. Kaviany, Principles of Heat Transfer in Porous Media, Springer, New York, 1995.
[265] A. Sellitto, D. Jou, V.A. Cimmelli, A phenomenological study of pore-size dependent thermal conductivity of porous silicon, Acta Appl. Math. 122 (2012) 435–445.
[266] J.-P.M. Peraud, N.G. Hadjiconstantinou, Efficient simulation of multidimensional phonon transport using energy-based variance-reduced Monte Carlo formulations, Phys. Rev. B 84 (2011) 205331.
[267] J.-P.M. Peraud, N.G. Hadjiconstantinou, An alternative approach to efficient simulation of micro/nanoscale phonon transport, Appl. Phys. Lett. 101 (2012) 153114.
[268] C.D. Landon, N.G. Hadjiconstantinou, Deviational simulation of phonon transport in graphene ribbons with ab initio scattering, J. Appl. Phys. 116 (2014) 163502.
[269] Y. Dong, B.-Y. Cao, Z.-Y. Guo, General expression for entropy production in transport processes based on the thermomass model, Phys. Rev. E 85 (2012) 061107.
[270] Y. Dong, B.-Y. Cao, Z.-Y. Guo, Temperature in nonequilibrium states and non-Fourier heat conduction, Phys. Rev. E 87 (2013) 032150.
[271] F.X. Alvarez, J. Casas-Vazquez, D. Jou, Robustness of the nonequilibrium entropy related to the Maxwell-Cattaneo heat equation, Phys. Rev. E 77 (2008) 031110.
[272] J. Casas-Vázquez, D. Jou, Nonequilibrium temperature versus local-equilibrium temperature, Phys. Rev. E 49 (1994) 1040–1048.
[273] J. Casas-Vázquez, D. Jou, Temperature in non-equilibrium states: a review of open problems and current proposals, Rep. Progr. Phys. 66 (2003) 1937–2023.
[274] D.Y. Tzou, Longitudinal and transverse phonon transport in dielectric crystals, J. Heat Transfer 136 (2014) 042401.
[275] M. Zakari, D. Jou, Nonequilibrium Lagrange multipliers and heat-flux saturation, J. Non-Equilib. Thermodyn. 20 (1995) 342–349.
[276] A. Sellitto, V.A. Cimmelli, Flux limiters in radial heat transport in silicon nanolayers, J. Heat Transfer 136 (2014) 071301.
[277] V.A. Cimmelli, A. Sellitto, D. Jou, Nonlinear evolution and stability of the heat flow in nanosystems: Beyond linear phonon hydrodynamics, Phys. Rev. B 82 (2010) 184302.
[278] A. Sellitto, V.A. Cimmelli, D. Jou, Analysis of three nonlinear effects in a continuum approach to heat transport in nanosystems, Physica D 241 (2012) 1344–1350.
[279] A. Matthiessen, C. Vogt, On the influence of temperature on the electric conducting-power of alloys, Philos. Trans. R. Soc. Lond. 154 (1864) 167–200.
[280] G.F. Xie, Y. Guo, B.H. Li, L.W. Yang, K.W. Zhang, M.H. Tang, G. Zhang, Phonon surface scattering controlled length dependence of thermal conductivity of silicon nanowires, Phys. Chem. Chem. Phys. 15 (2013) 14647–14652.
[281] X.J. Wang, B.L. Huang, Computational study of in-plane phonon transport in si thin films, Sci. Rep. 4 (2014) 1–9.
[282] D. Singh, J.Y. Murthy, T.S. Fisher, Spectral phonon conduction and dominant scattering pathways in graphene, J. Appl. Phys. 110 (2011) 094312.

[283] X.L. Zhang, H. Xie, M. Hu, H. Bao, S.Y. Yue, G.Z. Qin, G. Su, Thermal conductivity of silicene calculated using an optimized Stillinger-Weber potential, Phys. Rev. B 89 (2014) 054310.
[284] S. Lee, D. Broido, K. Esfarjani, G. Chen, Hydrodynamic phonon transport in suspended graphene, Nature Commun. 6 (2015) 6290.
[285] A. Cepellotti, G. Fugallo, L. Paulatto, M. Lazzeri, F. Mauri, N. Marzari, Phonon hydrodynamics in two-dimensional materials, Nature Commun. 6 (2015) 6400.
[286] J. Hartmann, P. Voigt, M. Reichling, Measuring local thermal conductivity in polycrystalline diamond with a high resolution photothermal microscope, J. Appl. Phys. 81 (1997) 2966–2972.
[287] S. Uma, A.D. Mcconnell, M. Asheghi, K. Kurabayashi, K.E. Goodson, Temperature-dependent thermal conductivity of undoped polycrystalline silicon layers, Int. J. Thermophys. 22 (2001) 605–616.
[288] T. Maekawa, K. Kurosaki, S. Yamanaka, Thermophysical properties of BaY2O4: A new candidate material for thermal barrier coatings, Mater. Lett. 61 (2007) 2303–2306.
[289] N.A. Roberts, D.G. Walker, A review of thermal rectification observations and models in solid materials, Int. J. Therm. Sci. 50 (2011) 648–662.
[290] M. Maldovan, Sound and heat revolutions in phononics, Nature 503 (2013) 209–217.
[291] N. Li, J. Ren, L. Wang, G. Zhang, P. Haenggi, B. Li, Colloquium: Phononics: Manipulating heat flow with electronic analogs and beyond, Rev. Modern Phys. 84 (2012) 1045–1066.
[292] S.R. Sklan, Splash, pop, sizzle: Information processing with phononic computing, AIP Adv. 5 (2015) 053302.
[293] M. Kadic, T. Bückmann, R. Schittny, M. Wegener, Metamaterials beyond electromagnetism, Rep. Progr. Phys. 76 (2013) 126501.
[294] S. Narayana, Y. Sato, Heat flux manipulation with engineered thermal materials, Phys. Rev. Lett. 108 (2012) 214303.
[295] T. Han, T. Yuan, B. Li, C.-W. Qiu, Homogeneous thermal cloak with constant conductivity and tunable heat localization, Sci. Rep. 3 (2013) 1593.
[296] T. Han, X. Bai, J.T. Thong, B. Li, C.W. Qiu, Full control and manipulation of heat signatures: Cloaking, camouflage and thermal metamaterials, Adv. Mater. 26 (2014) 1731–1734.
[297] M. Terraneo, M. Peyrard, G. Casati, Controlling the energy flow in nonlinear lattices: A model for a thermal rectifier, Phys. Rev. Lett. 88 (2002) 094302.
[298] B.W. Li, L. Wang, G. Casati, Thermal diode: Rectification of heat flux, Phys. Rev. Lett. 93 (2004) 184301.
[299] N. Yang, G. Zhang, B. Li, Thermal rectification in asymmetric graphene ribbons, Appl. Phys. Lett. 95 (2009) 033107.
[300] Y. Wang, A. Vallabhaneni, J. Hu, B. Qiu, Y.P. Chen, X. Ruan, Phonon lateral confinement enables thermal rectification in asymmetric single-material nanostructures, Nano Lett. 14 (2014) 592–596.
[301] S. Ju, X. Liang, Thermal rectification and phonon scattering in asymmetric silicon nanoribbons, J. Appl. Phys. 112 (2012) 024307.
[302] N. Yang, G. Zhang, B. Li, Carbon nanocone: A promising thermal rectifier, Appl. Phys. Lett. 93 (2008) 243111.
[303] M. Hu, J.V. Goicochea, B. Michel, D. Poulikakos, Thermal rectification at water/functionalized silica interfaces, Appl. Phys. Lett. 95 (2009) 151903.
[304] W.S. Kim, J.L.G. Hector, M.N. Ozisik, Hyperbolic heat conduction due to axisymmetric continuous or pulsed surface heat sources, J. Appl. Phys. 68 (1990) 5478–5485.
[305] D.W. Tang, N. Araki, Wavy, wavelike, diffusive thermal responses of finite rigid slabs to high-speed heating of laser-pulses, Int. J. Heat Mass Transfer 42 (1999) 855–860.
[306] M.N. Özisik, D.Y. Tzou, On the wave theory in heat conduction, J. Heat Transfer 116 (1994) 526–535.
[307] S. Volz, J.-B. Saulnier, M. Lallemand, B. Perrin, P. Depondt, M. Mareschal, Transient Fourier-law deviation by molecular dynamics in solid argon, Phys. Rev. B 54 (1996) 340.
[308] J. Shiomi, S. Maruyama, Non-Fourier heat conduction in a single-walled carbon nanotube: Classical molecular dynamics simulations, Phys. Rev. B 73 (2006) 205420.
[309] J. Zhang, X. Huang, Y. Yue, J. Wang, X. Wang, Dynamic response of graphene to thermal impulse, Phys. Rev. B 84 (2011) 235416.
[310] J. Xu, X.W. Wang, Simulation of ballistic and non-Fourier thermal transport in ultra-fast laser heating, Physica B 351 (2004) 213–226.
[311] W. Kaminski, Hyperbolic heat conduction equation for materials with a nonhomogeneous inner structure, J. Heat Transfer 112 (1990) 555–560.
[312] K. Mitra, S. Kumar, A. Vedevarz, M. Moallemi, Experimental evidence of hyperbolic heat conduction in processed meat, J. Heat Transfer 117 (1995) 568–573.
[313] H. Herwig, K. Beckert, Experimental evidence about the controversy concerning Fourier or non-Fourier heat conduction in materials with a nonhomogeneous inner structure, Heat Mass Transf. 36 (2000) 387–392.
[314] H. Herwig, K. Beckert, Fourier versus non-Fourier heat conduction in materials with a nonhomogeneous inner structure, J. Heat Transfer 122 (2000) 363–365.
[315] E.P. Scott, M. Tilahun, B. Vick, The question of thermal waves in heterogeneous and biological materials, J. Biomech. Eng. 131 (2009) 074518.
[316] D.W. Tang, N. Araki, N. Yamagishi, Transient temperature responses in biological materials under pulsed IR irradiation, Heat Mass Transf. 43 (2007) 579–585.
[317] T. Bright, Z. Zhang, Common misperceptions of the hyperbolic heat equation, J. Thermophys. Heat Transfer 23 (2009) 601–607.
[318] Z. Zhang, T. Bright, G. Peterson, Reexamination of the statistical derivations of Fourier's law and Cattaneo's equation, Nanosc. Microsc. Thermophys. Eng. 15 (2011) 220–228.